

Electronic Thesis and Dissertation Repository

6-4-2012 12:00 AM

The Synthesis and Reactivity of New Pnictogen(III) Cations

Allison L. Brazeau
The University of Western Ontario

Supervisor
Paul J. Ragogna
The University of Western Ontario

Graduate Program in Chemistry
A thesis submitted in partial fulfillment of the requirements for the degree in Doctor of
Philosophy
© Allison L. Brazeau 2012

Follow this and additional works at: <https://ir.lib.uwo.ca/etd>

 Part of the [Inorganic Chemistry Commons](#)

Recommended Citation

Brazeau, Allison L., "The Synthesis and Reactivity of New Pnictogen(III) Cations" (2012). *Electronic Thesis and Dissertation Repository*. 576.
<https://ir.lib.uwo.ca/etd/576>

This Dissertation/Thesis is brought to you for free and open access by Scholarship@Western. It has been accepted for inclusion in Electronic Thesis and Dissertation Repository by an authorized administrator of Scholarship@Western. For more information, please contact wlsadmin@uwo.ca.

The Synthesis and Reactivity of New Pnictogen(III) Cations
(Spine title: The Synthesis and Reactivity of New Pnictogen(III) Cations)
(Thesis format: Integrated Article)

by

Allison L. Brazeau

Graduate Program in Chemistry

A thesis submitted in partial fulfillment
of the requirements for the degree of
Doctor of Philosophy

The School of Graduate and Postdoctoral Studies
The University of Western Ontario
London, Ontario, Canada

© Allison L. Brazeau 2012

CERTIFICATE OF EXAMINATION

Joint Supervisor

Examiners

Dr. Paul J. Ragona

Dr. Eric Rivard

Joint Supervisor

Dr. Richard J. Puddephatt

Dr. Nathan D. Jones

Dr. John F. Corrigan

Dr. Lyudmila Goncharova

The thesis by

Allison L. Brazeau

entitled:

The Synthesis and Reactivity of New Pnictogen(III) Cations

is accepted in partial fulfillment of the
requirements for the degree of
Doctor of Philosophy

Date

Chair of the Thesis Examination Board

Abstract

Chelating nitrogen based ligands are well known for their use with transition metals while their chemistry with p-block elements has been relatively underdeveloped. This thesis examines the structure, bonding and reactivity of group 15 elements supported by a pyridyl tethered 1,2-bis(imino)acenaphthene (“clamshell”) and various homo- and heteroleptic guanidinate frameworks.

The unique “clamshell” ligand contains a pendant Lewis base and has been used to support *N*-heterocyclic phosphonium and arsenium cations. Reactivity studies with the phosphorus analogue demonstrate the ability of the ligand to act as a Lewis base, while the phosphorus centre provides a Lewis acidic site, showing the amphoteric nature of such a molecule. Cobaltocene has been used as a new one-electron reductant in the facile, high yielding synthesis of a diaminochloroarsine supported by the “clamshell” ligand. Unfortunately this method was not suitable for all Group 15 elements and resulted in low yields for phosphorus and insoluble black material for antimony and bismuth. In the absence of a reductant the “clamshell” ligand can be used to form hypervalent donor-acceptor complexes with heavy main group elements (Sn, Sb and Bi). The addition of a salt metathesis reagent to the hypervalent Sb and Bi complexes results in base-stabilized SbCl_2^+ and BiCl_2^+ cations.

A series of diaminochlorophosphines has been synthesized with various dianionic guanidinate ligands, and their reluctance to release a chloride ion using halide abstracting reagents has been noted. A comprehensive study of their reactivity has been completed and the following were observed: (i) that the chloride ion could be removed with the addition of a chelating base; (ii) that carbodiimide can be eliminated chemically and thermally from the four-membered ring; and, (iii) that a rare ring expansion by the insertion of a chloro(imino)phosphine into a P–N bond of the P–N–C–N framework takes place. The analogous chemistry with heavier pnictogens to form diaminochloropnictines does not occur; rather the products are diaminodichloropnictines where the guanidinate ligand is monoanionic. Halide abstraction from these molecules is facile for As and Sb and the addition of a chelating base allows for the removal of the second chloride ion to give base-stabilized dicationic species.

Keywords

phosphenium cation • pnictogen • pnictenium cation • synthesis • structure and bonding • *N,N*-chelating ligands • guanidinate

Co-Authorship Statement

This thesis includes material from four previously published manuscripts presented in Chapters 2, 3, 4 and 5. The article presented in Chapter 2 was co-authored by A. L. Brazeau, C. A. Caputo, C. D. Martin, N. D. Jones and P. J. Ragogna (*Dalton Trans.* **2010**, 39, 11069). All of the experimental work was performed by ALB. X-ray diffraction data were collected and solved by CDM. CAC initially started the project, and is given credit for her early attempts. This work was started under the supervision of NDJ (CAC and ALB) and his NSERC grant continued to support the project. ALB and PJR. assembled the manuscript collaboratively.

The work described in Chapter 3 is accepted for publication in a manuscript co-authored by A. L. Brazeau, N. D. Jones and P. J. Ragogna and was an invited submission to appear in a themed issue of Dalton Transactions: *New Talent Americas* (*Dalton Trans.* **2012**, DOI: 10.1039/c2dt30171g). ALB conducted all experiments and solved the X-ray diffraction data. This project was funded by grant money belonging to NDJ. ALB was responsible for writing the manuscript, which was edited by PJR

The material presented in Chapter 4 was published in an article co-authored by A. L. Brazeau, M. M. Hänninen, H. M. Tuononen, N. D. Jones and P. J. Ragogna (*J. Am. Chem. Soc.* **2012**, 134, 5398). Theoretical calculations were conducted by MMH and HMT at the University of Jyväskylä, Finland. All experimental work was completed by ALB. The experimental work was originally started under the supervision of NDJ, and later taken over by PJR. The experimental and X-ray crystallographic portions of the manuscript were composed by ALB and edited by PJR, while the computational section was written by MMH and HMT.

A portion of the work in Chapter 5 was published in a communication co-authored by A. L. Brazeau, A. S. Nikouline and P. J. Ragogna (*Chem. Commun.* **2011**, 47, 4817). ASN is credited for the initial synthesis of all compounds, which were then comprehensively characterized by ALB. The manuscript was mainly written by ALB and heavily edited by PJR.

Acknowledgments

I would like to start by thanking Paul Ragona for being a great mentor. Not only have I learned so much under his supervision in the lab, but I have also come to depend on him as a life coach and value his opinion in the highest regard. His door is always open for a chat and it was always comforting that he “remembered what it was like to be in grad school.” Thank you to Nathan Jones, whose enthusiasm for chemistry brought me to Western and for supporting me in my decision to switch projects and join “Team Phosphonium” one year into my PhD. His mentorship and encouragement were greatly appreciated.

I would also like to thank all the staff members of the Chemistry department. Specifically, Dr. Mathew Willans for help with NMR spectroscopy, Dr. Ben Cooper for collecting X-ray diffraction data on my countless thin, plate-like crystals, Doug Hairsine for mass spectrometry, Yves Rambour for fixing and creating essential glassware (especially my Schlenk line!), John Vanstone and Jon Aukema for being masters of all trades and especially for being drybox repairmen, Darlene McDonald for keeping on top of deadlines that have slipped my mind, and the ChemBio Stores staff, specifically Sherrie McPhee, Don Yakobchuk, Monica Chirigel and especially Marylou Hart for remembering to order N₂ dewars even when I forgot.

I acknowledge Western University, OGS and NSERC for generous funding over the last 4.5 years.

I would also like to thank my committee members, Prof. Eric Rivard, Prof. Lyudmila Goncharova, Prof. Richard Puddephatt and Prof. John Corrigan, for reading my thesis and for their feedback.

I thank all the members, past and present, of the Ragona Lab for contributing to such a great working environment. I would especially like to thank Dr. Caleb Martin, Jonathan Dube and Jacquelyn Price for collecting X-ray diffraction data, solving

structures, teaching me how to solve my own and for being great friends in and out of the lab. I would also like to thank the original Jones lab. A special shout out goes to Team Awesome (Dr. Christine Caputo and Jacquelyn Price) for being awesome labmates, workout partners and friends.

Thank you to my “non-chemistry” friends (Jen and Janice) who remind me that sometimes its good to not talk science on the weekend. Thanks to my roommates (Nicole, Bianca, April and Laura) who are always willing for a spontaneous night out, a trip to Kiwi Kraze, or a night in on the couch for Jersday Thursday. I would also like to thank Sarah Anderson (my “wife”) for always being available for a chat or ready to jump in the car to drive six hours down the 401 when I need cheering up and of course for being my dance partner at DTKB.

I would especially like to thank my parents, Ana and Bill Brazeau, for always supporting me, reminding me to take things one step at a time when I was overwhelmed and for being incredible role models. I am the person I am today because of them. Thank you to my sister Nicole for always being there and helping me find ways to deal with stress.

Lastly, I would like to thank Phil Medeiros, my best friend and future husband, who has been a constant source of support, encouragement and comfort for my entire university career. You are an incredible person. I love you and I can’t wait to start our life together in the “real” world.

Table of Contents

CERTIFICATE OF EXAMINATION	ii
Abstract.....	iii
Keywords.....	iv
Co-Authorship Statement.....	v
Acknowledgments.....	vi
Table of Contents.....	viii
List of Figures.....	xii
List of Schemes.....	xv
List of Charts.....	xvii
List of Tables.....	xviii
List of Appendices.....	xix
List of Symbols and Abbreviations.....	xx
Chapter 1.....	1
1 Phosphenium cations.....	1
1.1 General introduction.....	1
1.2 History.....	1
1.3 Synthesis.....	3
1.3.1 Halide abstraction.....	3
1.3.2 Protic attack.....	4
1.3.3 Electrophilic attack.....	4
1.3.4 Redox route.....	5
1.3.4.1 External reductant.....	5
1.3.4.2 Internal reductant.....	6

1.4	Reactivity	7
1.4.1	Lewis acidity	8
1.4.2	Metal complexes	10
1.4.3	Bond activation	10
1.4.4	Polycations.....	12
1.5	<i>N</i> -Heterocyclic phosphonium cations (NHP).....	13
1.6	Scope of thesis.....	16
1.7	References	18
Chapter 2.....		22
2	A new approach to internal Lewis pairs featuring a phosphonium acid and a pyridine base.....	22
2.1	Introduction	22
2.2	Results and discussion	23
2.2.1	Synthesis	23
2.2.2	X-ray crystallography.....	27
2.3	Conclusions	31
2.4	Experimental section.....	31
2.4.1	Synthetic procedures	31
2.5	References	36
Chapter 3.....		37
3	Chemistry of the heavy group 15 elements with the “clamshell” ligand.....	37
3.1	Introduction	37
3.2	Results and discussion	38
3.2.1	Synthesis	38
3.2.2	X-ray crystallography.....	43
3.3	Conclusions	49

3.4	Experimental section.....	49
3.4.1	Synthetic procedures	49
3.5	References	57
Chapter 4.....		59
4	Synthesis, reactivity, and computational analysis of <i>N</i> -heterocyclic halophosphines supported by dianionic guanidinate ligands.....	59
4.1	Introduction	59
4.2	Results and discussion	63
4.2.1	Synthesis	63
4.2.2	Reactivity	66
4.2.3	X-ray crystallographic studies	77
4.2.4	Computational studies [†]	89
4.3	Conclusion.....	94
4.4	Experimental section.....	95
4.4.1	Synthesis	95
4.4.2	Computational details [†]	109
4.5	References	111
Chapter 5.....		116
5	Reactions of trichloropnictogens with a bulky guanidinate ligand.....	116
5.1	Introduction	116
5.2	Results and discussion	117
5.2.1	Synthesis	117
5.2.2	X-ray crystallography.....	120
5.3	Conclusions	125
5.4	Experimental section.....	125
5.4.1	Synthetic procedures	125

5.5 References	131
Chapter 6.....	133
6 Conclusions and future directions	133
6.1 Conclusions	133
6.2 Future directions.....	135
6.3 References	137
Appendices.....	138
Appendix 1: General considerations	138
A1.1 General experimental considerations	138
A1.2 General crystallography considerations	139
A1.3 References.....	139
Appendix 2: Copyright permission	140
A2.1 American Chemical Society's policy on theses and dissertations.....	140
A2.2 Royal Society of Chemistry rights retained by journal authors.....	142
Appendix 3: Supplementary data.....	143
A3.1 Corroborating ¹ H NMR spectra for elemental analyses of compounds 3.3-3.5	143

List of Figures

Figure 1.1: Analogous class of compounds.....	1
Figure 1.2: Frontier molecular orbitals for model diamminophosphonium cation $[(\text{H}_2\text{N})_2\text{P}]^{6,17}$	7
Figure 1.3: Amphoteric nature of a phosphonium cation.....	9
Figure 1.4: (a) Linear and (b) bent binding modes of metal-phosphonium complexes, and their analogy to NO^+	10
Figure 1.2: <i>N,N'</i> -chelating frameworks for NHPns (Pn = P, As, Sb, Bi) examined in this thesis.....	16
Figure 2.1: BIAN derivative featuring a pyridine donor (1).....	23
Figure 2.2: Stacked plot of ^1H NMR spectra (in CDCl_3) of the alkyl region for (a) 2.4 and (b) 2.3	26
Figure 2.3: Solid-state structures of 2.1-2.5 . Ellipsoids are drawn to 30% probability. Non-essential hydrogen atoms, solvate molecules and counteranions are omitted for clarity.....	28
Figure 3.1: Stacked plot of the ^1H NMR spectra for the reaction of 1 , AsCl_3 and SnCl_2 : (a) crystals of 3.1 ; (b) crude material; and, (c) supernatant.....	39
Figure 3.2: Solid-state structures of compounds 3.1-3.4 with thermal ellipsoids presented at 50% probability. Hydrogen atoms, solvates and non-coordinating anions are omitted for clarity. Refer to Table 3.1 for metrical parameters.....	44
Figure 3.3: Solid-state structures of compounds 3.5-3.8 with thermal ellipsoids presented at 50% probability. Hydrogen atoms, solvates and non-coordinating anions are omitted for clarity. Refer to Table 3.1 for metrical parameters.....	45

Figure 4.1: Stacked plot of the ^1H NMR spectra for (a) pure <i>N,N'</i> -bis(Mes)carbodiimide, (b) crude 4.9 , and (c) purified 4.9 .	69
Figure 4.2: Stacked plot of the ^1H NMR spectra for (a) 4.1 and (b) 4.12 .	73
Figure 4.3: (a) Plot of the integration of δ_{P} 4.1 , 4.12 , and 4.13 relative to normalized PPh_3 and the sum of the integrations as a function of time. (b) Stacked plot of $^{31}\text{P}\{^1\text{H}\}$ NMR spectra for monitoring the production of 4.13 from 4.1 in CDCl_3 .	76
Figure 4.4: Stack plot of ^1H NMR spectra for (a) pure 4.13 , (b) crude completed ring expansion, and (c) pure <i>N,N'</i> -bis(Mes)carbodiimide.	77
Figure 4.5: Solid-state structures of 2 , 4 , and 5 . Ellipsoids are drawn to 50% probability.	79
Figure 4.6: Solid-state structures of 4.1-4.4 . Ellipsoids are drawn to 50% probability. The methyl groups on the ^iPr substituents, and the hydrogen atoms have been omitted for clarity.	80
Figure 4.7: Solid-state structures of 4.6 , 4.7 , 4.10 . Ellipsoids are drawn to 50% probability. The hydrogen atoms and the triflate anion (4.10) have been omitted for clarity.	81
Figure 4.8: Isotropic solid-state structure of cation 4.9 . Ellipsoids are drawn to 30% probability.	83
Figure 4.9: Solid-state structures of 4.11-4.13 . Ellipsoids are drawn to 50% probability. Hydrogen atoms and solvates have been omitted for clarity. The view along the P–P bond of 4.11 has all but the <i>ipso</i> carbons removed from the Mes substituents for simplicity.	85
Figure 4.10: Lowest unoccupied molecular orbitals of the studied <i>N</i> -heterocyclic phosphines and their orbital energies (eV, in parenthesis).	91

Figure 4.11: Correlation between (a) the covalent contribution and the charge difference in the P–Cl bond of the studied chlorophosphines, and (b) correlation between the LUMO energies of the studied NHPs and the EDA P–Cl interaction energies of the studied chlorophosphines.....	93
Figure 4.12: Two of the lowest unoccupied molecular orbitals of 4.14	94
Figure 5.1: Stacked plot of the ¹ H NMR spectra for 5.6 : (a) crude; (b) yellow; and (c) white material.....	119
Figure 5.4: (a) Lewis structure and (b) dative bonding models for 5.7 and 5.8	121
Figure 5.2: Solid-state structures of 5.1 , 5.2 , 5.4 and 5.7 . Ellipsoids are drawn to 30% probability. Non-essential hydrogen atoms, solvates and non-interacting anions are removed for clarity.....	122
Figure A3.1: Corroborating ¹ H NMR spectrum for the elemental analysis of 3.3 showing ¼ equivalents of CH ₂ Cl ₂ (blue) and ¼ equivalents of Et ₂ O (red).....	143
Figure A3.2: Corroborating ¹ H NMR spectrum for the elemental analysis of 3.4 showing ¼ equivalents of CH ₂ Cl ₂ (blue) and ¼ equivalents of Et ₂ O (red).....	144
Figure A3.3: Corroborating ¹ H NMR spectrum for the elemental analysis of 3.5 showing ¼ equivalents of CH ₃ CN.	144

List of Schemes

Scheme 1.1: Synthesis of the first phosphonium cation.....	1
Scheme 1.2: Fragmentation pathway for <i>N,N'</i> -dimethyl-2-R-2-phospha-1,3-diazacyclohexanes.....	2
Scheme 1.3: Synthesis of the first acyclic phosphonium cation.....	3
Scheme 1.4: Halide abstraction from the parent halophosphine by (a) salt metathesis and (b) addition of a halide acceptor.....	3
Scheme 1.5: Protonation of an (a) amino and (b) imino group to give a phosphonium cation.	4
Scheme 1.6: (a) General and (b) specific example of an electrophilic attack for the synthesis of a phosphonium cation.....	5
Scheme 1.7: Pioneering work of Schmidpeter <i>et al.</i> on the reduction of P(III), giving cyclic triphosphonium cations.....	6
Scheme 1.8: Proposed mechanism for redox processes involving PX_3 ($X = Cl, Br, I$) and reducible α -diimines.....	6
Scheme 1.9: Baker and coworkers example of inserting $Pt(PPh_3)$ into the $P \leftarrow NHC$ bond of a cyclic phosphonium. ²²	9
Scheme 1.10: Reactivity of phosphonium cations.....	11
Scheme 1.11: Cationic phosphorus clusters <i>via</i> P_4 activation.....	12
Scheme 1.12: Synthesis of (a) acyclic and (b) cyclic catena-polyphosphorus cations.....	12
Scheme 1.13: General synthetic approach used in this thesis.....	16

Scheme 2.1: Redox reactions for the synthesis of 2.1 , 2.2 and the halide abstraction reaction giving 2.3	24
Scheme 2.2: Lewis acidic and basic reactivity of 2.3	25
Scheme 3.1: Anticipated (A) and observed (B) reactivity of 1 with AsCl ₃ and SnCl ₂	39
Scheme 3.2: Redox reactions for the synthesis of 3.2 and 3.3 , and the halide abstraction reaction giving 3.6	40
Scheme 3.3: Synthesis of base-stabilized 3.4 and 3.5 , and cationic 3.7 and 3.8	42
Scheme 4.1: Synthetic route for <i>N,N',N''</i> -tris(<i>aryl</i>)guanidines (2-5).....	64
Scheme 4.2: General method for synthesizing halophosphines with (dianionic)guanidinate ligands.....	65
Scheme 4.3: Lewis acid/Lewis base adduct formation of 4.7 and 4.8	67
Scheme 4.5: Synthesis of base-stabilized cationic 4.10	70
Scheme 4.6: Redox reaction for the synthesis of 4.11	71
Scheme 4.7: Carbodiimide elimination and ring expansion producing 4.12 and 4.13	73
Scheme 4.8a: Proposed route to 4.13 by insertion of MesNPCl.....	74
Scheme 4.8b: Proposed route to 4.13 by insertion of carbodiimide.....	75
Scheme 5.1: Anticipated and observed (5.1-5.3) reactivity of 2 with PnCl ₃ and NEt ₃ ; i) PnCl ₃ , 2 eq NEt ₃	118
Scheme 5.2: Synthesis of mono- (5.4-5.6) and dicationic (5.7-5.9) Pn(III) complexes.	120
Scheme 6.1: Proposed synthesis for the diphosphenium dication and its coordination to metals and formation of Lewis acid/Lewis base adducts.....	136

List of Charts

Chart 1.1: (a) Lewis structure and (b) dative bonding model for representing the triphosphenium cation.	6
Chart 1.2: Representations for $[\text{Me}_2\text{PPMe}_3]^+$ as the (a) dative model phosphino-phosphenium and (b) Lewis structure phosphinophosponium.	8
Chart 1.3: Examples of (a) dicationic and (b) tricationic base-stabilized P(III).....	13
Chart 4.1: Known and target four-membered NHP species.....	61
Chart 4.2: (a) Monoanionic vs. (b) dianionic guanidinate ligands, and (c) amidinate ligands.....	61
Chart 4.3: Literature examples of (a) monomeric (monoanionic)amidinate, (b) dimeric (monoanionic)amidinate, (c) (monoanionic)guanidinate, and (d) (dianionic)guanidinate ligands.....	62
Chart 4.4: (a) Symmetric and (b) asymmetric chelating guanidates for 4.3	66
Chart 4.5: Possible bonding descriptions of 4.9	83
Chart 4.6: Compounds studied computationally.....	89
Chart 6.1: (a) “Frustrated” internal Lewis pairs; (b) metal complexes; and, (c) NHC with the “clamshell” ligand.	137

List of Tables

Table 2.1: Selected metrical parameters for 2.1-2.5 . Bond lengths are in angstroms (Å) and bond angles in degrees (°).....	29
Table 2.2: X-ray details for 2.1-2.5	30
Table 3.1: Selected metrical parameters for 3.1-3.8 . Bond lengths are in angstroms (Å) and bond angles in degrees (°).....	46
Table 3.2: X-Ray details for 3.1-3.4	47
Table 3.3: X-Ray details for 3.5-3.8	48
Table 4.1: Selected bond lengths (Å) and bond angles (°) for 2 and 4	79
Table 4.2: Selected bond lengths (Å) and bond angles (°) for 4.1-4.4 , 4.6 and 4.7	81
Table 4.3: Selected bond lengths (Å) and bond angles (°) for 4.11-4.13	86
Table 4.4: X-ray details for 2 , 4 , 4.1-4.4	87
Table 4.5: X-ray details for 4.6 , 4.7 , and 4.11-4.13	88
Table 4.6: Atomic partial charges (δ) as obtained from the natural population analysis of the studied chlorophosphines.....	90
Table 4.7: LUMO energies (in eV) of 4.5⁺ and 4.14⁺-4.21⁺	91
Table 4.8: Results from energy decomposition analyses of P–Cl bonding in the studied chlorophosphines. ^a	92
Table 5.1: Selected bond lengths (Å) and bond angles (°) for compounds 5.1 , 5.2 , 5.4 and 5.7	123
Table 5.2: Refinement details for compounds 5.1 , 5.2 , 5.4 and 5.7	124

List of Appendices

Appendix 1: General considerations	138
A1.1 General experimental considerations	138
A1.2 General crystallography considerations	139
Appendix 2: Copyright permission	140
A2.1 American Chemical Society's policy on theses and dissertations	140
A2.2 Royal Society of Chemistry rights retained by journal authors.....	142
Appendix 3: Supplementary data.....	143
A3.1 Corroborating ¹ H NMR spectra for elemental analyses of compounds 3.3-3.5	143

List of Symbols and Abbreviations

Abbreviation	Definition
ang	angle
AO	atomic orbital
avg	average
BAr _F	tetrakis(3,5-bis(trifluoromethyl)phenyl)borate;
BIAN	1,2-bis(imino)acenaphthene
bpy	2,2'-bipyridine
br	broad
Calcd	calculated
<i>cf.</i>	<i>confer</i> (compare)
cm	centimetre
Cp	cyclopentadienyl
Cy	cyclohexyl
d	doublet
dd	doublet of doublets
ddd	doublet of doublets of doublets
DAB	diazabutadiene
DBN	1,5-diazabicyclo[4.3.0]non-5-ene
DBU	1,8-diazabicyclo[5.4.0]undec-7-ene
DFT	density functional theory
DIMPY	diiminopyridine
Dipp	2,6-diisopropylphenyl
DMAP	4-dimethylaminopyridine
Dmp	2,6-dimethylphenyl
d.p.	decomposition point
EDA	energy decomposition analysis
e.g.	<i>exempli gratia</i> (for example)
Et	ethyl
<i>et al.</i>	<i>et alii</i> (and others)

eV	electronvolt
FLP	frustrated Lewis pairs
FT	fourier transform
g	gram
h	hour(s)
HOMO	highest occupied molecular orbital
HRMS	high resolution mass spectrometry
Hz	hertz
ⁱ Pr	isopropyl
IR	infrared
<i>J</i>	coupling constant (Hz)
kJ	kilojoule
LUMO	lowest unoccupied molecular orbital
m	multiplet
M	molar
<i>m</i> -	meta
Me	methyl
Mes	2,4,6-trimethylphenyl; mesityl
MHz	megahertz
min	minute(s)
mL	milliliter
mmol	millimole
MO	molecular orbital
mol	mole
m.p.	melting point
ⁿ BuLi	<i>normal</i> butyllithium
NHC	<i>N</i> -heterocyclic carbene
NHP	<i>N</i> -heterocyclic phosphonium cation
NHPn	<i>N</i> -heterocyclic pnictenium cation
NMR	nuclear magnetic resonance
NPA	natural population analysis

<i>o</i> -	ortho
Oct	octyl
OTf	trifluoromethanesulfonate; triflate; CF_3SO_3^-
<i>P</i>	primitive unit cell
<i>p</i> -	para
Pn	pnictogen
ppm	parts per million
<i>R</i>	rhombohedrally centred
rt	room temperature
s	singlet
sept	septet
t	triplet
THF	tetrahydrofuran
vdW	van der Waals
Å	angstrom
°	degrees
°C	degrees Celsius
δ	chemical shift (ppm)
δ_{B}	boron chemical shift (ppm)
δ_{C}	carbon chemical shift (ppm)
δ_{F}	fluorine chemical shift (ppm)
δ_{H}	proton chemical shift (ppm)
δ_{P}	phosphorus chemical shift (ppm)
$\Delta\delta$	change in chemical shift (ppm)
{ ^1H }	proton decoupled
μL	microlitre

Chapter 1

1 Phosphenium cations

1.1 General introduction

Phosphenium cations are an interesting class of molecules that are defined as a two-coordinate P(III) species with a lone pair of electrons, an empty π orbital, and a localized positive charge on the central phosphorus atom. The cationic nature causes a characteristic downfield chemical shift in their ^{31}P NMR spectrum in the range of $\delta_{\text{P}} = 200\text{-}500$. Given this description they are considered as group 15 analogues of singlet state carbenes (Figure 1.1).

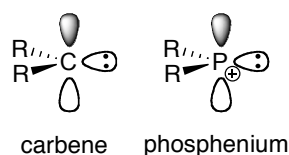
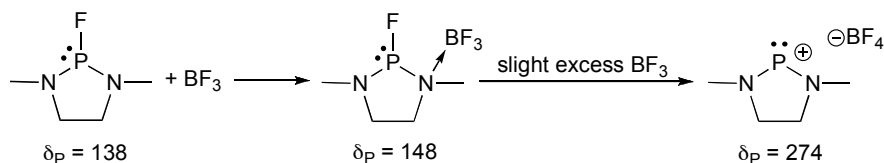


Figure 1.1: Analogous class of compounds.

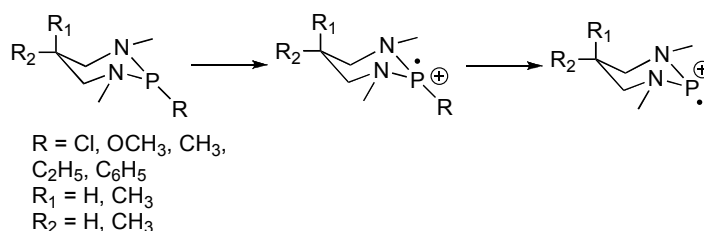
1.2 History

The first reported synthesis of a phosphenium cation was in 1972 by Fleming *et al.*¹ This was accomplished by using an excess of trifluoroborane to abstract a fluoride ion from cyclic fluorodialkylaminophosphine (Scheme 1.1) and upon formation of the cation-anion pair a significant downfield chemical shift was observed in the ^{31}P NMR spectrum ($\delta_{\text{P}} = 274$, $\Delta\delta_{\text{P}} = 126$).¹



Scheme 1.1: Synthesis of the first phosphenium cation.

Shortly after these findings a second report was published by Hutchins *et al.*, in which a mass spectrometric study of *N,N'*-dimethyl-2-R-2-phospha-1,3-diazacyclohexanes (R = Cl, OCH₃, CH₃, C₂H₅, C₆H₅) revealed a fragmentation pathway resulting from the loss of R (Scheme 1.2).² The most intense peak corresponding to a long-lived phosphonium cation was observed in all spectra. Analogous compounds with flanking oxygen and sulfur atoms were studied and it was found that the base peak did not correspond to a phosphonium ion. If both nitrogen atoms were in a bridgehead position, giving a bicyclic aminophosphine, then the mass spectral fragmentation pattern is different from that observed previously for (mono)cyclic species, disfavoring the production of a phosphonium cation. From the two previous observations it was concluded that delocalization by flanking nitrogen atoms with available axial lone pairs had a stabilizing effect on the electron deficient phosphorus atom.²

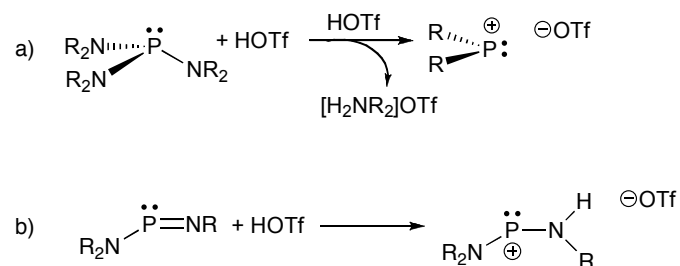


Scheme 1.2: Fragmentation pathway for *N,N'*-dimethyl-2-R-2-phospha-1,3-diazacyclohexanes.

The first two literature reports of dicoordinate P(III) species were of cyclic diaminophosphonium cations.^{1,2} It was not until four years later that Parry *et al.* published back-to-back articles describing the synthesis of the first acyclic diaminophosphonium cation.^{3,4} The initial studies were of the reactions of bis(dimethylamido)chlorophosphorus(III), ((H₃C)₂N)₂PCl, with AlCl₃. It was discovered that Lewis acid/Lewis base 1:1 adducts are produced, but the unexpected result of a 2:1 adduct is also possible if a second stoichiometric equivalent of ((H₃C)₂N)₂PCl or ((CH₃)₂N)₃P is added (Scheme 1.3).³ Conductivity studies revealed that the 2:1 adduct was actually an ionic species and multinuclear NMR spectroscopy confirmed the presence of inequivalent four- and three-coordinate phosphorus atoms.⁴ While solid-state structures are not reported, the comprehensive characterization suggests the

1.3.2 Protic attack

In the case of the parent phosphine being an aminophosphine or an iminophosphine, the method of protic attack can be conveniently employed to generate a phosphonium cation.⁶ The goal in this approach is to protonate the amino group to liberate NHR_2 , or add a proton across the $\text{P}=\text{N}$ bond. Both can be accomplished by using a proton source, such as triflic acid (HOTf). Dahl has illustrated that the 1:2 stoichiometric reaction of $\text{P}(\text{NMe}_2)_3$ and HOTf (Scheme 1.5a) results in the protonation of one NMe_2 group to give a phosphonium cation with an OTf^- ion and HNMe_2 . The second equivalent of HOTf then reacts with the secondary amine to form the ammonium salt $[\text{H}_2\text{NMe}_2]\text{OTf}$. It is desirable to use a proton donor that gives a weak nucleophile as an anion, such as OTf^- , since more nucleophilic anions have the tendency to give substitution products.⁹ Romanenko *et al* demonstrated that stable cations could be synthesized by the addition of HOTf to an aminoiminophosphine (Scheme 1.5b).¹⁰

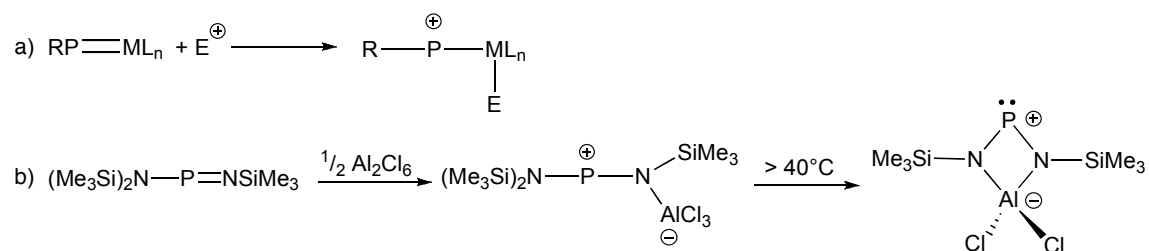


Scheme 1.5: Protonation of an (a) amino and (b) imino group to give a phosphonium cation.

1.3.3 Electrophilic attack

Electrophilic attack at element-phosphorus double bonds can result in phosphonium cations as shown in the general case in Scheme 1.6a.^{6,10} A specific example is that from Niecke and Kroher where AlCl_3 attacks the nitrogen of a $\text{P}=\text{N}$ bond, resulting in a two-coordinate phosphorus atom bearing a positive charge (Scheme 1.6b).¹¹ Cyclization of this compound occurs above $40\text{ }^\circ\text{C}$ to give a four-membered zwitterionic ring. The downfield chemical shifts in the ^{31}P NMR spectra of these zwitterions suggest a highly

localized positive charge at phosphorus and thus these compounds are considered to be phosphonium cations.¹¹

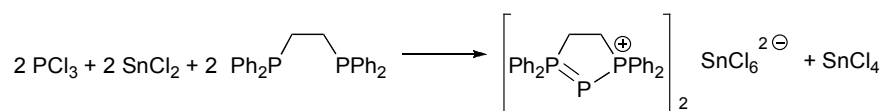


Scheme 1.6: (a) General and (b) specific example of an electrophilic attack for the synthesis of a phosphonium cation.

1.3.4 Redox route

1.3.4.1 External reductant

The use of an external reductant to reduce P(III) to a P(I) species was pioneered by Schmidpeter *et al.* in 1982. It was demonstrated that if PCl_3 is reduced by $SnCl_2$ in the presence of a chelating phosphine, a triphosphonium cation results (Scheme 1.7).¹² However, there are several different ways this molecule can be illustrated depending on if a Lewis or dative bonding model is used (Chart 1.1). With a chemical shift of $\delta_P = -232$ ¹² this molecule is better assigned as a P(I) cation stabilized by a chelating (dative) phosphine (Chart 1.1b), where each chelating phosphorus donates its lone pairs to $P(I)^+$. This same redox approach can be applied to P(III) in the presence of an α -diimine, as shown by Cowley *et al.* (Scheme 1.8). The 1:1:1 stoichiometric reaction of PCl_3 , $SnCl_2$ and α -diimine results in the *N*-heterocyclic phosphonium cation (NHP) with a $SnCl_5^-$ counteranion.¹³ The mechanism is thought to be concerted and occur by the Lewis basic α -diimine forming a donor-acceptor complex with P(III), which is then reduced by $SnCl_2$ to the fleeting P(I) species and concomitantly generates $SnCl_4$. The low energy LUMO of the α -diimine can accept two electrons from P(I), which reduces the ligand and oxidizes P(I) back to P(III) in an overall cyclization reaction. The chloride ion is removed by $SnCl_4$ (acceptor) resulting in an NHP with a $SnCl_5^-$ anion. This approach has also been successful for the synthesis of arsenium cations.¹³



Scheme 1.7: Pioneering work of Schmidpeter *et al.* on the reduction of P(III), giving cyclic triphosphenium cations.

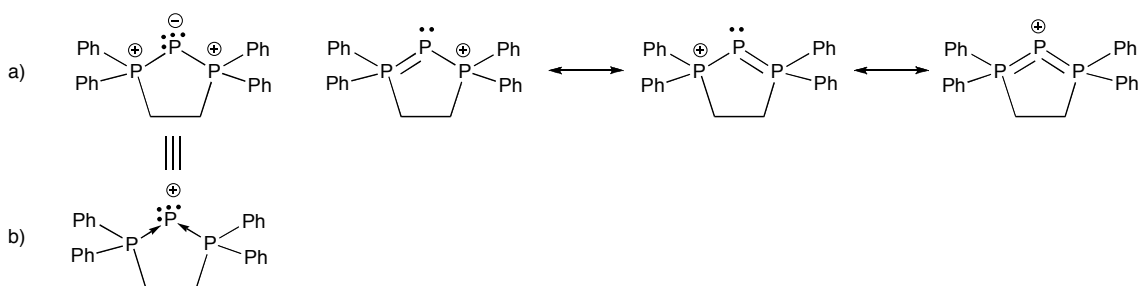
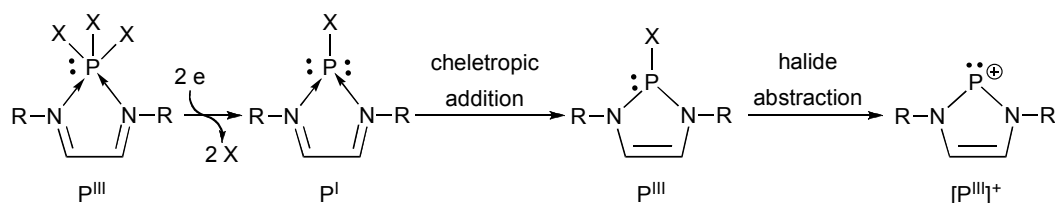


Chart 1.1: (a) Lewis structure and (b) dative bonding model for representing the triphosphenium cation.



Scheme 1.8: Proposed mechanism for redox processes involving PX_3 ($\text{X} = \text{Cl}, \text{Br}, \text{I}$) and reducible α -diimines.

1.3.4.2 Internal reductant

Similar to the synthesis of triphosphenium cations by Schmidpeter, Macdonald *et al.* isolated P(I) cations stabilized by chelating phosphines, but without the use of an external reductant. Macdonald demonstrated that if PI_3 was used as the P(III) source, I_2 is reductively eliminated to give a P(I) cation with an iodide anion.¹⁴ Cowley has demonstrated the convenience of this method in the facile synthesis of NHPs.^{13,15} Similar to the chemistry described in the previous section, the 1:1 stoichiometric reaction of PI_3 and a α -diimine undergoes reduction to P(I), cyclization with the reducible ligand and oxidation to P(III)⁺. The counteranion in Cowley's work is I_3^- , where the I_2 acts as a

halide abstracting reagent.^{13,15} This is a convenient one-pot synthesis to NHP with no byproducts, and analogous chemistry has been observed for AsI_3 .¹³

1.4 Reactivity

The cationic charge, Lewis acidity and coordinative unsaturation of phosphonium cations are the key factors in the observed reactivity of this class of molecules. Inverse electronic properties are observed for phosphonium cations compared to their carbene group 14 analogues, and therefore they are poor σ -donors but excellent π -acceptors.¹⁶ Examination of the frontier molecular orbitals for a diaminophosphonium cation (Figure 1.2) reveals that the LUMO is represented by the anti-bonding molecular orbital in which an empty π -orbital is on phosphorus, giving rise to its Lewis acidic nature. The lone pair of electrons on phosphorus is represented by the HOMO-1 rendering the phosphonium weakly Lewis basic.^{6,17,18}

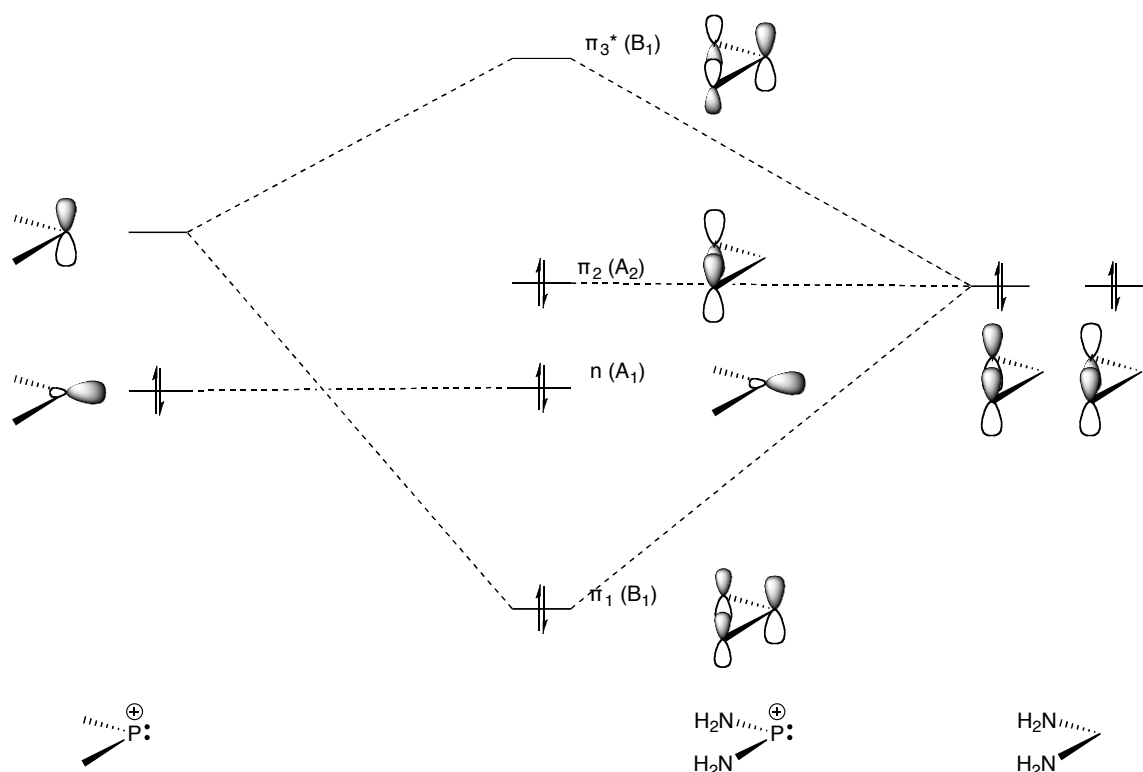


Figure 1.2: Frontier molecular orbitals for model diaminophosphonium cation $[(\text{H}_2\text{N})_2\text{P}]^+$.^{6,17}

1.4.1 Lewis acidity

The Lewis acidity of phosphonium cations is underscored by the ability to form adducts with Lewis bases, such as amines, phosphines, and carbenes. A quantitative study of the Lewis acidity of various phosphonium cations (cyclic, acyclic, diamino-, dithia-) by examining the $\Delta\delta_C$ of the *para*-carbon in the donating pyridine found that Lewis acidity trends of the cations were as follows: cyclic < acyclic and diamino < dithia.¹⁹ Bertrand *et al.* also demonstrated the donating power of amines to dicoordinate cationic phosphorus species with the bicyclic amidine DBU (1,8-diazabicyclo[5.4.0]undec-7-ene). Upon coordination the positive charge is delocalized throughout the cluster as evidenced from the C–N bond lengths of the N–C–N framework and the upfield chemical shift of phosphorus ($\delta_P = 108$, *cf.* $\delta_P = 313$ for $(i\text{Pr}_2\text{N})_2\text{P}^+$).²⁰

The first synthesis of an acyclic phosphonium cation, as mentioned in Section 1.2, was by Parry who recognized a 2:1 adduct when a second equivalent of phosphine was added to a 1:1 Lewis acid/Lewis base adduct. Parry's synthesis of the first acyclic phosphonium cation, also marks the synthesis of the first phosphino-phosphonium complex.^{3,4} Depending on the representation (Chart 1.2) these species can be considered as phosphino-phosphonium (dative model, Chart 1.2a) or phosphino-phosphonium (Lewis model, Chart 1.2b) cations. Evidence for the dative coordinative nature of the phosphine was demonstrated by the ability of $[\text{Ph}_2\text{P}(\text{Ph}_2\text{PCl})]\text{GaCl}_4$ to undergo ligand exchange with PPh_3 to form $[\text{Ph}_2\text{P}(\text{Ph}_3\text{P})]\text{GaCl}_4$.^{7d} The weaker Lewis acidic cyclic diaminophosphonium has also been shown to form adducts with phosphines by the reversible donor-acceptor complex with PMe_3 .^{7b}

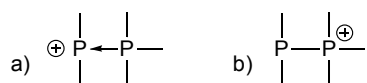
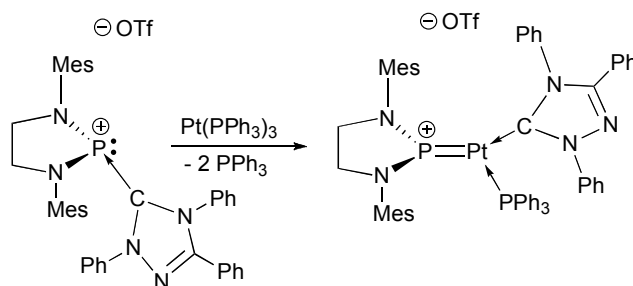


Chart 1.2: Representations for $[\text{Me}_2\text{PPMe}_3]^+$ as the (a) dative model phosphino-phosphonium and (b) Lewis structure phosphinophosphonium.

The first $[\text{R}_2\text{P}\leftarrow\text{NHC}]^+$ adduct was illustrated by Kuhn *et al.* by the reaction of an NHC with Ph_2PCl which forms a stable adduct upon addition of AlCl_3 .²¹ Baker and coworkers

also demonstrated the ability of phosphonium cations to form stable donor-acceptor complexes with an NHC by addition of a carbene to a cyclic diaminophosphonium. Unlike in the case of a phosphine donor (e.g. PMe_3), the stronger σ -donating NHC does not show reversible coordination at room temperature. However, the NHC donor can be displaced upon reaction of the adduct with $\text{Pt}(\text{PPh}_3)_3$ in which two phosphines are displaced and the Pt inserts into the $\text{P}\leftarrow\text{NHC}$ bond to give $[\text{Pt}(\text{PPh}_3)(\text{NHP})(\text{NHC})]^+$ (Scheme 1.9).²²



Scheme 1.9: Baker and coworkers example of inserting $\text{Pt}(\text{PPh}_3)$ into the $\text{P}\leftarrow\text{NHC}$ bond of a cyclic phosphonium.²²

An interesting feature of these donor-acceptor complexes is the conservation of the stereochemically active lone pair on the phosphonium cation, which is available to act as a Lewis donor. Burford and coworkers have elegantly confirmed the weak Lewis basicity of these lone pairs by the reversible (in solution) coordination to a Lewis acid. The solid-state structure clearly shows an “in series” coordination where a phosphine base coordinates to a Lewis acidic phosphonium cation, which forms an adduct with GaCl_3 (Figure 1.3).²³

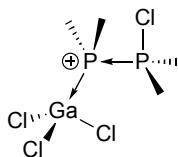


Figure 1.3: Amphoteric nature of a phosphonium cation.

1.4.2 Metal complexes

The amphoteric nature of phosphonium cations is a consequence of phosphorus possessing both a lone pair of electrons and an empty π -orbital. This property makes them ideal to form coordination complexes with low valent transition metals,^{8a} as they have been described as “bulky CO” or NO^+ equivalents.^{7a,24,25} Their analogy to NO^+ seems more appropriate given that they are both cationic and can adopt either linear or bent binding modes to transition metals (Figure 1.4). Phosphonium cations have been used as ancillary ligands for primarily group 6-10 metals^{7a,17,24,26-29} and in all cases short M–P bonds are observed. This is indicative of significant metal-to-ligand backbonding in addition to phosphorus donating its lone pair to the electron-rich metal.²⁴ Reactivity studies for these metal-phosphonium cationic complexes most commonly involve ligand exchange and reactions with nucleophiles, which leads to isomerization.^{27,28} The general claim for the application of metal-phosphonium complexes is that they are ideal for catalysis because of the π -accepting ability of the phosphonium ligand, however there have been limited investigations conducted in this area.³⁰⁻³²

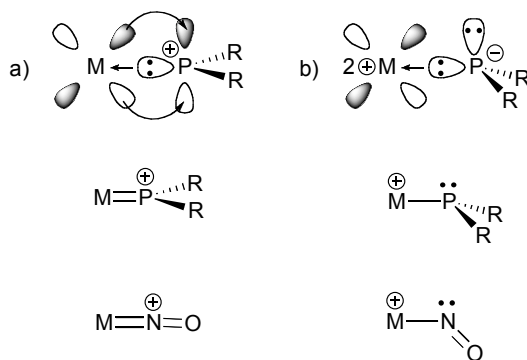
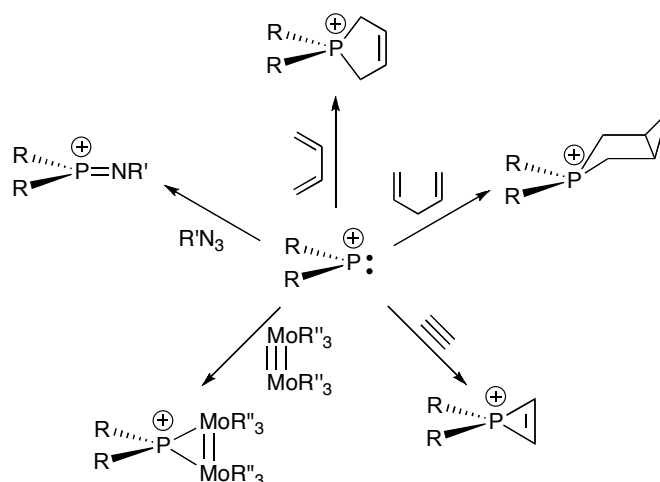


Figure 1.4: (a) Linear and (b) bent binding modes of metal-phosphonium complexes, and their analogy to NO^+ .

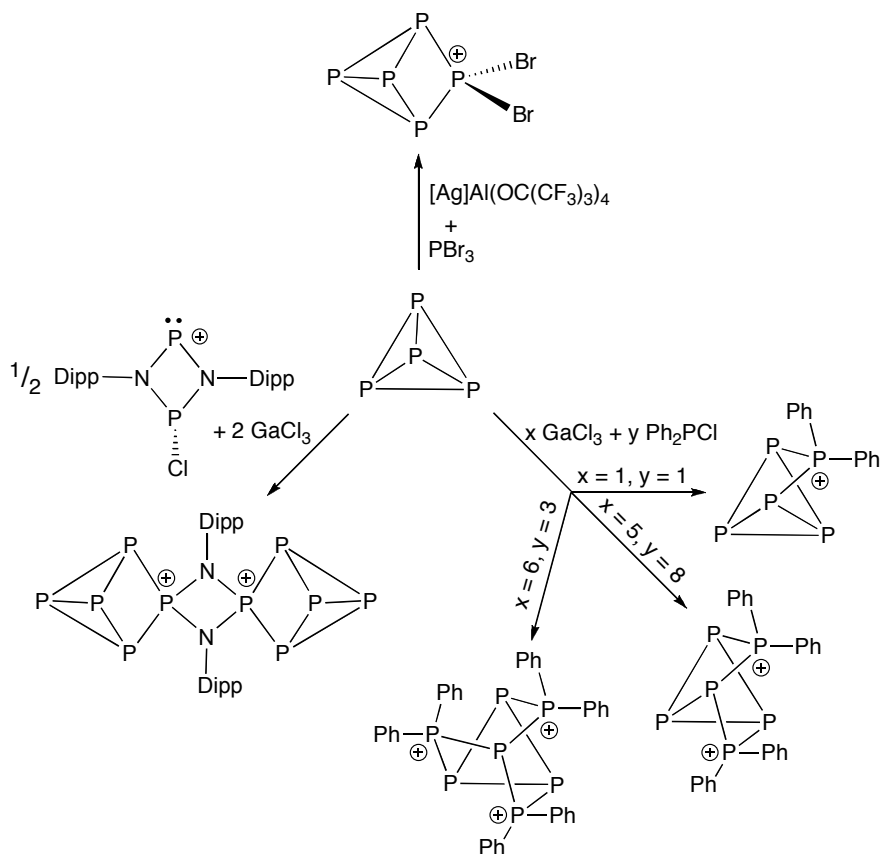
1.4.3 Bond activation

The reactivity of phosphonium cations towards unsaturated molecules has been studied in great detail. For example, they have been observed to undergo cycloadditions with 1,3-dienes,^{7f,33-36} 1,4-dienes,^{35,37} insert into alkynes^{6,38,39} and metal-metal triple bonds,⁶ and react with azides to form iminophosphonium ions⁴⁰ (Scheme 1.10).

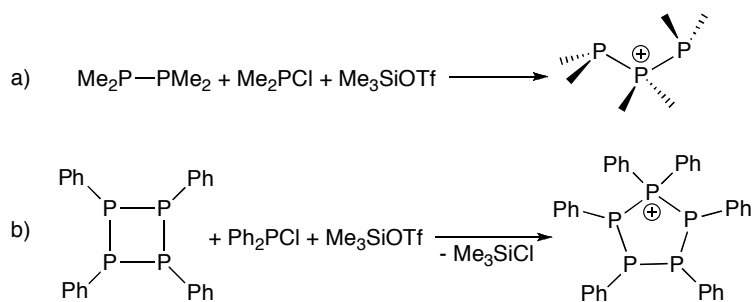


Scheme 1.10: Reactivity of phosphonium cations.

Investigating the insertion of phosphonium cations into element-element bonds of main group molecules has been a relatively new area of research for this class of molecules and has resulted in interesting reactivity, and bonding motifs. Crossing and coworkers were the first to report a P_5^+ cationic cluster *via* the insertion of a phosphonium cation into a P_4 tetrahedron.⁴¹ This has been followed by several examples from Weigand *et al.* where it was demonstrated that polycationic clusters were accessible by varying the stoichiometry in reactions with P_4 , $GaCl_3$ and Ph_2PCl .⁴² Weigand has also shown that the bifunctional phosphonium $[DippNP]_2^{2+}$ is capable of forming P_5 cationic clusters at both P^+ sites (Scheme 1.11).^{8d} Phosphonium cations have also been inserted into the P–P bonds of diphosphines and cyclophosphines to synthesize new catena-polyphosphorus cations (Scheme 1.12).^{7d,43}



Scheme 1.11: Cationic phosphorus clusters *via* P₄ activation.



Scheme 1.12: Synthesis of (a) acyclic and (b) cyclic catena-polyphosphorus cations.

1.4.4 Polycations

While the majority of the reports on cationic phosphorus(III) concern phosphonium (mono)cations, there are an increasing number of studies on polycationic P(III), in which the charge is +2 or +3 (Chart 1.3). These typically require additional stabilization from a base that is capable of delocalizing the positive charge. The first report was in 1991 by

Weiss and Engel where the reaction of PX_3 ($X = Cl, Br, I$) with DMAP or quinuclidine generates P(III) tricationic species, however this was not confirmed by X-ray diffraction studies. Similarly, Bertrand *et al.* were able to make di- and tricationic P(III) compounds using DBU or DBN.^{20,44} More recently, the groups of Weigand and Alcarazo have utilized carbenes for delocalizing the cationic charge on $P(III)^{2+}$ and $P(III)^{3+}$, respectively.^{45,46} The use of cyclopropenium⁴⁶ as the carbene precursor as opposed to the more common imidazolium⁴⁵ salt allowed for the isolation of a $[(\text{carbene})_3P]^{3+}$ species as opposed to the latter which can only be used in the synthesis of mono- and dicationic P(III).

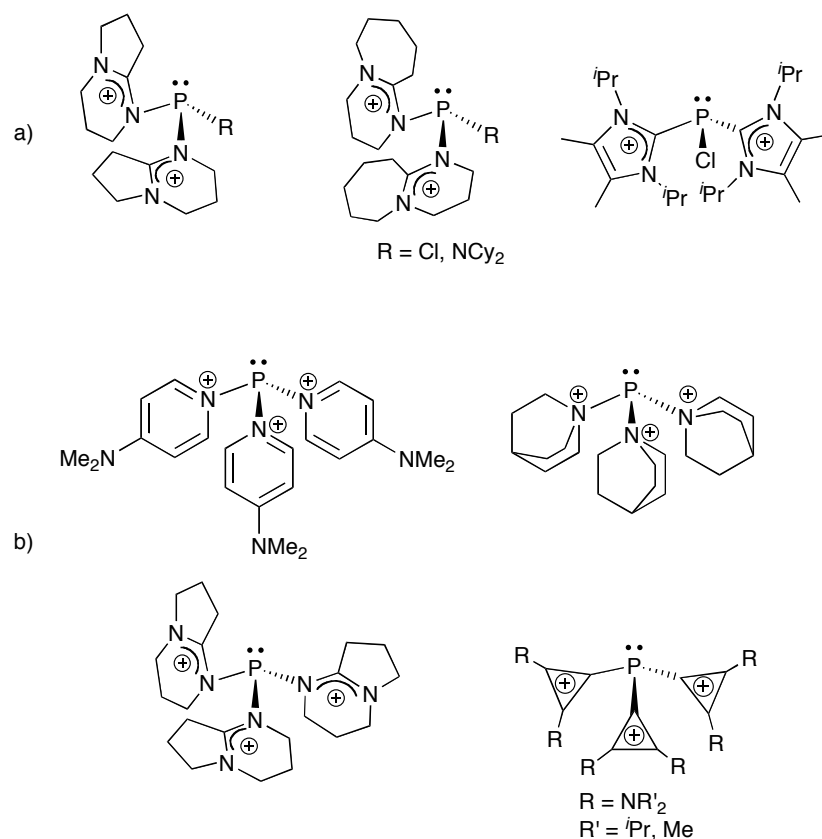


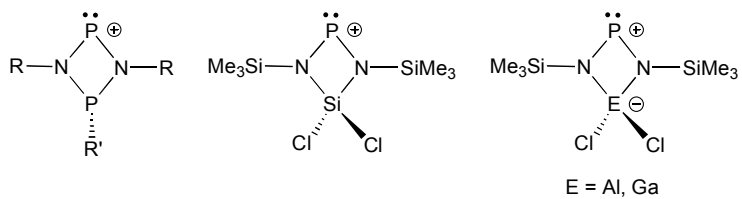
Chart 1.3: Examples of (a) dicationic and (b) tricationic base-stabilized P(III).

1.5 N-Heterocyclic phosphonium cations (NHP)

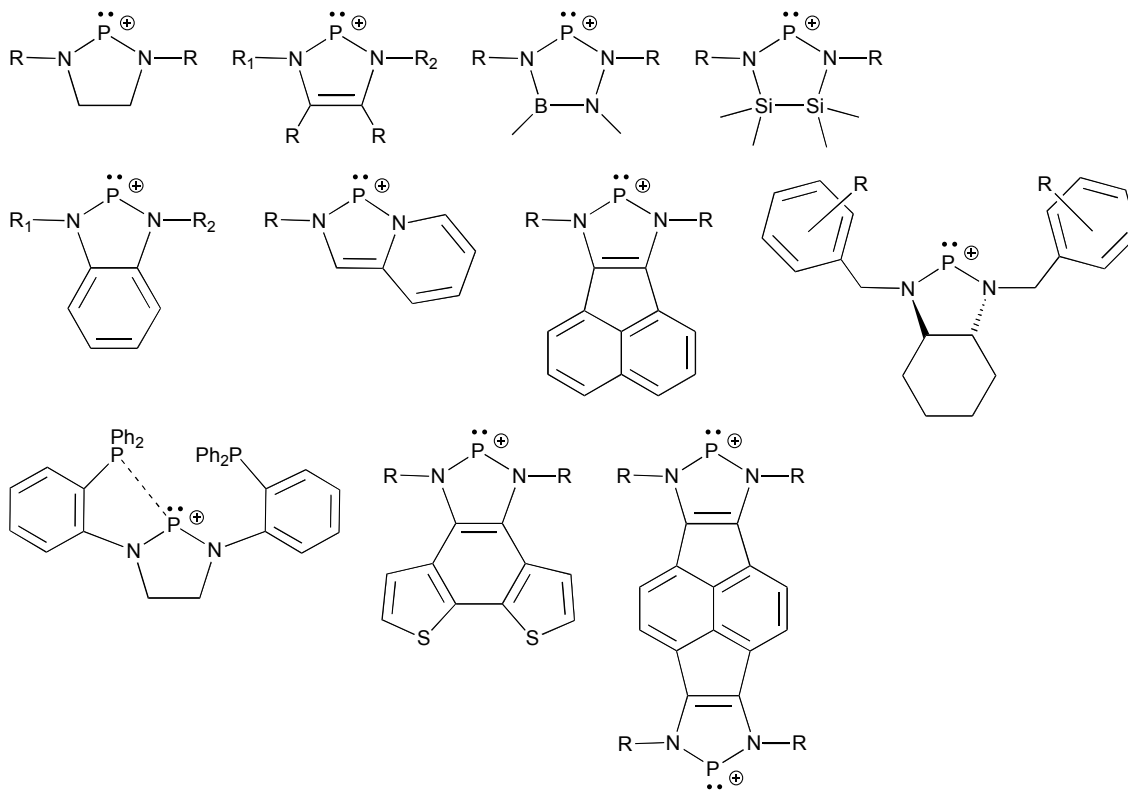
The NHPs are a well studied class of species, and are supported by a variety of N-based ligands, in which there is chelation by two tethered nitrogen atoms to the central P(III)

cation. The ring size of the NHP is dependent on the number of atoms linking the nitrogen atoms. NHPs with four-, five-, and six-membered rings are known in the literature. However, the five-membered rings dominate this group of compounds, with such ligands as diazabutadiene (DAB), ethylenediamine, and bis(imino)acenaphthene (BIAN). Chart 1.4 provides a generalized, extensive list of reported NHPs categorized by ring size.^{1,2,7a,7e-g,8d-e,11,13,47-49}

a) Four-membered rings



b) Five-membered rings



c) Six-membered rings

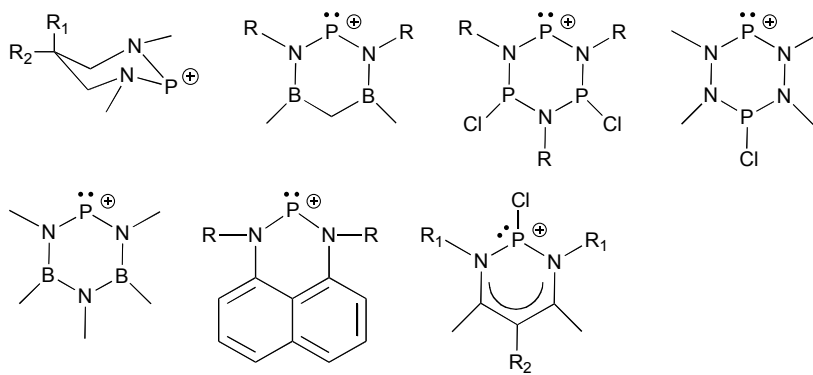


Chart 1.4: Examples of NHPs as (a) four-, (b) five-, and (c) six-membered rings.

1.6 Scope of thesis

In light of the above discussion, the work presented in this thesis targets the synthesis of new NHPs with increased utility and heightened reactivity, by incorporating proximal functional groups, ring strain and increasing the charge at the phosphorus centre. This will be accomplished utilizing previously known *N,N'*-chelating frameworks (Figure 1.2) ubiquitously known as ligands for transition metals, but rarely used with p-block elements. The unknown coordination of a pyridyl tethered 1,2-bis(imino)acenaphthene and a dianionic guanidinate to phosphorus and the reactivity of these molecular entities will be explored. Analogous studies for the heavier Group 15 elements (As, Sb, Bi) are also investigated. These fundamental studies are aimed at investigating the structure, bonding and reactivity of new NHPs and their heavier congeners.

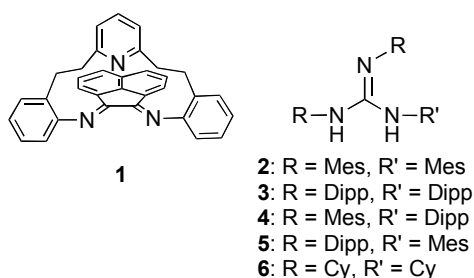
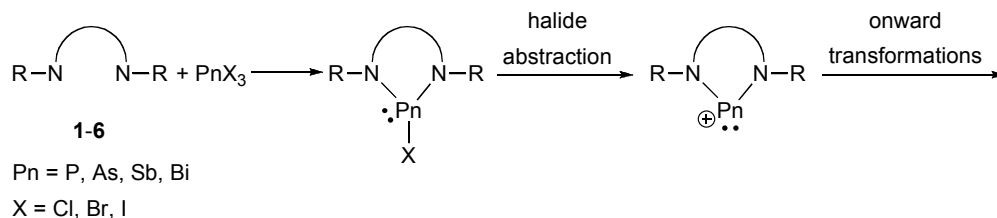


Figure 1.2: *N,N'*-chelating frameworks for NHPns (Pn = P, As, Sb, Bi) examined in this thesis.

The synthetic approach (Scheme 1.13) for generating NHPs is to first synthesize the parent halophosphine by redox or dehydrohalogenation routes, and subsequently abstract the halide by salt metathesis to obtain the cation. Investigations on the reactivity and properties of the new NHPs will be performed.



Scheme 1.13: General synthetic approach used in this thesis.

Chapter two will focus on the synthesis of an NHP with a pyridyl tethered 1,2-bis(imino)acenaphthene “clamshell” ligand (**1**, Figure 1.2) and the evaluation of the Lewis acidity/basicity of the resulting phosphonium complexes. Chapter 3 will examine the synthesis of heavy *N*-heterocyclic pnictenium cation (NHPn) analogues (Pn = pnictenium = As, Sb, Bi), utilizing a different reducing agent than those used previously in the literature. A comprehensive study towards the synthesis of an NHP supported by a dianionic guanidinate ligand (**2-6**, Figure 1.2) is detailed in Chapter 4, along with an extensive look at the reactivity and thermal stability of the starting diaminochlorophosphine. The synthesis of heavy NHPns (Pn = As, Sb, Bi) with the guanidine **2** and how they differ from the phosphorus analogues is examined in Chapter 5, along with the rare synthesis of pnictetidine dications. A collective summary, conclusions and future directions for the projects comprising this thesis will be given in Chapter 6.

1.7 References

- (1) Fleming, S.; Lupton, M. K.; Jekot, K. *Inorg. Chem.* **1972**, *11*, 2534.
- (2) Maryanoff, B. E.; Hutchins, R. O. *J. Org. Chem.* **1972**, *37*, 3475.
- (3) Kopp, R. W.; Bond, A. C.; Parry, R. W. *Inorg. Chem.* **1976**, *15*, 3042.
- (4) Schultz, C. W.; Parry, R. W. *Inorg. Chem.* **1976**, *15*, 3046.
- (5) Igau, A.; Grutzmacher, H.; Baceiredo, A.; Bertrand, G. *J. Am. Chem. Soc.* **1988**, *110*, 6463.
- (6) Cowley, A. H.; Kemp, R. A. *Chem. Rev.* **1985**, *85*, 367.
- (7) For example, see: (a) Abrams, M. B.; Scott, B. L.; Baker, R. T. *Organometallics* **2000**, *19*, 4944. (b) Gudat, D.; Haghverdi, A.; Hupfer, H.; Nieger, M. *Chem. Eur. J.* **2000**, *6*, 3414. (c) Burford, N.; Cameron, T. S.; Ragona, P. J. *J. Am. Chem. Soc.* **2001**, *123*, 7947. (d) Burford, N.; Dyker, C. A.; Decken, A. *Angew. Chem. Int. Ed.* **2005**, *44*, 2364. (e) Spinney, H. A.; Yap, G. P. A.; Korobkov, I.; DiLabio, G.; Richeson, D. S. *Organometallics* **2006**, *25*, 3541. (f) Caputo, C. A.; Price, J. T.; Jennings, M. C.; McDonald, R.; Jones, N. D. *Dalton Trans.* **2008**, 3461. (g) Dube, J. W.; Farrar, G. J.; Norton, E. L.; Szekely, K. L. S.; Cooper, B. F. T.; Macdonald, C. L. B. *Organometallics* **2009**, *28*, 4377.
- (8) For example, see: (a) Cowley, A. H.; Cushner, M. C.; Szobota, J. S. *J. Am. Chem. Soc.* **1978**, *100*, 7784. (b) Spinney, H. A.; Korobkov, I.; DiLabio, G. A.; Yap, G. P. A.; Richeson, D. S. *Organometallics* **2007**, *26*, 4972. (c) Weigand, J. J.; Burford, N.; Decken, A. *Eur. J. Inorg. Chem.* **2008**, 4343. (d) Holthausen, M. H.; Weigand, J. J. *J. Am. Chem. Soc.* **2009**, *131*, 14210. (e) Denk, M. K.; Gupta, S.; Ramachandran, R. *Tetrahedron Lett.* **1996**, *37*, 9025.
- (9) Dahl, O. *Tetrahedron Lett.* **1982**, *23*, 1493.
- (10) Drapailo, A. B.; Chernega, A. N.; Romanenko, V. D.; Madhouni, R.; Sotiropoulos, J.-M.; Lamandé, L.; Sanchez, M. *J. Chem. Soc., Dalton Trans.* **1994**, 2925.
- (11) Niecke, E.; Kröher, R. *Angew. Chem. Int. Ed. Engl.* **1976**, *15*, 692.
- (12) Schmidpeter, A.; Lochschmidt, S.; Sheldrick, W. S. *Angew. Chem. Int. Ed. Engl.* **1982**, *21*, 63.
- (13) Reeske, G.; Hoberg, C. R.; Hill, N. J.; Cowley, A. H. *J. Am. Chem. Soc.* **2006**, *128*, 2800.
- (14) Ellis, B. D.; Carlesimo, M.; Macdonald, C. L. B. *Chem. Commun.* **2003**, 1946.

- (15) Reeske, G.; Cowley, A. H. *Inorg. Chem.* **2007**, *46*, 1426.
- (16) Tuononen, H. M.; Roesler, R.; Dutton, J. L.; Ragogna, P. J. *Inorg. Chem.* **2007**, *46*, 10693.
- (17) Gudat, D. *Coord. Chem. Rev.* **1997**, *163*, 71.
- (18) Schoeller, W. W.; Tubbesing, U. *Journal of Molecular Structure (Theochem)* **1995**, *343*, 49.
- (19) Payraastre, C.; Madaule, Y.; Wolf, J. G.; Kim, T. C.; Mazières, M.-R.; Wolf, R.; Sanchez, M. *Heteroat. Chem.* **1992**, *3*, 157.
- (20) Reed, R.; Réau, R.; Dahan, F.; Bertrand, G. *Angew. Chem. Int. Ed. Engl.* **1993**, *32*, 399.
- (21) Kuhn, N.; Fahl, J.; Bläser, D.; Boese, R. *Z. Anorg. Allg. Chem.* **1999**, *625*, 729.
- (22) Hardman, N. J.; Abrams, M. B.; Pribisko, M. A.; Gilbert, T. M.; Martin, R. L.; Kubas, G. J.; Baker, R. T. *Angew. Chem. Int. Ed.* **2004**, *43*, 1955.
- (23) Burford, N.; Losier, P.; Sereda, S. V.; Cameron, T. S.; Wu, G. *J. Am. Chem. Soc.* **1994**, *116*, 6474.
- (24) Caputo, C. A.; Jennings, M. C.; Tuononen, H. M.; Jones, N. D. *Organometallics* **2009**, *28*, 990.
- (25) Pan, B.; Xu, Z.; Bezpalko, M. W.; Foxman, B. M.; Thomas, C. M. *Inorg. Chem.* **2012**, *51*, 4170.
- (26) Montemayor, R. G.; Sauer, D. T.; Fleming, S. S.; Bennett, D. W.; Thomas, M. G.; Parry, R. W. *J. Am. Chem. Soc.* **1978**, *100*, 2231.
- (27) Nakazawa, H. *J. Organomet. Chem.* **2000**, *611*, 349.
- (28) Rosenberg, L. *Coord. Chem. Rev.* **2012**, *256*, 606.
- (29) Burck, S.; Daniels, J.; Gans-Eichler, T.; Gudat, D.; Nättinen, K.; Nieger, M. *Z. Anorg. Allg. Chem.* **2005**, *631*, 1403.
- (30) Breit, B. *Chem. Commun.* **1996**, 2071.
- (31) Sakakibara, K.; Yamashita, M.; Nozaki, K. *Tetrahedron Lett.* **2005**, *46*, 959.
- (32) Breit, B. *J. Mol. Catal. A: Chem.* **1999**, *143*, 143.
- (33) SooHoo, C. K.; Baxter, S. G. *J. Am. Chem. Soc.* **1983**, *105*, 7443.

- (34) Cowley, A. H.; Kemp, R. A.; Lasch, J. G.; Norman, N. C.; Stewart, C. A. *J. Am. Chem. Soc.* **1983**, *105*, 7444.
- (35) Cowley, A. H.; Kemp, R. A.; Lasch, J. G.; Norman, N. C.; Stewart, C. A.; Whittlesey, B. R.; Wright, T. C. *Inorg. Chem.* **1986**, *25*, 740.
- (36) Boyd, R. J.; Burford, N.; Macdonald, C. L. B. *Organometallics* **1998**, *17*, 4014.
- (37) Cowley, A. H.; Stewart, C. A.; Whittlesey, B. R.; Wright, T. C. *Tetrahedron Lett.* **1984**, *25*, 851.
- (38) Fongers, K. S.; Hogeveen, H.; Kingma, R. F. *Tetrahedron Lett.* **1983**, *24*, 643.
- (39) Breslow, R.; Deuring, L. A. *Tetrahedron Lett.* **1984**, *25*, 1345.
- (40) Marre, M.-R.; Sanchez, M.; Wolf, R. *J. Chem. Soc., Chem. Commun.* **1984**, 566.
- (41) Krossing, I.; Raabe, I. *Angew. Chem. Int. Ed.* **2001**, *40*, 4406.
- (42) Weigand, J. J.; Holthausen, M.; Fröhlich, R. *Angew. Chem. Int. Ed.* **2009**, *48*, 295.
- (43) Weigand, J. J.; Burford, N.; Lumsden, M. D.; Decken, A. *Angew. Chem. Int. Ed.* **2006**, *45*, 6733.
- (44) Bouhadir, G.; Reed, R. W.; Réau, R.; Bertrand, G. *Heteroat. Chem.* **1995**, *6*, 371.
- (45) Weigand, J. J.; Feldman, K.-O.; Henne, F. D. *J. Am. Chem. Soc.* **2010**, *132*, 16321.
- (46) Petušková, J.; Patil, M.; Holle, S.; Lehmann, C. W.; Thiel, W.; Alcarazo, M. *J. Am. Chem. Soc.* **2011**, *133*, 20758.
- (47) For examples of four-membered NHPs, see: (a) Scherer, O. J.; Schnabl, G. *Chem. Ber.* **1976**, *109*, 2996. (b) Oberdörfer, R.; Nieger, M.; Niecke, E. *Chem. Ber.* **1994**, *127*, 2397. (c) Holthausen, M. H.; Richter, C.; Hepp, A.; Weigand, J. J. *Chem. Commun.* **2010**, *46*, 6921.
- (48) For examples of five-membered NHPs, see: (a) Barlos, K.; Nöth, H.; Wrackmeyer, B.; McFarlane, W. *J. Chem. Soc., Dalton Trans.* **1979**, 801. (b) Burford, N.; Dipchand, A. I.; Royan, B. W. *Acta Crystallogr., Sect. C: Cryst. Struct. Commun.* **1989**, *45*, 1485. (c) Wrackmeyer, B.; Schiller, J. Z. *Naturforsch., B: Chem. Sci.* **1992**, *47*, 662. (d) Carmalt, C. J.; Lomeli, V.; McBurnett, B. G.; Cowley, A. H. *Chem. Commun.* **1997**, 2095. (e) Jones, V. A.; Thornton-Pett, M.; Kee, T. P. *Chem. Commun.* **1997**, 1317. (f) Caputo, C. A.; Brazeau, A. L.; Hynes, Z.; Price, J. T.; Tuononen, H. M.; Jones, N. D. *Organometallics* **2009**, *28*, 5261. (g) Schmid, D.; Bubrin, D.; Förster, D.; Nieger, M.; Roeben, E.; Strobel, S.; Gudat, D. *C. R. Chimie* **2010**, *13*, 998. (h) Day, G. S.; Pan, B.; Kellenberger, D. L.; Foxman, B. M.; Thomas, C. M. *Chem. Commun.* **2011**, *47*, 3634. (i) Price, J. T.; Lui, M.; Jones, N. D.; Ragogna, P. J. *Inorg. Chem.* **2011**, *50*, 12810. (j)

Vasudevan, K. V.; Findlater, M.; Vargas-Baca, I.; Cowley, A. H. *J. Am. Chem. Soc.* **2012**, *134*, 176.

(49) For examples of six-membered NHPs, see: (a) Noeth, H.; Ullmann, R. *Chem. Ber.* **1976**, *109*, 1942. (b) Ederer, B.; Ederle, H.; Noeth, H. *Chem. Ber.* **1992**, *125*, 2213. (c) Burford, N.; Conroy, K. D.; Landry, J. C.; Ragogna, P. J.; Ferguson, M. J.; McDonald, R. *Inorg. Chem.* **2004**, *43*, 8245. (d) Vidovic, D.; Lu, Z.; Reeske, G.; Moore, J. A.; Cowley, A. H. *Chem. Commun.* **2006**, 3501.

Chapter 2

2 A new approach to internal Lewis pairs featuring a phosphonium acid and a pyridine base^φ

2.1 Introduction

N-Heterocyclic phosphonium cations (NHPs) are analogous to the well known and widely exploited Arduengo type carbenes (NHCs).^{1,2} They have inverse electronic properties relative to NHCs, in that they are poor σ -donors but excellent π -acceptors, and it is the cationic nature of the system that dominates in the observed reactivity, which is underscored by their Lewis acidity.³

Typical frameworks for NHPs involve five- and six-membered rings with phosphorus being the lone reactive site. Universally, the focus of NHP chemistry has been to harness the utility of the low coordinate, cationic phosphorus centre only. There have been no reports of making multifunctional NHPs, where incorporation of additional functional groups on the ligand framework, proximal to phosphorus, could open the door to tandem or cooperative reactivity. Recent studies by Guan *et al.* involved the design of a unique bis(imino)acenaphthene (BIAN) derivative (**1**) featuring a tethered pyridine donor in an axial position relative to the *N,N'* BIAN chelate (Figure 2.1).⁴ This ligand not only has the diimine framework, for which there is developed and emerging chemistry for the p-block elements, but having the pyridine donor in such close proximity to the Lewis acidic phosphonium centre is anticipated to provide secondary reactivity to the Lewis amphoteric phosphorus.

^φ This work is published in Brazeau, A. L.; Caputo, C. A.; Martin, C. D.; Jones, N. D.; Ragona, P. J. *Dalton Trans.* **2010**, 39, 11069. Reproduced by permission of The Royal Society of Chemistry (RSC). See Appendix 2.2.

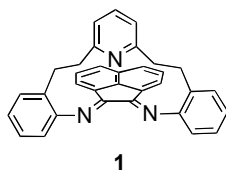


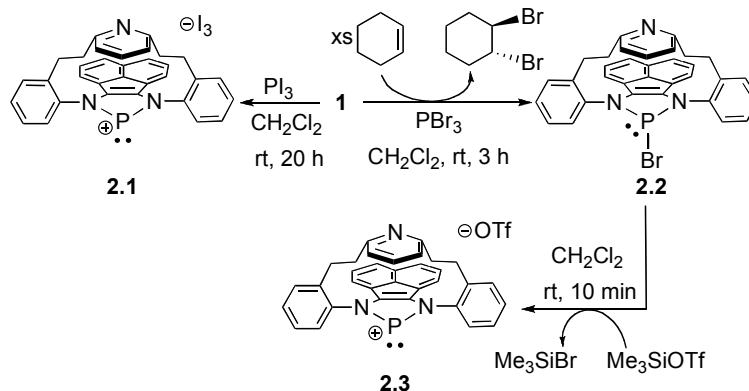
Figure 2.1: BIAN derivative featuring a pyridine donor (**1**).

In this context, we report the synthesis and characterization of a new bromophosphine and phosphonium cation utilizing the “clamshell” ligand **1**. This is the first application of such a system to the p-block and it represents the ability to access simultaneous Lewis acidic and basic chemistry within a phosphonium system. Coordination *to* BH_3 and *by* 4-dimethylaminopyridine (DMAP) demonstrates that both the empty π -orbital on P and the lone pair on the pyridine can be accessed

2.2 Results and discussion

2.2.1 Synthesis

The addition of a stoichiometric equivalent of PI_3 (in CH_2Cl_2) to a CH_2Cl_2 solution of **1** resulted in an immediate colour change from red and orange solutions, respectively, to a dark brown reaction mixture (Scheme 2.1).⁵ After no further colour change, an aliquot was taken for analysis by $^{31}\text{P}\{^1\text{H}\}$ NMR spectroscopy and revealed the complete consumption of PI_3 and the appearance of a downfield signal at $\delta_{\text{P}} = 230$ (*cf.* PI_3 , $\delta_{\text{P}} = 178$), which is consistent with the production of a phosphonium cation.^{5,6} The volatiles were removed *in vacuo* leaving a brown powder of **2.1**. A sample of the powder was redissolved and the $^{31}\text{P}\{^1\text{H}\}$ NMR spectrum of the sample gave an identical chemical shift to that observed in the reaction mixture. X-ray quality crystals (Figure 2.3) were grown from the bulk material in CH_2Cl_2 by liquid diffusion of Et_2O at $-30\text{ }^\circ\text{C}$. X-ray diffraction experiments confirmed that the phosphonium cation as an I_3^- salt was produced in essentially quantitative yield. While the reaction for **2.1** was clean and high yielding, further attempts to study the molecule resulted in undesirable reactivity with the triiodide anion, rather than with the cation, thus a new ion pairing was sought.

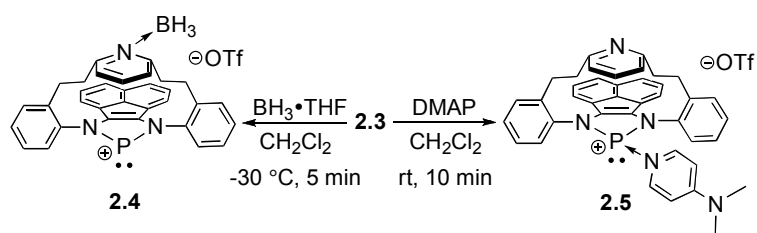


Scheme 2.1: Redox reactions for the synthesis of **2.1**, **2.2** and the halide abstraction reaction giving **2.3**.

The 1:1 stoichiometric reaction between PBr₃ and **1** in the presence of excess cyclohexene,⁷ yielded a red/brown solution (Scheme 2.1). Analysis of a sample of the reaction mixture showed a single resonance in the ³¹P{¹H} NMR spectrum at δ_P = 200, indicative of the production of **2.2**.⁷ Removal of the volatiles gave a deep red/brown solid, which was recrystallized from a 1:1 CH₂Cl₂/Et₂O solution. Single crystal X-ray diffraction studies (Figure 2.3) confirmed the production of **2.2**, isolated as a crystalline solid with a yield of 74%. Synthesis of the NHP triflate salt was achieved by the addition of a stoichiometric amount of Me₃SiOTf (OTf = [CF₃SO₃]⁻) to a CH₂Cl₂ solution of **2.2** (Scheme 2.1), which resulted in a colour change from red to orange. The reaction process was monitored using ³¹P{¹H} NMR spectroscopy, indicating that conversion was complete after 10 min by the disappearance of the signal for **2.2** and the appearance of a new downfield singlet at δ_P = 230, identical to the shift for the cation **2.1**. Identification of the triflate salt **2.3** was confirmed by X-ray diffraction experiments (Figure 2.3), where the salt was produced in quantitative yields. It should be noted that it was of the utmost importance to ensure that **2.2** was of exceptional purity by ¹H NMR spectroscopy before continuing with the halide abstraction, otherwise production of the NHP was unsuccessful.

With the bifunctional phosphonium cation in hand, the reactivity of **2.3** was probed to examine its propensity for dual reactivity (Scheme 2.2). To investigate the Lewis basic nature of the system, a reaction of excess BH₃•THF with **2.3** was carried out

in CH_2Cl_2 at $-30\text{ }^\circ\text{C}$ for 5 min; the colour of the solution changed from yellow to red. Monitoring the reaction progress by $^{31}\text{P}\{^1\text{H}\}$ NMR spectroscopy, showed only a slight change in the resonance for the phosphorus centre ($\delta_{\text{P}} = 228$). A bright yellow solid was precipitated from the reaction mixture using Et_2O , which was dried *in vacuo*. A sample of the bulk material was redissolved for ^1H NMR spectroscopy, which revealed a dramatic change in the signals for the ethyl tethers (Figure 2.2). Unlike the poorly resolved signals in **2.3**, after the reaction with borane, these signals became four well resolved doublet of doublets of doublets representing each of the CH_2 protons. In addition, a new broad proton signal, integrating to 3, at $\delta_{\text{H}} = 1.9$ was observed, indicative of BH_3 incorporation. The $^{11}\text{B}\{^1\text{H}\}$ NMR spectrum had a broad single peak at $\delta_{\text{B}} = -18.0$, consistent with a Lewis base adduct of BH_3 .^{8,9} Single crystals suitable for X-ray diffraction studies were grown from a $\text{CH}_2\text{Cl}_2/\text{Et}_2\text{O}$ solution at $-30\text{ }^\circ\text{C}$ (Figure 2.3) and confirmed the production of **2.4**, which was obtained in 62% yield.



Scheme 2.2: Lewis acidic and basic reactivity of **2.3**.

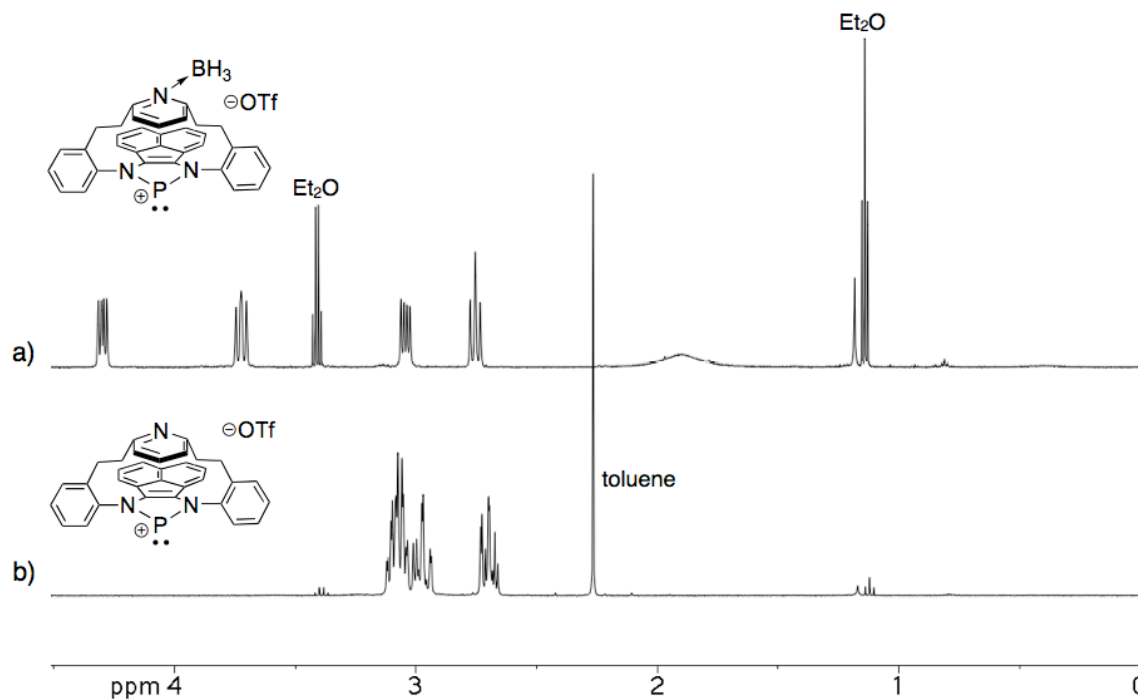


Figure 2.2: Stacked plot of ^1H NMR spectra (in CDCl_3) of the alkyl region for (a) **2.4** and (b) **2.3**.

To probe the retention of the Lewis acidic P centre, **2.3** was treated with the Lewis bases PMe_3 and pyridine. Monitoring these reaction mixtures by $^{31}\text{P}\{^1\text{H}\}$ and ^1H NMR spectroscopy indicated that no reaction had occurred. This was somewhat surprising, as NHPs are well known to form the corresponding complexes.¹⁰⁻¹³ The use of a stoichiometric amount of the strong σ -donor DMAP (Scheme 2.2) resulted in an instant colour change from yellow to deep red/purple and an upfield chemical shift in the $^{31}\text{P}\{^1\text{H}\}$ NMR spectrum ($\delta_{\text{P}} = 170$, $\Delta\delta_{\text{P}} = 60$). Variable temperature $^{31}\text{P}\{^1\text{H}\}$ NMR spectroscopy shifted the resonance even further upfield to a more phosphine-like chemical shift at $\delta_{\text{P}} = 131$ (-80 °C). Single crystals of the phosphonium–DMAP adduct were grown by vapour diffusion of Et_2O into a concentrated CDCl_3 solution at room temperature and were used in X-ray diffraction studies which confirmed the Lewis acid–base adduct **2.5** (Figure 2.3).

2.2.2 X-ray crystallography

All compounds (**2.1-2.5**) have been characterized by single crystal X-ray diffraction studies. Selected bond lengths (Å) and bond angles (°) are given in Table 2.1. Refinement details are summarized in Table 2.2.

Examination of the solid-state structures revealed that the metrical parameters for the C₂N₂P five-membered ring were consistent with two C–N single bonds (1.357(4)–1.409(6) Å, compared to 1.272(3) Å (avg), double bonds in the free ligand) and a C–C double bond (1.357(6)–1.383(9) Å vs. 1.517(3) Å in **1**).⁴ The lengthening of C–N and shortening of C–C bonds were congruous with a two-electron reduction of the BIAN fragment as expected for the cyclization reactions of **2.1** and **2.2**.⁷

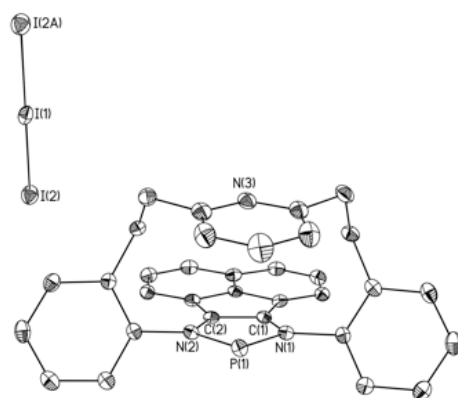
Unlike compound **1**, the tethered pyridine ring in all the solid-state structures adopted a conformation of lying almost coplanar (interplanar angle: 8.3–19.3°) to the BIAN framework, whereas in **1** it was situated perpendicular to the BIAN plane and is an interestingly substantial deviation of the ligand behaviour from the Pd complex, which retained the perpendicular orientation.⁴

Compound **2.2** featured a characteristically long P–Br bond (2.686(2) Å) common to 2-bromo-1,3-diaryl-1,3,2-diazaphospholenes (*ca.* 2.43–2.95 Å) attributed to the hyperconjugation of $\pi(\text{C}_2\text{N}_2)\text{--}\sigma^*(\text{P--X})$.^{2,7,14,15} The phosphorus atom was pyramidal ($\Sigma_{\text{ang}} = 292.8^\circ$), as expected for a three-coordinate phosphorus centre with a lone pair.

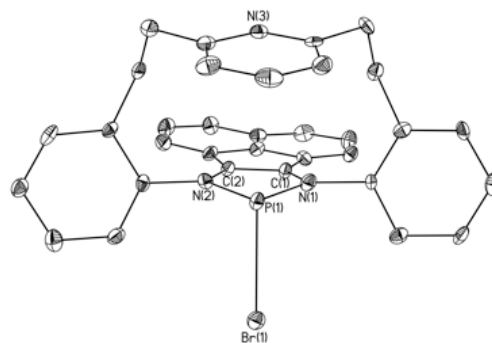
The closest phosphorus-oxygen contact in the solid-state for the cation-anion pair in **2.3** was 3.06 Å, which is shorter than the van der Waals distance of 3.35 Å for a P–O interaction, indicating a weak cation-anion interaction in the solid-state.

The nitrogen-boron bond in **2.4** (N(3)–B(1) 1.627(6) Å) was within the range of observed σ donations of nitrogen to BH₃ (1.56–1.66 Å).^{8,9} The added steric bulk of BH₃ caused the plane of the pyridine ring to deviate from being parallel with the BIAN plane by 19.3° and was tilted by 5.0° from **2.3**.

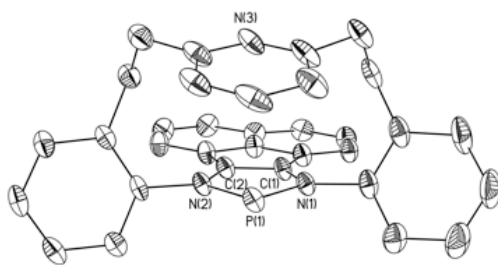
In **2.5** the P(1)–N(4) bond length was within the range of P–N_{DMAP} dative bonds (1.854(3) *cf.* 1.774(2)–1.879(2) Å).^{16,17} The DMAP adduct maximum deviation (0.08 Å) from planarity increased within the C₂N₂P ring.



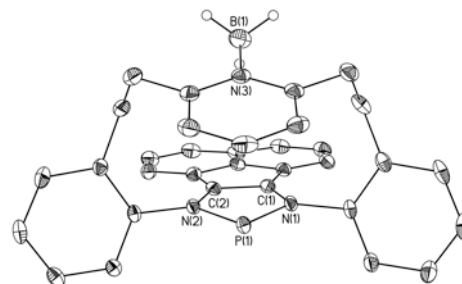
2.1



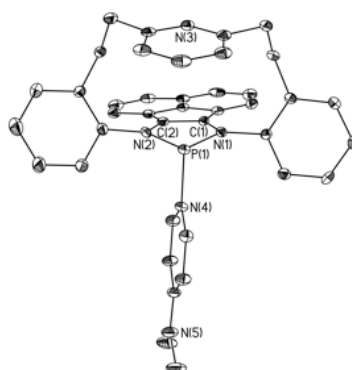
2.2



2.3



2.4



2.5

Figure 2.3: Solid-state structures of **2.1–2.5**. Ellipsoids are drawn to 30% probability. Non-essential hydrogen atoms, solvate molecules and counteranions are omitted for clarity.

Table 2.1: Selected metrical parameters for **2.1-2.5**. Bond lengths are in angstroms (Å) and bond angles in degrees (°).

Bond \ Compound	2.1	2.2 X = Br, n = 1	2.3	2.4	2.5 X = N, n = 4
P(1)–N(1)	1.691(5)	1.678(8)	1.688(3)	1.680(3)	1.697(4)
P(1)–N(2)	1.684(5)	1.683(6)	1.686(2)	1.680(3)	1.703(4)
C(1)–C(2)	1.377(9)	1.383(9)	1.376(4)	1.377(5)	1.357(6)
N(1)–C(1)	1.359(8)	1.384(8)	1.364(4)	1.364(4)	1.409(6)
N(2)–C(2)	1.364(8)	1.397(8)	1.365(4)	1.357(4)	1.402(6)
P(1)–X(n)	–	2.686(2)	–	–	1.854(3)
N(3)–B(1)	–	–	–	1.627(6)	–
N(1)–P(1)–N(2)	90.3(3)	90.1(3)	89.97(12)	90.06(14)	90.68(18)
N(1)–P(1)–X(n)	–	101.0(3)	–	–	103.26(18)
N(2)–P(1)–X(n)	–	101.7(2)	–	–	99.20(18)

Table 2.2: X-ray details for **2.1-2.5**.

Compound	2.1	2.2	2.3	2.4	2.5
Empirical formula	C ₃₄ H ₂₇ Cl ₂ I ₃ N ₃ P ₁	C _{34.50} H ₂₇ Br ₁ Cl ₃ N ₃ P ₁	C ₃₄ H ₂₅ F ₃ N ₃ O ₃ P ₁ S ₁	C ₇₃ H ₆₆ B ₂ Cl ₂ F ₆ N ₆ O ₇ P ₂ S ₂	C ₄₂ H ₃₅ Cl ₂ F ₃ N ₅ O ₃ P ₁ S ₁
FW (g/mol)	960.16	700.82	643.6	1471.9	848.68
Crystal system	Triclinic	Orthorhombic	Triclinic	Triclinic	Orthorhombic
Space group	<i>P</i> $\bar{1}$	<i>Pna</i> 2 ₁	<i>P</i> $\bar{1}$	<i>P</i> $\bar{1}$	<i>P</i> 2 ₁ 2 ₁
<i>a</i> (Å)	10.811(2)	21.0725(6)	15.975(3)	12.260(3)	10.5053(5)
<i>b</i> (Å)	12.371(3)	14.0248(4)	16.350(3)	14.962(3)	17.6658(8)
<i>c</i> (Å)	13.303(3)	22.0431(6)	16.581(3)	19.811(4)	22.5701(11)
<i>a</i> (deg)	82.17(3)	90	117.72(3)	88.78(3)	90
<i>b</i> (deg)	82.44(3)	90	105.64(3)	77.03(3)	90
<i>g</i> (deg)	77.46(3)	90	103.78(3)	83.08(3)	90
<i>V</i> (Å ³)	1711.0(6)	6514.6(3)	3338.7(12)	3515.5(12)	4188.7(3)
<i>Z</i>	2	8	4	2	4
<i>D_c</i> (mg m ⁻³)	1.864	1.429	1.28	1.39	1.346
<i>R</i> 1[<i>I</i> > 2σ <i>I</i>] ^a	0.0457	0.0601	0.0642	0.0588	0.0668
<i>wR</i> 2(<i>F</i> ²) ^a	0.1348	0.1712	0.1647	0.1396	0.1756
GOF (<i>S</i>) ^a	1.198	1.058	1.096	1.028	1.055

^a $R1(F[I > 2(I)]) = \sum || |F_o| - |F_c| || / \sum |F_o|$; $wR2(F^2 [all data]) = [w(F_o^2 - F_c^2)^2]^{1/2}$; $S(all data) = [w(F_o^2 - F_c^2)^2 / (n - p)]^{1/2}$ (n = no. of data; p = no. of parameters varied; $w = 1 / [\sigma^2(F_o^2) + (aP)^2 + bP]$ where $P = (F_o^2 + 2F_c^2) / 3$ and a and b are constants suggested by the refinement program.

2.3 Conclusions

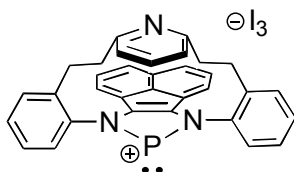
We have synthesized a new NHP with a BIAN framework featuring a tethered pyridine, which represents the first example of this framework with a p-block element. The amphoteric NHP has shown dual reactivity towards a Lewis acid and base.

2.4 Experimental section

General synthetic and crystallography experimental details can be found in Appendix 1.

2.4.1 Synthetic procedures

Compound 2.1



A solution of **1** (0.399 g, 0.860 mmol) in CH₂Cl₂ (4 mL) was added dropwise to a solution of PI₃ (0.354 g, 0.860 mmol) in CH₂Cl₂ (4 mL) over 20 min. The dark brown reaction mixture was stirred for 20 h at rt. The solvent was removed *in vacuo*.

The resulting brown powder was washed with Et₂O (3 x 3 mL) and dried *in vacuo*.

Yield: 84% (0.635 g, 0.725 mmol);

d.p.: 175-177 °C;

¹H NMR: δ 8.16 (d, 2H, *aryl*, ³J_{H-H} = 8.0), 7.92 (d, 2H, *aryl*, ³J_{H-H} = 8.4), 7.72 (m, 4H, *aryl*), 7.59 (dt, 2H, *aryl*, ³J_{H-H} = 8.0, ⁴J_{H-H} = 2.0), 7.49 (dd, 2H, *aryl*, ³J_{H-H} = 8.4, ³J_{H-H} = 7.2), 7.30 (t, 1H, *aryl*, ³J_{H-H} = 7.6), 7.05 (d, 2H, *aryl*, ³J_{H-H} = 6.8), 6.68 (d, 2H, *aryl*, ³J_{H-H} = 7.6), 3.18 (m, 4H, CH₂), 3.09 (m, 2H, CH₂), 2.83 (m, 2H, CH₂);

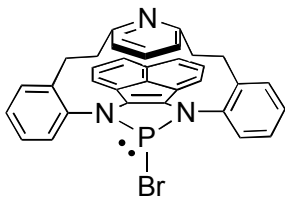
¹³C{¹H} NMR: δ 160.9, 143.7, 138.7 (d, ³J_{13C-P} = 3.8 Hz), 138.4 (d, ³J_{13C-P} = 3.8), 132.5, 132.4, 132.1, 131.9, 130.5, 130.1, 129.0, 128.3, 127.2 (d, ²J_{13C-P} = 4.8), 125.1 (d, ²J_{13C-P} = 4.5), 123.3 (d, ³J_{13C-P} = 1.5), 122.4 (d, ³J_{13C-P} = 2.7), 41.2, 31.4;

³¹P{¹H} NMR: δ 230 (s);

FT-IR (cm⁻¹(relative intensities)): 486(10), 725(13), 745(4), 764(1), 797(8), 819(5), 1037(15), 1144(14), 1221(12), 1261(9), 1345(11), 1412(7), 1437(2), 1448(3), 1487(6);

FT-Raman (cm⁻¹(relative intensities)): 117(1), 138(2), 168(3), 214(6), 361(8), 405(7), 487(13), 563(10), 956(5), 1210(12), 1344(15), 1436(11), 1471(9), 1609(4), 3059(14).

Compound 2.2



Phosphorus(III) bromide (107 μL , 1.14 mmol) and cyclohexene (691 μL , 6.82 mmol) were sequentially added dropwise to a solution of **1** (0.527 g, 1.14 mmol) in CH_2Cl_2 (10 mL). The dark red solution was stirred at rt for 3 h. The solvent was removed *in vacuo* to give a red solid, which was washed with Et_2O (3 x 3 mL) and dried. The crude material was then redissolved in CH_2Cl_2 (10 mL) and Et_2O (10 mL) was added to the solution, which was stored overnight at $-20\text{ }^\circ\text{C}$, yielding a crop of crystals.

Yield: 74% (0.483 g, 0.841 mmol);

m.p.: 268-271 $^\circ\text{C}$;

^1H NMR: δ 8.32 (d, 2H, *aryl*, $^3J_{\text{H-H}} = 7.6$), 7.64 (d, 2H, *aryl*, $^3J_{\text{H-H}} = 8.4$), 7.55 (m, 4H, *aryl*), 7.43 (m, 2H, *aryl*), 7.26 (t, 2H, *aryl*, $^3J_{\text{H-H}} = 7.2$), 7.06 (t, 1H, *aryl*, $^3J_{\text{H-H}} = 7.6$), 6.73 (d, 2H, *aryl*, $^3J_{\text{H-H}} = 7.2$), 6.48 (d, 2H, *aryl*, $^3J_{\text{H-H}} = 7.6$), 3.16 (m, 6H, CH_2), 2.79 (m, 2H, CH_2);

$^{13}\text{C}\{^1\text{H}\}$ NMR: δ 160.7, 139.8 (d, $^2J_{13\text{C-P}} = 5.7$), 137.4 (d, $^3J_{13\text{C-P}} = 3.9$), 134.8, 134.7, 131.4, 130.3, 130.2, 129.0, 128.0, 127.9, 127.6, 127.5 (d, $^3J_{13\text{C-P}} = 3.0$), 127.0 (d, $^2J_{13\text{C-P}} = 7.3$), 121.5 (d, $^3J_{13\text{C-P}} = 2.5$), 120.9, 41.3, 31.5;

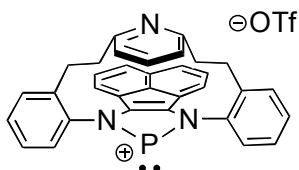
$^{31}\text{P}\{^1\text{H}\}$ NMR: δ 200 (s);

FT-IR (cm^{-1} (relative intensities)): 720(13), 734(10), 749(7), 767(1), 781(4), 817(6), 980(8), 1151(14), 1269(15), 1361(9), 1450(2), 1466(3), 1490(5), 1571(12), 1587(11);

FT-Raman (cm^{-1} (relative intensities)): 175(11), 215(15), 564(6), 735(12), 953(4), 981(1), 1044(14), 1210(8), 1260(9), 1342(13), 1439(7), 1469(5), 1521(2), 1611(3), 3062(10);

HRMS: $\text{C}_{33}\text{H}_{25}\text{N}_3\text{P}_1^+$ calcd (found) 494.1786 (494.1791).

Compound 2.3



To a red solution of **2.2** (0.654 g, 1.14 mmol) in CH_2Cl_2 (5 mL) the halide abstracting agent Me_3SiOTf (200 μL , 1.14 mmol) was added dropwise. The orange reaction mixture was stirred at rt for 10 min. The volatiles were removed *in vacuo*. The product was washed with Et_2O (2 x 3 mL) and dried under reduced pressure.

Yield: 95% (0.691 g, 1.07 mmol);

d.p.: 151-154 °C;

¹H NMR: δ 8.09 (d, 2H, *aryl*, ³*J*_{H-H} = 8.0), 7.91 (d, 2H, *aryl*, ³*J*_{H-H} = 8.0), 7.70 (m, 4H, *aryl*), 7.55 (dt, 2H, *aryl*, ³*J*_{H-H} = 8.4, ⁴*J*_{H-H} = 2.0), 7.47 (dd, 2H, *aryl*, ³*J*_{H-H} = 7.6, ³*J*_{H-H} = 6.8), 7.25 (t, 1H, *aryl*, ³*J*_{H-H} = 7.6), 7.04 (d, 2H, *aryl*, ³*J*_{H-H} = 6.8), 6.62 (d, 2H, *aryl*, ³*J*_{H-H} = 7.6), 3.15 (m, 2H, *CH*₂), 3.06 (m, 2H, *CH*₂), 2.78 (m, 2H, *CH*₂);

¹³C{¹H} NMR: δ 161.1, 143.7, 138.3 (d, ³*J*_{13C-P} = 3.6), 138.1 (d, ³*J*_{13C-P} = 4.1), 133.4, 132.2, 132.1, 131.7, 130.5, 130.0, 129.1, 128.2, 128.1 (d, ²*J*_{13C-P} = 5.5), 124.8 (d, ²*J*_{13C-P} = 4.3), 123.2, 122.3, 41.3, 31.4;

³¹P{¹H} NMR: δ 230 (s);

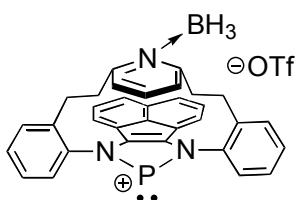
¹⁹F{¹H} NMR: δ -78.5 (s);

FT-IR (cm⁻¹(relative intensities)): 517(7), 571(13), 637(2), 733(12), 768(4), 801(15), 823(8), 1028(1), 1153(5), 1222(10), 1279(3), 1349(11), 1458(6), 1489(9), 1558(14);

FT-Raman (cm⁻¹(relative intensities)): 176(8), 213(14), 563(5), 731(13), 956(1), 976(6), 1028(10), 1212(9), 1255(11), 1344(12), 1415(15), 1437(4), 1483(3), 1614(2), 3061(7);

HRMS: C₃₃H₂₅N₃P₁⁺ calcd (found) 494.1786 (494.1782).

Compound 2.4



A solution of **2.3** (0.0730 g, 0.113 mmol) in CH₂Cl₂ (7 ml) and BH₃·THF (1.0 M in THF, 0.340 mL, 0.340 mmol) were cooled to -30 °C. With rapid stirring, BH₃·THF was added quickly to the CH₂Cl₂ solution of **2.3**. Diethyl ether (5 mL) was then

added with rapid stirring, which resulted in the precipitation of a yellow solid. The supernatant was decanted and the discoloured yellow precipitate was dried *in vacuo*. The powder was washed with Et₂O (3 x 3 mL) and dried *in vacuo*, yielding a yellow powder.

Yield: 62% (0.0456 g, 0.0698 mmol);

d.p.: 166-169 °C;

¹H NMR (CD₂Cl₂): δ 8.08 (d, 2H, *aryl*, ³*J*_{H-H} = 8.4), 7.82 (m, 6H, *aryl*), 7.59 (m, 3H, *aryl*), 7.31 (d, 2H, *aryl*, ³*J*_{H-H} = 6.8), 6.96 (d, 2H, *aryl*, ³*J*_{H-H} = 8.0), 4.32 (ddd, 2H, *CH*,

$^2J_{\text{H-H}} = 13.2$, $^3J_{\text{H-H}} = 7.6$, $^4J_{\text{H-H}} = 1.2$), 3.80 (t, 2H, CH, $^2J_{\text{H-H}} = 13.2$), 3.14 (ddd, 2H, CH, $^2J_{\text{H-H}} = 14.8$, $^3J_{\text{H-H}} = 7.6$, $^4J_{\text{H-H}} = 1.6$), 2.85 (t, 2H, CH, $^2J_{\text{H-H}} = 13.6$), 1.89 (br, 3H, BH₃);

$^{13}\text{C}\{^1\text{H}\}$ NMR (CD₂Cl₂): δ 161.8, 145.2, 141.4 (d, $^3J_{13\text{C-P}} = 4.9$), 138.2 (d, $^3J_{13\text{C-P}} = 3.8$), 133.5, 133.2, 132.3, 132.1, 131.8, 130.7, 129.7, 128.9, 128.2 (d, $^2J_{13\text{C-P}} = 6.3$), 127.7 (d, $^3J_{13\text{C-P}} = 2.8$), 124.7 (d, $^2J_{13\text{C-P}} = 4.4$), 124.4, 41.2, 28.8;

$^{31}\text{P}\{^1\text{H}\}$ NMR (CD₂Cl₂): δ 228 (s);

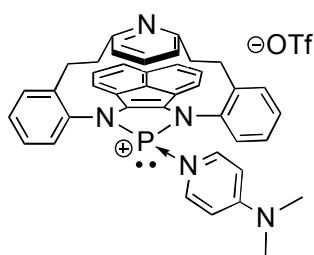
$^{19}\text{F}\{^1\text{H}\}$ NMR (CD₂Cl₂): δ -79.3 (s);

$^{11}\text{B}\{^1\text{H}\}$ NMR (CD₂Cl₂): δ -18.0 (br);

FT-IR (cm⁻¹(relative intensities)): 517(9), 563(13), 637(3), 750(14), 771(5), 825(8), 1030(2), 1152(6), 1222(10), 1259(1), 1416(11), 1470(4), 1493(15), 1610(7), 2371(12);

FT-Raman (cm⁻¹(relative intensities)): 209(9), 359(14), 564(4), 731(10), 798(15), 956(2), 1030(11), 1213(8), 1253(12), 1344(6), 1416(7), 1437(5), 1473(3), 1614(1), 3061(13).

Compound 2.5



A solution of DMAP (0.0177 g, 0.145 mmol) in CH₂Cl₂ (2 mL) was added dropwise to a CH₂Cl₂ solution (4 mL) of **2.3** (0.0935 g, 0.145 mmol). The colour of the solution changed from orange to red/purple upon addition of the DMAP. The reaction mixture was stirred for 10 min at rt and then the

volatiles were removed *in vacuo* yielding a dark purple wax. The wax was washed with Et₂O (2 x 3 mL) and dried under reduced pressure to yield a purple solid, which was redissolved in CH₂Cl₂ and precipitated by the addition of Et₂O. The mixture was held at -30 °C overnight after which the mother liquor was removed and the purple solid was dried *in vacuo*.

Yield: 76% (0.0844 g, 0.110 mmol);

m.p.: 158-162 °C;

^1H NMR: δ 8.09 (d, 2H, aryl, $^3J_{\text{H-H}} = 6.8$), 7.71 (d, 2H, aryl, $^3J_{\text{H-H}} = 8.4$), 7.58 (m, 4H, aryl), 7.35 (m, 4H, aryl), 7.19 (t, 1H, aryl, $^3J_{\text{H-H}} = 7.6$), 6.83 (d, 2H, aryl, $^3J_{\text{H-H}} = 6.8$), 6.72 (d, 2H, aryl, $^3J_{\text{H-H}} = 7.2$), 6.54 (d, 2H, aryl, $^3J_{\text{H-H}} = 7.6$), 3.30 (m, 2H, CH₂), 3.17 (m, 4H, CH₂), 3.15 (s, 6H, CH₃), 2.81 (m, 2H, CH₂);

$^{13}\text{C}\{^1\text{H}\}$ NMR: δ 160.7, 156.5, 143.6, 139.6 (d, $^3J_{13\text{C-P}} = 4.8$ Hz), 137.8, 137.7 (d, $^3J_{13\text{C-P}} = 3.9$), 134.0 (d, $^2J_{13\text{C-P}} = 13.3$), 132.1, 130.5, 130.2, 129.0, 128.6 (d, $^2J_{13\text{C-P}} = 12.1$), 127.8, 127.0 (d, $^2J_{13\text{C-P}} = 6.2$), 126.9 (d, $^3J_{13\text{C-P}} = 2.1$), 121.5 (d, $^3J_{13\text{C-P}} = 2.2$), 121.4, 107.9, 41.4, 40.1, 31.6;

$^{31}\text{P}\{^1\text{H}\}$ NMR: δ 170 (br);

$^{19}\text{F}\{^1\text{H}\}$ NMR: δ -78.5 (s);

FT-IR (cm^{-1} (relative intensities)): 515(15), 637(4), 764(10), 817(13), 968(11), 1008(8), 1031(2), 1150(6), 1223(7), 1269(1), 1350(12), 1459(5), 1491(14), 1555(9), 1635(3);

FT-Raman (cm^{-1} (relative intensities)): 168 (5), 442(15), 565(7), 762(14), 951(11), 968(4), 1033(10), 1206(13), 1259(12), 1391(6), 1441(9), 1461(2), 1554(3), 1607(1), 3063(8).

2.5 References

- (1) Arduengo, A. J., III; Harlow, R. L.; Kilne, M. *J. Am. Chem. Soc.* **1991**, *113*, 361.
- (2) Gudat, D.; Haghverdi, A.; Hupfer, H.; Nieger, M. *Chem. Eur. J.* **2000**, *6*, 3414.
- (3) Tuononen, H. M.; Roesler, R.; Dutton, J. L.; Ragona, P. J. *Inorg. Chem.* **2007**, *46*, 10693.
- (4) Leung, D. H.; Ziller, J. W.; Guan, Z. *J. Am. Chem. Soc.* **2008**, *130*, 7538.
- (5) Reeske, G.; Hoberg, C. R.; Hill, N. J.; Cowley, A. H. *J. Am. Chem. Soc.* **2006**, *128*, 2800.
- (6) Cowley, A. H.; Kemp, R. A. *Chem. Rev.* **1985**, *85*, 367.
- (7) Dube, J. W.; Farrar, G. J.; Norton, E. L.; Szekely, K. L. S.; Cooper, B. F. T.; Macdonald, C. L. B. *Organometallics* **2009**, *28*, 4377.
- (8) Ainscough, E. W.; Brodie, A. M.; Lowe, A. D.; Waters, J. M. *Inorg. Chim. Acta* **2000**, *303*, 128.
- (9) Dupart, J.-M.; Grand, A.; Pace, S.; Riess, J. G. *Inorg. Chem.* **1984**, *23*, 3776.
- (10) Kopp, R. W.; Bond, A. C.; Parry, R. W. *Inorg. Chem.* **1976**, *15*, 3042.
- (11) Schultz, C. W.; Parry, R. W. *Inorg. Chem.* **1976**, *15*, 3046.
- (12) Abrams, M. B.; Scott, B. L.; Baker, R. T. *Organometallics* **2000**, *19*, 4944.
- (13) Burford, N.; Ragona, P. J. *J. Chem. Soc., Dalton Trans.* **2002**, 4307.
- (14) Caputo, C. A.; Brazeau, A. L.; Hynes, Z.; Price, J. T.; Tuononen, H. M.; Jones, N. D. *Organometallics* **2009**, *28*, 5261.
- (15) Burck, S.; Gudat, D.; Nieger, M.; Benkő, Z.; Nyulászi, L. *Z. Anorg. Allg. Chem.* **2009**, *635*, 245.
- (16) Burford, N.; Spinney, H. A.; Ferguson, M. J.; McDonald, R. *Chem. Commun.* **2004**, 2696.
- (17) Davidson, R. J.; Weigand, J. J.; Burford, N.; Cameron, T. S.; Decken, A.; Werner-Zwanziger, U. *Chem. Commun.* **2007**, 4671.

Chapter 3

3 Chemistry of the heavy group 15 elements with the “clamshell” ligand^φ

3.1 Introduction

The reduction of pnictogen(III) (pnictogen = Pn = P, As) halides to yield Pn(I) centres has been known for many years, underscored by the pioneering work of Schmidpeter *et al.* who demonstrated that PCl₃ could be reduced in the presence of chelating or monodentate phosphines to produce triphosphenium cations (Chapter 1, Section 1.3.4.1).¹ More recently, Macdonald *et al.* have shown that low oxidation state Pn(I) compounds can be isolated without the use of an external reductant.² It was subsequently illustrated that ligand exchange reactions could be performed at the Pn(I) centre and these types of molecules could be considered sources of Pn(I).³ It has also been reported by Cowley *et al.* as well as our group, that the diiminopyridine (DIMPY) N-based ligand can be used in the isolation of Pn(I) cations.^{4,5}

Both Cowley and Macdonald have illustrated that α -diimines, such as 1,4-diaza-1,3-butadiene (DAB) and 1,2-bis(imino)acenaphthene (BIAN),⁶⁻⁸ can also be used in the stabilization of Pn centres, however the difference between the chelating phosphines and the DAB or BIAN ligands, is that the latter two can be easily reduced.⁹ The ability to reduce the N=C–C=N backbone of these ligand systems is a consequence of the low energy LUMOs, that can formally accept two electrons from the putative Pn(I) centre, in contrast to the DIMPY class, where no redox activity is observed. Although no mechanistic investigations have been completed, it is likely that a similar pathway to the Pn(I) systems with non-reducing ligands can be invoked, where the reduction/oxidation occurs after chelation of the pnictogen atom (refer to Chapter 1, Section 1.3.4.1).^{8,10} This synthetic route has proven to be a facile approach to making *N*-heterocyclic phosphonium cations.^{6-8,11,12} In our quest to make the analogous *N*-heterocyclic arsenium cations, we

^φ This work is published in Brazeau, A. L.; Jones, N. D.; Ragona, P. J. *Dalton Trans.* **2012**, DOI: 10.1039/c2dt30171g. Reproduced by permission of The Royal Society of Chemistry (RSC). See Appendix 2.2.

found the previously reported redox routes^{4,6} to be insufficient with our ligand of choice, pyridyl tethered 1,2-bis(imino)acenaphthene “clamshell” (**1**),¹³ because of unwanted by-products and the tendency of SnCl_5^- and I_3^- counteranions, generated during the chemistry, to be reactive in onward transformations.

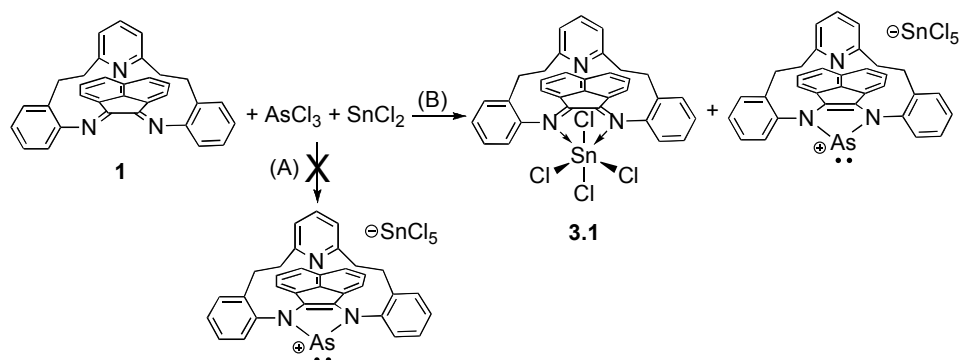
In this context, this chapter focuses on the one-electron reductant cobaltocene in the facile synthesis of *N*-heterocyclic chloropnictogens (Pn = P, As) as precursors to *N*-heterocyclic pnictenium cations (NHPn). Simple halide abstraction reactions give the NHPn with tailored counteranions. While the analogous redox reaction with Sb(III) and Bi(III) does not give Sb(I) or Bi(I), the “clamshell” ligand can be used as a donor to the Lewis acidic heavy pnictogen trichloride (Pn = Sb, Bi) and the corresponding dichloropnictenium cations. This work presents a new convenient redox route in the synthesis of *N*-heterocyclic chlorophosphines and chloroarsines.

3.2 Results and discussion

3.2.1 Synthesis

The addition of **1** to an equimolar solution of AsCl_3 and SnCl_2 in THF (Scheme 3.1) resulted in a colour change from colourless to brown/yellow. Removal of the volatiles gave a dark yellow solid, which was redissolved in CH_2Cl_2 and centrifuged to remove an insoluble black solid. The yellow solution was dried *in vacuo* and a sample of the yellow powder taken for analysis by ^1H NMR spectroscopy, which revealed the presence of two products, neither of which were the starting material **1** (Figure 3.1). Slow evaporation of a CH_2Cl_2 solution of the bulk crude material at room temperature produced X-ray quality orange crystals. X-ray diffraction studies revealed that one of the products was a hypervalent Sn centre, of **1** coordinating to SnCl_4 (**3.1**). Several of the orange crystals were redissolved in CDCl_3 and examined by ^1H NMR spectroscopy, showing a perfect match to one set of signals in the ^1H NMR spectrum of the crude material. The supernatant from the first crop of crystals was dried *in vacuo* and a ^1H NMR spectrum collected, which revealed that the mother liquor contained mostly the second product with a small amount of **3.1** remaining. The synthesis of **3.1** was also confirmed by the 1:1 stoichiometric reaction of **1** with SnCl_4 , which gave an identical ^1H NMR spectrum.

Despite numerous recrystallization attempts, crystalline material of the second product could not be obtained, but was likely the anticipated arsenium cation paired with the $[\text{SnCl}_5]^-$ anion. The reduction of AsCl_3 by SnCl_2 clearly took place, given that SnCl_4 was produced. Nevertheless this reaction route was undesirable given that two products were formed, thus an alternate route was sought.



Scheme 3.1: Anticipated (A) and observed (B) reactivity of **1** with AsCl_3 and SnCl_2 .

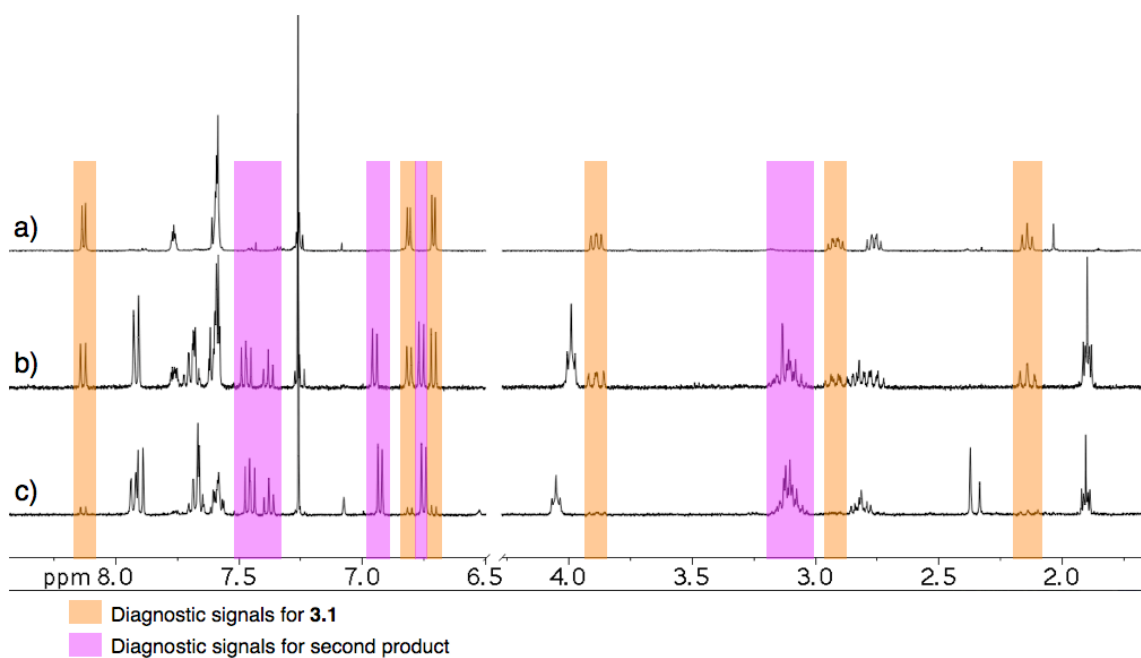
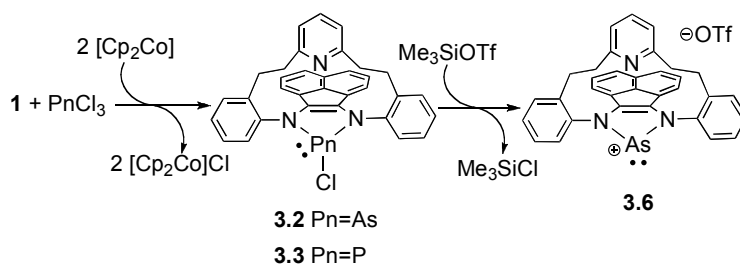


Figure 3.1: Stacked plot of the ^1H NMR spectra for the reaction of **1**, AsCl_3 and SnCl_2 : (a) crystals of **3.1**; (b) crude material; and, (c) supernatant.

Cobaltocene (Cp_2Co) is a well-known one-electron reductant and two stoichiometric equivalents of Cp_2Co were used in the reaction of AsCl_3 and **1** in THF (Scheme 3.2). The addition of Cp_2Co resulted in the immediate precipitation of a green solid from the purple solution. The precipitated solid was removed by centrifugation, and the ^1H NMR spectrum of the precipitate in CDCl_3 revealed a single peak at $\delta_{\text{H}} = 5.90$, corresponding to $[\text{Cp}_2\text{Co}]\text{Cl}$. The volatiles were removed from the decanted solution *in vacuo* to yield a dark purple solid. The crude material was analyzed by ^1H NMR spectroscopy, which revealed one major product, integrating to the expected 17 protons, in 75% purity. The impurities were removed by recrystallization at $-35\text{ }^\circ\text{C}$ by liquid diffusion of Et_2O into a concentrated CH_2Cl_2 solution of the bulk material, giving pure **3.2** with a good overall yield of 72%. A major difference between the ^1H NMR spectra of free and reduced **1** is observed in the CH_2 bridging arms in the range of $\delta_{\text{H}} = 2.4\text{--}3.5$, which changed from three broad signals to four distinct doublet of doublet of doublets, in a 2:2:2:2 integration for **3.2**. There was also a noticeable change in the downfield shift of the resonance corresponding to the proton on the *para*-carbon of the pyridine ring ($\Delta\delta_{\text{H}} \approx 0.2$). X-ray quality single crystals could be obtained by the same recrystallization method used above. Given the clean, facile isolation of **3.2**, the analogous reactions with PCl_3 , SbCl_3 and BiCl_3 were attempted to determine if a universal cobaltocene redox route could be used with all the trichloropnictines ($\text{Pn} = \text{P}, \text{As}, \text{Sb}, \text{Bi}$) to obtain diaminochloropnictines.



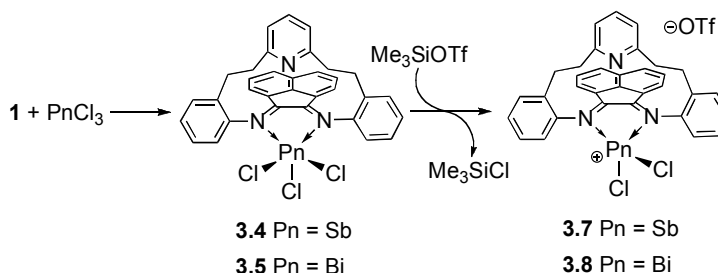
Scheme 3.2: Redox reactions for the synthesis of **3.2** and **3.3**, and the halide abstraction reaction giving **3.6**.

The 2:1:1 stoichiometric reaction of Cp_2Co , PCl_3 and **1**, respectively, resulted in the instantaneous precipitation of a green solid from a dark purple solution. An aliquot of

the reaction mixture was sampled after stirring at rt for 20 min and analyzed by $^{31}\text{P}\{^1\text{H}\}$ NMR spectroscopy, which showed one peak at $\delta_{\text{P}} = 179$ and no resonance for PCl_3 ($\delta_{\text{P}} = 220$). The volatiles were then removed from the aliquot *in vacuo* and the resulting dark purple solid was redissolved in CDCl_3 for analysis by ^1H NMR spectroscopy, which revealed three distinct products. There was a set of resonances assigned to unreacted **1**, a single peak at $\delta_{\text{H}} = 5.90$ (for $[\text{Cp}_2\text{Co}]\text{Cl}$), and a set of resonances belonging to the expected product **3.3**. The ratio for peaks belonging to **1** and **3.3** were 2:1, respectively. Given that all PCl_3 had been consumed in the reaction, as observed by $^{31}\text{P}\{^1\text{H}\}$ NMR spectroscopy, a side reaction between Cp_2Co and PCl_3 was postulated to have occurred. The addition of more PCl_3 and Cp_2Co to the reaction mixture, eventually led to the complete consumption of **1**. The optimized reaction conditions require a 1:3:6 (**1**: PCl_3 : Cp_2Co) stoichiometric ratio which resulted in a purified yield of 40% after recrystallization.

Analogous cobaltocene reactions with SbCl_3 or BiCl_3 and **1**, resulted in the precipitation of black material, green $[\text{Cp}_2\text{Co}]\text{Cl}$, and unreacted **1** in solution. However, in the absence of the external reductant, the “clamshell” ligand can be used in the formation of hypervalent Sb and Bi. This is accomplished by the 1:1 stoichiometric reaction of **1** and PnCl_3 ($\text{Pn} = \text{Sb}, \text{Bi}$) in CH_2Cl_2 (Scheme 3.3). Upon addition of solid PnCl_3 to the CH_2Cl_2 solution of **1**, an instantaneous colour change was observed (red for Sb, and orange for Bi). The addition of Et_2O to the reaction mixture of SbCl_3 after 5 min resulted in the precipitation of a red solid. A sample of the isolated red powder was taken for analysis by ^1H NMR spectroscopy, revealing a single product that incorporated **1**. The analogous reaction involving BiCl_3 precipitated an orange powder on its own after stirring for 10 min at rt. This product was isolated by centrifugation, and it was found to be practically insoluble in all available solvents. It was possible to get a small amount to dissolve in CDCl_3 to collect a ^1H NMR spectrum, where a single product with resonances corresponding to the coordinated “clamshell” ligand was observed. A downfield chemical shift of $\Delta\delta_{\text{H}} \approx 0.5$ was observed for the proton on the *para*-carbon of the pyridine ring for coordinated compared to free **1**. Single crystals of the antimony species were grown by liquid diffusion of pentane into a CH_2Cl_2 solution of the bulk material at -

35 °C after two days, and a saturated CH₃CN solution for the bismuth product produced suitable crystals after two weeks at -30 °C. X-ray diffraction studies confirmed the synthesis of coordinated **1** to SbCl₃ and BiCl₃, **3.4** and **3.5**, respectively.



Scheme 3.3: Synthesis of base-stabilized **3.4** and **3.5**, and cationic **3.7** and **3.8**.

Halide abstraction reactions were attempted using Me₃SiOTf with **3.2**, **3.4**, or **3.5** in anticipation of obtaining the corresponding pnictenium cations.^{14,15} One stoichiometric equivalent of Me₃SiOTf was added to each of a CH₂Cl₂ solution of **3.2** (Scheme 3.2), **3.4**, and **3.5** (Scheme 3.3). The addition to **3.2** resulted in an immediate colour change from dark purple to yellow. The colour change for **3.4** and **3.5** was minimal, but a notable solubility change was observed, especially for **3.5**, which was nearly insoluble in CH₂Cl₂ but became completely soluble 5 min after the addition of Me₃SiOTf. Removal of the volatiles *in vacuo* gave yellow (As), red (Sb) and orange (Bi) coloured powders. Samples of the bulk powders were redissolved in CDCl₃ and the ¹⁹F{¹H} NMR spectra had a single peak in the range of δ_F = -78 to -79, indicative of an ionic triflate in solution (*cf.* MeOTf, δ_F = -75.4; [NOct₄]OTf δ_F = -79.0). The ¹H NMR spectra of the materials had similar patterns to the chloropnictine precursors, with no telltale changes in the chemical shifts. In the case of Pn = Sb and Bi a common impurity was present in low quantities (<10%) with resonances resembling a species containing **1** and an acidic proton at δ_H = 14.8. The acidic proton was indicative of a pyridinium version of **1**, where the nitrogen in the pyridine ring is protonated.¹⁶ If the products were left at room temperature overnight, the impurities continued to grow, as observed by ¹H NMR spectroscopy. Single crystals could be grown for all pnictenium species, which confirmed the abstraction of one chloride in each case resulting in the *N*-heterocyclic arsenium cation **3.6** and the base-stabilized dichloropnictenium cations **3.7** and **3.8**.

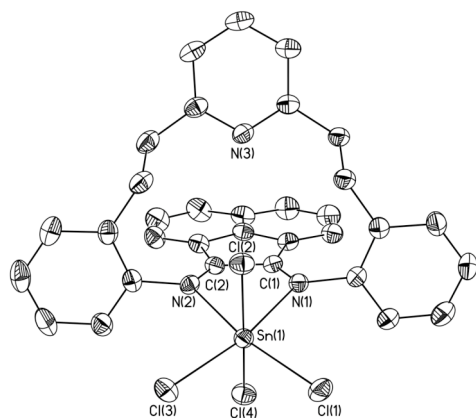
3.2.2 X-ray crystallography

All compounds (**3.1-3.8**) have been characterized by single crystal X-ray diffraction studies. Selected bond lengths and bond angles are given in Table 3.1. Refinement details are summarized in Tables 3.2 and 3.3.

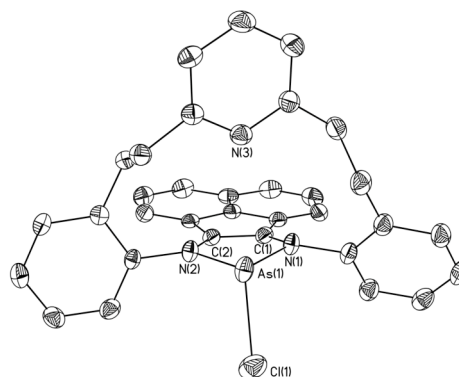
Examination of the solid-state structures of **3.2** and **3.3** (Figure 3.2) revealed that the metrical parameters for the C₂N₂Pn five-membered ring were consistent with a cheletropic addition. The two-electron reduction of the N=C–C=N backbone of **1** resulted in two C–N single bonds (1.355(5)–1.439(5) Å, *cf.* 1.272(3) Å (avg) in **1**)¹³ and a C=C double bond (1.322(6)–1.398(6) Å, *cf.* 1.517(3) in **1**).¹³ The Pn–Cl bond was characteristically long (2.3745(10) and 2.3859(11) Å (As) and 2.3832(17) and 2.4122(17) Å (P))¹⁷⁻¹⁹ and the central main group element had a pyramidal geometry expected for a As(III) ($\Sigma_{\text{ang}} = 284.9$ and 286.7°)^{17,19} or P(III) ($\Sigma_{\text{ang}} = 293.9^\circ$)¹⁸ with a lone pair.

Compounds **3.1**, **3.4** (Figure 3.2) and **3.5** (Figure 3.3) all feature hypervalent central atoms with the “clamshell” ligand. The metrical parameters of coordinated **1** (C=N 1.282(7) Å (avg), C–C 1.514(11) Å (avg)) indicate that a reduction did not occur and that the ligand is datively bound (Sn–N 2.259(3) and 2.291(4) Å, Sb–N 2.449(3) and 2.570(3) Å, Bi–N 2.540(5) and 2.648(5) Å). These types of bonding arrangements are common for SnCl₄, SbCl₃ and BiCl₃ with α -diimines.^{9,20,21}

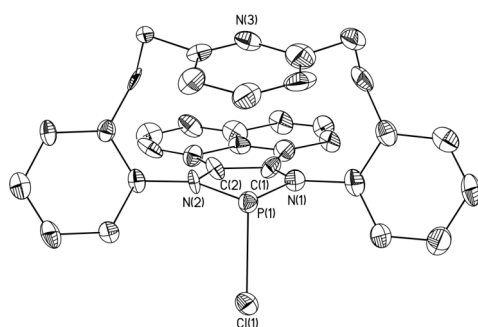
The closest Pn–O contacts in the solid state for the cation-anion pairs of **3.6-3.8** were 3.224(4), 2.733(6) and 2.652(3) Å, respectively, which are all within the sum of the van der Waals distance of 3.37, 3.58 and 3.59 Å for Pn = As, Sb and Bi, respectively.²² The corresponding triflate S–O bonds in **3.6** and **3.8** were crystallographically inequivalent with a range of bond lengths from 1.424(3)–1.440(3) and 1.415(3)–1.452(3) Å, respectively, indicating a substantial cation-anion interaction in the solid state. However the Pn–O bonds for these compounds were significantly longer than known As–O (1.987(2) Å)²³ and Bi–O (2.091(8) Å)²⁴ covalent bonds. On the contrary, the S–O bonds in **3.7** were of similar length (1.430(2) Å (avg)) and the weakly coordinated triflate is thus best described as an electrostatic interaction in the solid-state.



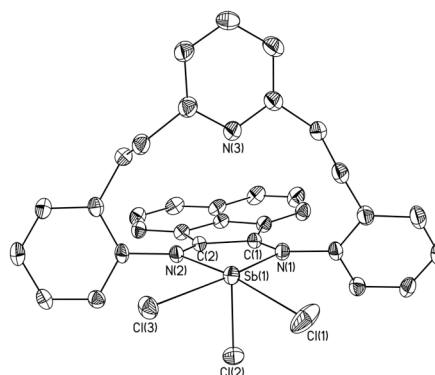
3.1



3.2

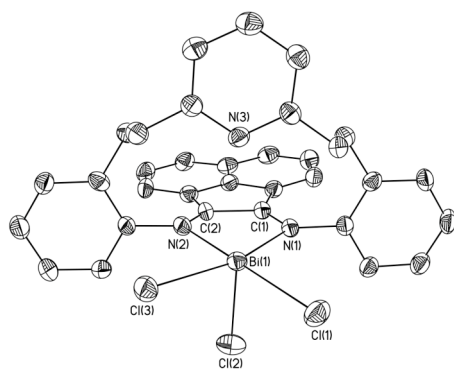


3.3

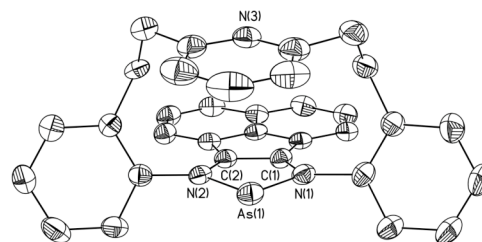


3.4

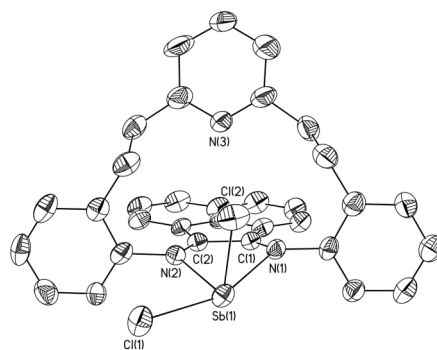
Figure 3.2: Solid-state structures of compounds **3.1-3.4** with thermal ellipsoids presented at 50% probability. Hydrogen atoms, solvates and non-coordinating anions are omitted for clarity. Refer to Table 3.1 for metrical parameters.



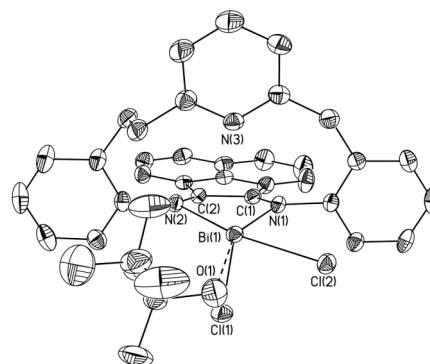
3.5



3.6



3.7



3.8

Figure 3.3: Solid-state structures of compounds 3.5-3.8 with thermal ellipsoids presented at 50% probability. Hydrogen atoms, solvates and non-coordinating anions are omitted for clarity. Refer to Table 3.1 for metrical parameters.

Table 3.1: Selected metrical parameters for **3.1-3.8**. Bond lengths are in angstroms (Å) and bond angles in degrees (°).

Compound \ Bond	3.1 E = Sn	3.2 [§] E = As	3.3 [§] E = P	3.4 E = Sb	3.5 E = Bi	3.6 E = As	3.7 E = Sb	3.8 E = Bi
N(1)–C(1)	1.283(5)	1.393(3)	1.376(5)	1.282(4)	1.286(7)	1.361(4)	1.266(10)	1.286(4)
N(2)–C(2)	1.269(6)	1.387(3)	1.355(5)	1.290(4)	1.280(7)	1.355(4)	1.282(10)	1.280(4)
C(1)–C(2)	1.502(6)	1.370(3)	1.398(6)	1.522(4)	1.518(8)	1.383(5)	1.505(11)	1.520(4)
E(1)–N(1)	2.291(4)	1.839(2)	1.683(4)	2.570(3)	2.648(5)	1.826(3)	2.518(6)	2.448(3)
E(1)–N(2)	2.259(3)	1.825(2)	1.738(4)	2.449(3)	2.540(5)	1.830(3)	2.283(6)	2.626(3)
E(1)–Cl(1)	2.3360(12)	2.3859(11)	2.4122(17)	2.5202(11)	2.6385(15)	–	2.401(2)	2.5116(8)
E(1)–Cl(2)	2.4045(13)	–	–	2.3813(10)	2.5033(16)	–	2.365(2)	2.5269(8)
E(1)–Cl(3)	2.3742(12)	–	–	2.4531(10)	2.5299(16)	–	–	–
E(1)–Cl(4)	2.4268(13)	–	–	–	–	–	–	–
E(1)–O	–	–	–	–	–	3.224(4)	2.733(6), 2.796(6)	2.652(3)
N(1)–E(1)– N(2)	73.55(13)	87.19(9)	90.73(16)	68.57(9)	65.48(14)	85.44(12)	69.3(2)	66.68(8)

[§]Selected bond lengths and bond angles are from one of the two molecules in the asymmetric unit.

Table 3.2: X-Ray details for 3.1-3.4.

Compound	3.1	3.2	3.3	3.4
Empirical formula	C ₃₄ H ₂₇ Cl ₆ N ₃ Sn ₁	C ₃₃ H ₂₅ As ₁ Cl ₁ N ₃	C ₃₃ H ₂₅ Cl ₁ N ₃ P ₁	C ₃₄ H ₂₇ Cl ₅ N ₃ Sb ₁
FW (g/mol)	808.98	573.93	529.98	776.59
Crystal system	Monoclinic	Triclinic	Orthorhombic	Triclinic
Space group	<i>P</i> 2 ₁ / <i>c</i>	<i>P</i> $\bar{1}$	<i>Pna</i> 2 ₁	<i>P</i> $\bar{1}$
<i>a</i> (Å)	11.498(2)	11.106(2)	20.871(4)	10.222(2)
<i>b</i> (Å)	17.844(4)	14.813(3)	13.861(3)	11.568(2)
<i>c</i> (Å)	18.107(6)	16.560(3)	22.172(4)	14.686(3)
α (deg)	90	103.03(3)	90	101.08(3)
β (deg)	113.49(2)	99.79(3)	90	91.95(3)
γ (deg)	90	94.54(3)	90	108.62(3)
<i>V</i> (Å ³)	3407.2(15)	2595.8(9)	6414(2)	1606.5(5)
<i>Z</i>	4	4	8	2
<i>D_c</i> (mg m ⁻³)	1.577	1.469	1.098	1.605
<i>R</i> _{int}	0.025	0.0434	0.0817	0.0243
<i>R</i> 1[<i>I</i> > 2σ(<i>I</i>)] ^a	0.0574	0.036	0.0654	0.0346
<i>wR</i> 2(<i>F</i> ²) ^a	0.1584	0.0824	0.1653	0.0911
GOF(<i>S</i>) ^a	1.085	1.054	1.063	1.142

^a $R1(F[I > 2(I)]) = \sum || |F_o| - |F_c| || / \sum |F_o|$; $wR2(F^2 [\text{all data}]) = [w(F_o^2 - F_c^2)^2]^{1/2}$; $S(\text{all data}) = [w(F_o^2 - F_c^2)^2 / (n - p)]^{1/2}$ (*n* = no. of data; *p* = no. of parameters varied; $w = 1/[\sigma^2(F_o^2) + (aP)^2 + bP]$ where $P = (F_o^2 + 2F_c^2)/3$ and *a* and *b* are constants suggested by the refinement program.

Table 3.3: X-Ray details for 3.5-3.8.

Compound	3.5	3.6	3.7	3.8
Empirical formula	C ₃₅ H ₂₈ Bi ₁ Cl ₃ N ₄	C ₃₅ H ₂₇ As ₁ Cl ₂ F ₃ N ₃ O ₃ S ₁	C _{36.2} H ₂₅ Cl ₂ F ₃ N ₃ O _{3.55} S ₁ Sb ₁	C ₃₆ H ₂₉ Bi ₁ Cl ₆ F ₃ N ₃ O ₃ S ₁
FW (g/mol)	819.94	772.48	840.5	1062.36
Crystal system	Orthorhombic	Monoclinic	Monoclinic	Monoclinic
Space group	<i>Pbca</i>	<i>P2₁/c</i>	<i>P2₁/c</i>	<i>C2/c</i>
<i>a</i> (Å)	15.192(3)	11.010(2)	12.5743(10)	42.4663(17)
<i>b</i> (Å)	18.558(4)	15.943(3)	20.9295(17)	9.7165(5)
<i>c</i> (Å)	22.275(4)	23.006(6)	14.7300(11)	20.6524(8)
α (deg)	90	90	90	90
β (deg)	90	115.88(2)	93.609(2)	110.538(2)
γ (deg)	90	90	90	90
<i>V</i> (Å ³)	6280(2)	3633.3(13)	3868.9(5)	7980.0(6)
<i>Z</i>	8	4	4	8
<i>D_c</i> (mg m ⁻³)	1.734	1.412	1.443	1.769
<i>R_{int}</i>	0.0326	0.0624	0.1551	0.0817
<i>R1</i> [<i>I</i> > 2 σ (<i>I</i>)] ^a	0.044	0.0576	0.0577	0.0399
<i>wR2</i> (<i>F</i> ²) ^a	0.1085	0.1629	0.1584	0.0765
GOF(<i>S</i>) ^a	1.001	1.044	1.073	1.009

^a $R1(F[I > 2(I)]) = \sum || |F_o| - |F_c| || / \sum |F_o|$; $wR2(F^2 [\text{all data}]) = [w(F_o^2 - F_c^2)^2]^{1/2}$; $S(\text{all data}) = [w(F_o^2 - F_c^2)^2 / (n - p)]^{1/2}$ (n = no. of data; p = no. of parameters varied; $w = 1/[\sigma^2(F_o^2) + (aP)^2 + bP]$ where $P = (F_o^2 + 2F_c^2)/3$ and a and b are constants suggested by the refinement program.

3.3 Conclusions

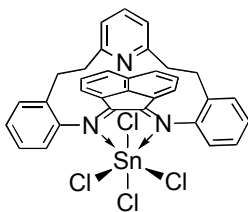
Precursors to *N*-heterocyclic phospheniums and arseniums have been synthesized utilizing cobaltocene as a one-electron reductant in a convenient redox method. Unfortunately this method was not suitable for all group 15 elements, and gave an insoluble black material when SbCl₃ or BiCl₃ were used as reagents. While the “clamshell” ligand can easily undergo cycloaddition reactions, it can also be used as a chelating Lewis base to form donor-acceptor complexes by datively bonding to SnCl₄, SbCl₃ and BiCl₃ through the lone pairs on nitrogen. With the additional support, halide abstraction was possible and base-stabilized dichlorostibenium and -bismuthenium cations were isolated. Although the group 15 compounds are prone to decomposition at ambient temperature, they have been characterized comprehensively and represent an interesting class of molecules.

3.4 Experimental section

General synthetic and crystallography experimental details can be found in Appendix 1.

3.4.1 Synthetic procedures[†]

Compound 3.1



The addition of neat SnCl₄ (21.0 μL, 0.179 mmol) to a THF solution (6 mL) of **1** (0.0829 g, 0.179 mmol), resulted in an instantaneous colour change from dark orange to a lighter shade of orange and the precipitation of an orange solid after stirring at rt for 3 min. The solution continued to stir at rt for 30 min. The precipitate was allowed to settle and the supernatant was decanted, the orange solid was dried *in vacuo*. The product was washed with hexanes (3 mL), which was decanted and the orange solid was dried *in vacuo*.

[†] Elemental analyses of air sensitive compounds were not weighed under nitrogen. All compounds show some degree of decomposition if kept at room temperature. Samples for elemental analysis were not performed in house. All samples were dried *in vacuo* for 24 h and some retained solvent, which could not be removed (see Appendix 3.1 for corroborating ¹H NMR spectra of **3.2-3.4**).

Yield: 72% (0.0937 g, 0.129 mmol);

d.p.: 277-281 °C;

¹H NMR (599.52 MHz, CD₂Cl₂): δ 8.18 (d, 2H, *aryl*, ³J_{H-H} = 7.8), 7.71 (d, 2H, *aryl*, ³J_{H-H} = 6.6), 7.63 (m, 8H, *aryl*), 7.27 (t, 2H, *aryl*, ³J_{H-H} = 7.2), 6.84 (d, 2H, *aryl*, ³J_{H-H} = 7.2), 6.73 (d, 2H, *aryl*, ³J_{H-H} = 7.8), 3.84 (ddd, 2H, CH₂, ²J_{H-H} = 14.1, ³J_{H-H} = 11.1, ³J_{H-H} = 1.2), 2.92 (ddd, 2H, CH₂, ²J_{H-H} = 14.1, ³J_{H-H} = 11.4, ³J_{H-H} = 9.0), 2.79 (ddd, 2H, CH₂, ²J_{H-H} = 12.9, ³J_{H-H} = 10.8, ³J_{H-H} = 9.0), 2.14 (vt, 2H, CH₂, ³J_{H-H} = 12.0);

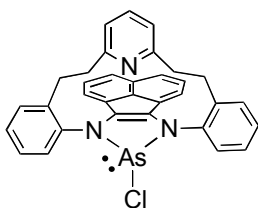
¹³C{¹H} NMR (150.76 MHz, CD₂Cl₂): δ 162.2, 161.6, 141.1, 141.07, 137.1, 135.5, 134.3, 132.4, 131.5, 130.1, 129.8, 128.9, 128.4, 126.4, 124.2, 120.3, 39.7, 33.6;

FT-IR (cm⁻¹ (relative intensities)): 767(11), 780(3), 834(6), 1051(14), 1125(10), 1186(15), 1253(9), 1297(7), 1420(12), 1455(5), 1482(4), 1588(2), 1635(1), 1674(8), 2951(13);

FT-Raman (cm⁻¹ (relative intensities)): 134(8), 232(14), 274(5), 327(6), 360(12), 965(10), 1039(13), 1125(11), 1220(3), 1345(15), 1420(7), 1599(2), 1634(1), 1674(9), 3067(4);

HRMS: C₃₃H₂₅Cl₃N₃Sn₁⁺ calcd (found) 688.0136 (688.0124).

Compound 3.2



To a THF solution (5 mL) of **1** (0.404 g, 0.871 mmol), AsCl₃ (73.0 μL, 0.871 mmol) was added and the solution stirred for 10 min at rt. A THF solution (3 mL) of Cp₂Co (0.334 g, 1.77 mmol) was added dropwise to the reaction mixture over 5 min, which caused the immediate precipitation of a green solid and a solution colour change from orange to purple. The reaction mixture was left to stir for 15 min at rt. The green solid was removed by centrifugation and washed with THF (2 x 3 mL). The volatiles of the combined purple solutions were removed *in vacuo*, giving a purple solid. A concentrated CH₂Cl₂ solution (3 mL) of the bulk material was layered with Et₂O (6 mL) and kept at -35 °C overnight. The mother liquor was decanted and the recrystallized product was dried *in vacuo*.

Yield: 72% (0.357 g, 0.621 mmol);

d.p.: 205-208 °C;

¹H NMR: δ 7.93 (dd, 2H, *aryl*, ³*J*_{H-H} = 8.0, ⁴*J*_{H-H} = 1.2), 7.54 (m, 5H, *aryl*), 7.50 (ddd, 2H, *aryl*, ³*J*_{H-H} = 7.6, ⁴*J*_{H-H} = 1.6), 7.40 (ddd, 2H, *aryl*, ³*J*_{H-H} = 7.6, ⁴*J*_{H-H} = 1.6), 7.19 (dd, 2H, *aryl*, ³*J*_{H-H} = 8.4, ³*J*_{H-H} = 8.0), 6.60 (ov. d, 4H, *aryl*, ³*J*_{H-H} = 7.6, ³*J*_{H-H} = 7.2), 3.36 (ddd, 2H, *CH*₂, ²*J*_{H-H} = 3.2, ³*J*_{H-H} = 10.4, ³*J*_{H-H} = 13.6), 3.18 (ddd, 2H, *CH*₂, ²*J*_{H-H} = 3.6, ³*J*_{H-H} = 7.6, ³*J*_{H-H} = 12.8), 3.04 (ddd, 2H, *CH*₂, ²*J*_{H-H} = 3.6, ³*J*_{H-H} = 7.6, ³*J*_{H-H} = 13.6), 2.77 (ddd, 2H, *CH*₂, ²*J*_{H-H} = 3.2, ³*J*_{H-H} = 10.4, ³*J*_{H-H} = 13.6);

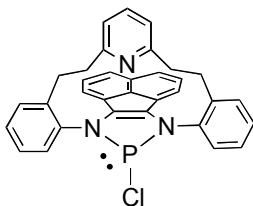
¹³C{¹H} NMR: δ 161.6, 139.9, 137.4, 137.3, 137.0, 131.3, 130.1, 129.5, 129.2, 128.7, 128.0, 127.4, 127.3, 126.7, 121.2, 119.8, 41.5, 31.9;

FT-IR (cm⁻¹ (relative intensities)): 444(15), 487(8), 763(2), 814(6), 921(11), 1145(9), 1265(10), 1358(4), 1389(7), 1457(1), 1486(3), 1532(14), 1572(12), 1593(5), 2927(13);

HRMS: C₃₃H₂₅As₁N₃⁺ calcd (found) 538.1264 (538.1263);

Elemental Analysis (%): calcd for C₃₃H₂₅As₁Cl₁N₃•¼(CH₃CH₂)₂O₁•¼CH₂Cl₂[†] C 67.03, H 4.60, N 6.85; found C 67.60, H 4.47, N 7.07.

Compound 3.3



Neat PCl₃ (144 μL, 1.65 mmol) was added to a THF solution (6 mL) of **1** (0.254 g, 0.549 mmol) and was stirred for 10 min at rt. A THF solution (4 mL) of Cp₂Co (0.619 g, 3.27 mmol) was prepared and added dropwise to the reaction mixture, which caused the precipitation of green solids from the dark purple solution. This was left to stir at rt for 2.5 h, at which time the precipitate was removed from the solution by centrifugation and washed with THF (2 x 3 mL), decanting and centrifuging between each wash. The purple solution and washings were combined and the volatiles were removed *in vacuo*. This gave a purple solid, which was redissolved in CH₂Cl₂ (4 mL) and layered with Et₂O (8 mL), producing purple crystals after two days at -35 °C.

Yield: 40% (0.115 g, 0.216 mmol);

d.p.: 196-200 °C;

¹H NMR: δ 8.03 (d, 2H, *aryl*, ³*J*_{H-H} = 7.6), 7.57-7.49 (m, 6H, *aryl*), 7.39 (ddd, 2H, *aryl*, ³*J*_{H-H} = 7.6, ³*J*_{H-H} = 7.5, ⁴*J*_{H-H} = 1.6), 7.22 (dd, 2H, *aryl*, ³*J*_{H-H} = 8.2, ³*J*_{H-H} = 6.8), 7.02 (t, 1H, *aryl*, ³*J*_{H-H} = 7.6), 6.68 (d, 2H, *aryl*, ³*J*_{H-H} = 6.8), 6.44 (d, 2H, *aryl*, ³*J*_{H-H} = 7.6), 3.30 (m, 2H, *CH*₂), 3.15 (m, 4H, *CH*₂), 2.80 (m, 2H, *CH*₂);

$^{13}\text{C}\{^1\text{H}\}$ NMR: δ 160.6, 140.2 (d, $^2J_{13\text{C-P}} = 5.9$), 137.1 (d, $^3J_{13\text{C-P}} = 3.3$), 136.0 (d, $^3J_{13\text{C-P}} = 5.6$), 135.5, 135.4, 131.5, 129.4, 128.6, 128.5, 127.8, 127.6 (d, $^2J_{13\text{C-P}} = 8.3$), 127.4, 127.0, 121.2, 120.1, 41.4, 31.6;

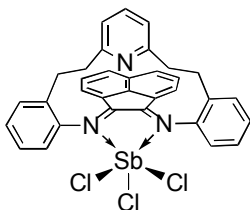
$^{31}\text{P}\{^1\text{H}\}$ NMR: δ 176 (s);

FT-IR (cm^{-1} (relative intensities)): 766(2), 780(10), 799(11), 816(5), 982(3), 1106(14), 1151(7), 1208(13), 1273(9), 1358(4), 1464(1), 1491(8), 1572(15), 1588(6), 2927(12);

FT-Raman (cm^{-1} (relative intensities)): 175(13), 564(5), 953(12), 983(3), 1209(7), 1262(14), 1395(15), 1440(11), 1465(4), 1536(2), 1610(1), 2061(6), 2117(9), 2185(10), 3062(8);

Elemental Analysis (%): calcd for $\text{C}_{33}\text{H}_{25}\text{P}_1\text{Cl}_1\text{N}_3 \cdot \frac{1}{4}(\text{CH}_3\text{CH}_2)_2\text{O}_1 \cdot \frac{1}{4}\text{CH}_2\text{Cl}_2^\ddagger$ C 72.20, H 5.95, N 7.38; found C 71.18, H 4.98, N 7.24.

Compound **3.4**[‡]



Solid SbCl_3 (0.0670 g, 0.294 mmol) was added to a CH_2Cl_2 solution (3 mL) of **1** (0.133 g, 0.287 mmol). The reaction mixture was left to stir for 30 min at rt. A red solid was precipitated from the reaction mixture by the addition of Et_2O with vigorous stirring.

The supernatant was decanted and the product was dried *in vacuo*.

X-ray quality single crystals were grown by liquid diffusion of pentane into a concentrated CH_2Cl_2 solution of the bulk powder at $-35\text{ }^\circ\text{C}$ for two days.

Yield: 82% (0.159 g, 0.229 mmol);

m.p.: 213-217 $^\circ\text{C}$;

^1H NMR: δ 7.98 (d, 2H, *aryl*, $^3J_{\text{H-H}} = 8.4$), 7.52-7.32 (m, 11H, *aryl*), 6.83 (d, 2H, *aryl*, $^3J_{\text{H-H}} = 7.6$), 6.79 (d, 2H, *aryl*, $^3J_{\text{H-H}} = 7.2$), 2.95-2.73 (m, 8H, CH_2);

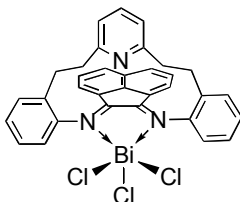
FT-IR (cm^{-1} (relative intensities)): 734(12), 765(14), 778(2), 831(4), 934(13), 1050(8), 1112(9), 1187(15), 1244(10), 1283(7), 1448(3), 1478(6), 1589(1), 1621(5), 2957(11);

[‡] Compounds **3.4** and **3.5** were extremely insoluble and attempts to acquire $^{13}\text{C}\{^1\text{H}\}$ NMR spectra failed because of the lack of material in solution.

FT-Raman (cm^{-1} (relative intensities)): 128(7), 237(5), 276(8), 330(3), 507(14), 958(10), 1041(11), 1113(13), 1157(15), 1218(4), 1434(9), 1589(1), 1621(2), 1651(12), 3068(6);

Elemental Analysis (%): calcd for $\text{C}_{33}\text{H}_{25}\text{Sb}_1\text{Cl}_3\text{N}_3 \cdot \frac{1}{4}\text{CH}_3\text{C}_1\text{N}_1^\dagger$ C 57.32, H 3.70, N 6.49; found C 56.53, H 3.49, N 6.28.

Compound 3.5[‡]



Solid BiCl_3 (0.142 g, 0.453 mmol) was added to a CH_2Cl_2 solution (4 mL) of **1** (0.216 g, 0.466 mmol) and the reaction mixture was stirred at rt. An orange solid precipitated from solution after 10 min and was separated by centrifugation after 2.5 h. The supernatant was decanted and the orange solid was washed with CH_3CN (3 mL), centrifuged and the supernatant decanted a second time. The orange solid was then suspended in CH_2Cl_2 and transferred to a vial. The volatiles were removed *in vacuo*. Single crystals were grown from a saturated CH_3CN solution at $-30\text{ }^\circ\text{C}$ after two weeks.

Yield: 84% (0.304 g, 0.391 mmol);

d.p.: 270-274 $^\circ\text{C}$;

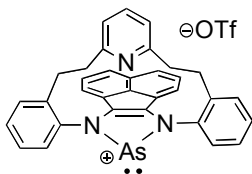
^1H NMR: δ 8.02 (d, 2H, *aryl*, $^3J_{\text{H-H}} = 8.0$), 7.55-7.39 (m, 11H, *aryl*), 7.01 (d, 2H, *aryl*, $^3J_{\text{H-H}} = 8.0$), 6.68 (d, 2H, *aryl*, $^3J_{\text{H-H}} = 7.6$), 3.24 (m, 4H, CH_2), 2.76 (m, 4H, CH_2);

FT-IR (cm^{-1} (relative intensities)): 779(2), 797(13), 834(5), 937(12), 1051(8), 1112(9), 1189(14), 1245(10), 1283(6), 1454(4), 1479(7), 1590(1), 1623(3), 1651(15), 2940(11);

FT-Raman (cm^{-1} (relative intensities)): 117(5), 147(8), 229(4), 282(2), 956(9), 1051(14), 1112(10), 1222(6), 1338(15), 1422(11), 1590(1), 1624(3), 1652(12), 2061(13), 3066(7);

Elemental Analysis (%): calcd for $\text{C}_{33}\text{H}_{25}\text{Bi}_1\text{Cl}_3\text{N}_3$ C 50.89, H 3.24, N 5.39; found C 50.34, H 2.97, N 5.33.

Compound 3.6



Neat Me_3SiOTf (70.0 μL , 0.387 mmol) was added to a CH_2Cl_2 solution (4 mL) of **3.2** (0.211 g, 0.367 mmol), causing an instantaneous colour change of the solution from purple to yellow.

After stirring for 10 min at rt the reaction was centrifuged and the solution was transferred to a vial. The volatiles were removed *in vacuo* leaving a yellow wax that became a yellow powder upon agitation in an Et₂O wash (3 mL). The yellow powder was dried *in vacuo*. Recrystallization at -35 °C overnight by liquid diffusion of Et₂O (6 mL) into a CH₂Cl₂ solution (2 mL) of the crude product yielded pure, microcrystalline, yellow powder, which was dried *in vacuo* after removal of the supernatant.

Yield: 85% (0.216 g, 0.313 mmol);

d.p.: 79-84 °C;

¹H NMR: δ 7.89 (d, 2H, *aryl*, ³J_{H-H} = 8.4), 7.82 (d, 2H, *aryl*, ³J_{H-H} = 8.0), 7.67 (m, 4H, *aryl*), 7.55 (ddd, 2H, *aryl*, ³J_{H-H} = 7.8, ³J_{H-H} = 6.4, ⁴J_{H-H} = 2.8), 7.44 (dd, 2H, *aryl*, ³J_{H-H} = 7.2, ³J_{H-H} = 8.0), 7.29 (t, 1H, *aryl*, ³J_{H-H} = 7.6), 6.90 (d, 2H, *aryl*, ³J_{H-H} = 6.8), 6.72 (d, 2H, *aryl*, ³J_{H-H} = 7.6), 3.09 (m, 6H, CH₂), 2.81 (m, 6H, CH₂);

¹³C{¹H} NMR: δ 161.2, 146.3, 137.9 (br), 135.3, 134.9, 131.8, 131.6, 130.2, 130.1, 128.9, 128.2, 127.4, 126.2, 123.0, 121.8, 40.9, 31.7;

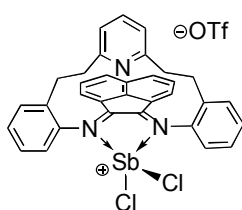
¹⁹F{¹H} NMR: δ -78.6 (s);

FT-IR (cm⁻¹ (relative intensities)): 636(2), 730(11), 772(4), 797(14), 824(7), 1028(3), 1154(6), 1223(12), 1269(1), 1415(8), 1455(5), 1491(9), 1571(15), 1588(10), 3059(13);

FT-Raman (cm⁻¹ (relative intensities)): 202(11), 284(4), 443(13), 558(9), 690(15), 916(6), 952(5), 1029(12), 1212(7), 1343(3), 1370(14), 1414(10), 1445(2), 1609(1), 3069(8);

HRMS: C₃₃H₂₅As₁N₃⁺ calcd (found) 538.1259 (538.1260).

Compound 3.7



Neat Me₃SiOTf (14.0 μL, 0.0774 mmol) was added to a CH₂Cl₂ suspension (3 mL) of **3.4** (0.0534 g, 0.0772 mmol), which changed the slurry to a translucent solution. The volatiles were removed *in vacuo* after stirring for 2 min to give a red powder. This was redissolved in CH₂Cl₂ (2 mL) and pentane (6 mL) was added with rapid stirring, causing the precipitation of a red powder. The supernatant was decanted and the powder dried *in vacuo*. Single crystals were grown at -35 °C by liquid diffusion of Et₂O into a CH₂Cl₂ solution of the bulk material.

Yield: 73% (0.0455 g, 0.0564 mmol);

d.p.: 180-196 °C;

¹H NMR (599.52 MHz): δ 8.12 (d, 2H, *aryl*, ³J_{H-H} = 6.0), 7.65 (br, 2H, *aryl*), 7.55 (m, 8H, *aryl*), 7.31 (t, 1H, *aryl*, ³J_{H-H} = 6.0), 6.81 (d, 2H, *aryl*, ³J_{H-H} = 6.0), 6.78 (d, 2H, *aryl*, ³J_{H-H} = 6.0), 3.44 (br, 2H, CH₂), 2.87 (br, 2H, CH₂), 2.34 (br, 2H, CH₂);

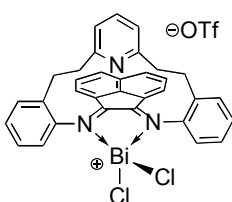
¹³C{¹H} NMR (150.76 MHz): δ 167.6, 161.2, 137.1, 133.4, 131.3, 131.2, 129.3, 129.2, 128.2, 127.41, 127.38, 126.5, 123.3, 120.1, 40.2, 33.7;

¹⁹F{¹H} NMR: δ -78.5(s);

FT-IR (cm⁻¹ (relative intensities)): 517(10), 574(14), 637(2), 779(5), 833(11), 1028(4), 1170(9), 1236(1), 1276(13), 1448(7), 1482(8), 1587(3), 1622(6), 2960(12), 3066(15);

FT-Raman (cm⁻¹ (relative intensities)): 121(2), 295(11), 344(6), 798(15), 962(10), 1025(9), 1042(13), 1123(12), 1218(4), 1344(14), 1422(7), 1586(1), 1621(3), 1665(8), 3069(5).

Compound 3.8



Compound **3.5** (0.0438 g, 0.0537 mmol) was suspended in CD₂Cl₂ (1 mL) and cooled to -60 °C. Neat Me₃SiOTf (10.0 μL, 0.0553 mmol) was added and the solution was stirred for 5 min at rt. The volatiles were removed *in vacuo*, giving an orange solid. Single crystals suitable for X-ray diffraction studies were grown after one week at -36 °C by liquid diffusion of Et₂O into a concentrated CH₃CN solution of the bulk material.

Yield: 91% (0.0439 g, 0.0492 mmol);

d.p.: 168-174 °C;

¹H NMR (CD₂Cl₂): δ 8.15 (d, 2H, *aryl*, ³J_{H-H} = 8.4), 7.60 (m, 5H, *aryl*), 7.49 (m, 6H, *aryl*), 7.06 (d, 2H, *aryl*, ³J_{H-H} = 7.6), 6.65 (d, 2H, *aryl*, ³J_{H-H} = 7.6), 3.21 (m, 4H, CH₂), 2.92 (m, 2H, CH₂), 2.64 (m, 2H, CH₂);

¹³C{¹H} NMR (CD₂Cl₂): δ 169.5, 162.7, 145.1, 144.8, 139.2, 133.2, 133.1, 131.7, 130.8, 129.6, 129.2, 128.8, 127.4, 127.3, 122.2, 121.6, 40.4, 33.3;

¹⁹F{¹H} NMR (CD₂Cl₂): δ -79.1(s);

FT-IR (cm^{-1} (relative intensities)): 636(2), 771(5), 832(10), 1012(4), 1052(13), 1086(15), 1117(12), 1201(1), 1294(8), 1456(7), 1481(9), 1587(3), 1624(6), 2961(11), 3065(14);

FT-Raman (cm^{-1} (relative intensities)): 123(13), 145(4), 284(2), 961(7), 1039(14), 1220(5), 1586(1), 1623(3), 2044(12), 2061(6), 2076(9), 2146(8), 2158(11), 2184(10), 3070(15).

3.5 References

- (1) Schmidpeter, A.; Lochschmidt, S.; Sheldrick, W. S. *Angew. Chem. Int. Ed. Engl.* **1982**, *21*, 63.
- (2) Ellis, B. D.; Carlesimo, M.; Macdonald, C. L. B. *Chem. Commun.* **2003**, 1946.
- (3) Ellis, B. D.; Dyker, C. A.; Decken, A.; Macdonald, C. L. B. *Chem. Commun.* **2005**, 1965.
- (4) Reeske, G.; Cowley, A. H. *Chem. Commun.* **2006**, 1784.
- (5) Martin, C. D.; Ragogna, P. J. *Dalton Trans.* **2011**, *40*, 11976.
- (6) Reeske, G.; Hoberg, C. R.; Hill, N. J.; Cowley, A. H. *J. Am. Chem. Soc.* **2006**, *128*, 2800.
- (7) Reeske, G.; Cowley, A. H. *Inorg. Chem.* **2007**, *46*, 1426.
- (8) Dube, J. W.; Farrar, G. J.; Norton, E. L.; Szekely, K. L. S.; Cooper, B. F. T.; Macdonald, C. L. B. *Organometallics* **2009**, *28*, 4377.
- (9) Hill, N. J.; Vargas-Baca, I.; Cowley, A. H. *Dalton Trans.* **2009**, 240.
- (10) Dillon, K. B.; Monks, P. K. *Dalton Trans.* **2007**, 1420.
- (11) Caputo, C. A.; Brazeau, A. L.; Hynes, Z.; Price, J. T.; Tuononen, H. M.; Jones, N. D. *Organometallics* **2009**, *28*, 5261.
- (12) Brazeau, A. L.; Caputo, C. A.; Martin, C. D.; Jones, N. D.; Ragogna, P. J. *Dalton Trans.* **2010**, *39*, 11069.
- (13) Leung, D. H.; Ziller, J. W.; Guan, Z. *J. Am. Chem. Soc.* **2008**, *130*, 7538.
- (14) Cowley, A. H.; Kemp, R. A. *Chem. Rev.* **1985**, *85*, 367.
- (15) Given that the phosphonium cation has been previously synthesized (**2.3**), the reaction of Me₃SiOTf and **3.3** was not performed.
- (16) The pyridinium version of the free ligand can be made separately by the addition of triflic acid to **1**.
- (17) Carmalt, C. J.; Lomeli, V.; McBurnett, B. G.; Cowley, A. H. *Chem. Commun.* **1997**, 2095.
- (18) Gudat, D.; Haghverdi, A.; Hupfer, H.; Nieger, M. *Chem. Eur. J.* **2000**, *6*, 3414.

- (19) Burford, N.; Macdonald, C. L. B.; Parks, T. M.; Wu, G.; Borecka, B.; Kwiatkowski, W.; Cameron, T. S. *Can. J. Chem.* **1996**, *74*, 2209.
- (20) Hill, N. J.; Vasudevan, K.; Cowley, A. H. *JJC* **2006**, *1*, 47.
- (21) Fedushkin, I. L.; Khvoynova, N. M.; Baurin, A. Y.; Chudakova, V. A.; Skatova, A. A.; Cherkasov, V. K.; Fukin, G. K.; Baranov, E. V. *Russ. Chem. Bull., Int. Ed.* **2006**, *55*, 74.
- (22) Mantina, M.; Valero, R.; Cramer, C. J.; Truhlar, D. G. In *CRC Handbook of Chemistry and Physics*; 92 ed.; Haynes, W. M., Ed.; CRC Press: 2011.
- (23) Michalik, D.; Schulz, A.; Villinger, A. *Inorg. Chem.* **2008**, *47*, 11798.
- (24) Matano, Y.; Azuma, N.; Suzuki, H. *J. Chem. Soc., Perkin Trans. I* **1994**, 1739.

Chapter 4

4 Synthesis, reactivity, and computational analysis of *N*-heterocyclic halophosphines supported by dianionic guanidinate ligands^ϕ

4.1 Introduction

A major theme in the field of synthetic main group chemistry is to push the limits of the bonding environments surrounding a central p-block element and impose a stress that will then allow for access to unprecedented yet controlled reactivity. There are many variables associated with forcing such a condition within a molecule that include modifications to the electronics, sterics, charge and ring strain. Over the past decade there has been a shift in research efforts to design main group molecules that are capable of reactivity previously reserved for the transition metals. Highlights include the ability of “frustrated Lewis pairs,” low-valent group 13 species, and heavy group 14 analogues of *N*-heterocyclic carbenes, alkenes and alkynes to activate small molecules, including H₂, NH₃, PH₃, and P₄.

Power *et al.* were the first to demonstrate the bifurcation of dihydrogen by a main group metal, with the addition of H₂ across the Ge-Ge bond in unsaturated digermynes at ambient temperature and pressure to give a combination of digermenes and germanes.¹ Several years later the Power group also showed the addition of dihydrogen to distannynes to give tin(II) hydrides.²⁻⁸ A notable surge in the reported reactivity of “frustrated Lewis pairs” (FLP) was kickstarted by Stephan *et al.*, where they reported metal-free reversible hydrogen activation by the unquenched reactivity of a phosphine-borane ((C₆H₂Me₃)₂P(C₆F₄)B(C₆F₅)₂), which features a Lewis acidic boron and Lewis basic phosphorus.⁹ Since then, many different FLP systems have been developed¹⁰ and

^ϕ This work is published and reproduced with permission from Brazeau, A. L.; Hänninen, M. M.; Tuononen, H. M.; Jones, N. D.; Ragona, P. J. *J. Am. Chem. Soc.* **2012**, *134*, 5398. Copyright 2012 American Chemical Society. See Appendix 2.1.

reactivity with a variety of substrates has been observed, including B–H bonds,¹¹ CO₂,^{12,13} unsaturated bonds¹⁰ and even catalytic, metal-free hydrogenation.¹⁴⁻¹⁸

The silylene LSi (L = CH{(C=CH₂)(CMe)(2,6-*i*-Pr₂C₆H₃N)₂}) will oxidatively add ammonia to give four-coordinate LSi(H)NH₂¹⁹ and is the only reported main group molecule that has been successfully used in the activation of PH₃, yielding LSi(H)PH₂.²⁰

Phosphenium cations have a rich history of reactivity, including reactions with Lewis bases,²¹⁻²³ inorganic and organic unsaturated bonds,²⁴ and as ligands on transition metals.²⁵⁻³² Phosphenium cations are also known to catenate,³³ activate white phosphorus,^{34,35} and undergo substitution reactions.³⁶ The Lewis amphoteric phosphenium cation presents a unique environment, which opens the floodgates for unique structures, bonding arrangements and reactivity.

We envisaged designing a NHP within a highly strained four-membered ring so that the phosphorus atom could be probed for new and unobserved reactivity. While several four-membered rings incorporating NHP are known (Chart 4.1) they are all of the type P–N–X–N where X = P,^{34,37} Si or Al,^{35,38} all electropositive elements, however the example where X = C has surprisingly been absent from the literature. We sought to extend this series and fill the void by using the nitrogen-based, chelating, guanidinate ligand (Chart 4.2a,b), which despite its wide spread use for supporting metallic elements spanning the periodic table, little is known about the role in stabilizing group 15 centres in the +3 oxidation state. Jones *et al.* have synthesized several (monoanionic)guanidinate pnictogen(III) dihalides (pnictogen = Pn = P, As, Sb) as precursors to amido-dipnictenes (Chart 4.3c).³⁹ Related (monoanionic)amidinate ligands (Chart 4.2c) have been used in stabilizing heavier group 15 atoms (As, Sb, Bi)⁴⁰⁻⁴³ as shown in Chart 4.3a,b. We have previously reported a (monoanionic)guanidinate ligand capable of supporting a dicationic arsenic centre with additional stabilization from a Lewis base (Chart 4.3c).⁴⁴ For the synthesis of an NHP it would be ideal to have the “free” cation, which therefore calls for the use of a (dianionic)guanidinate (Chart 4.2b). There is only one previous report of a (dianionic)guanidinate being used to support a group 15 atom involving antimony⁴⁵

(Chart 4.3d), and one example of a phosphorus centre³⁹ being supported by a guanidinate ligand.

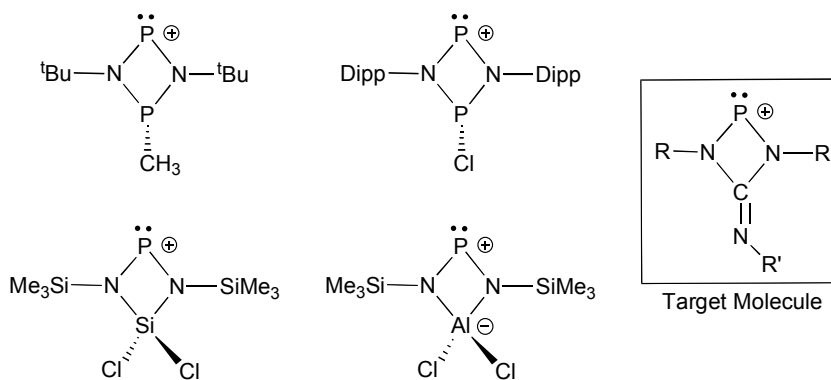


Chart 4.1: Known and target four-membered NHP species.

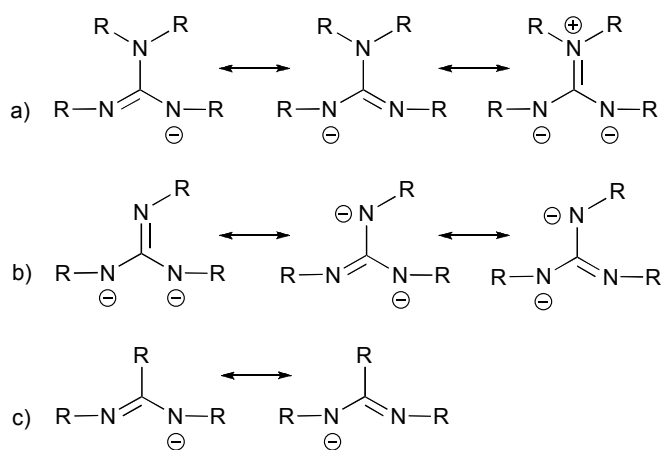


Chart 4.2: (a) Monoanionic vs. (b) dianionic guanidinate ligands, and (c) amidinate ligands.

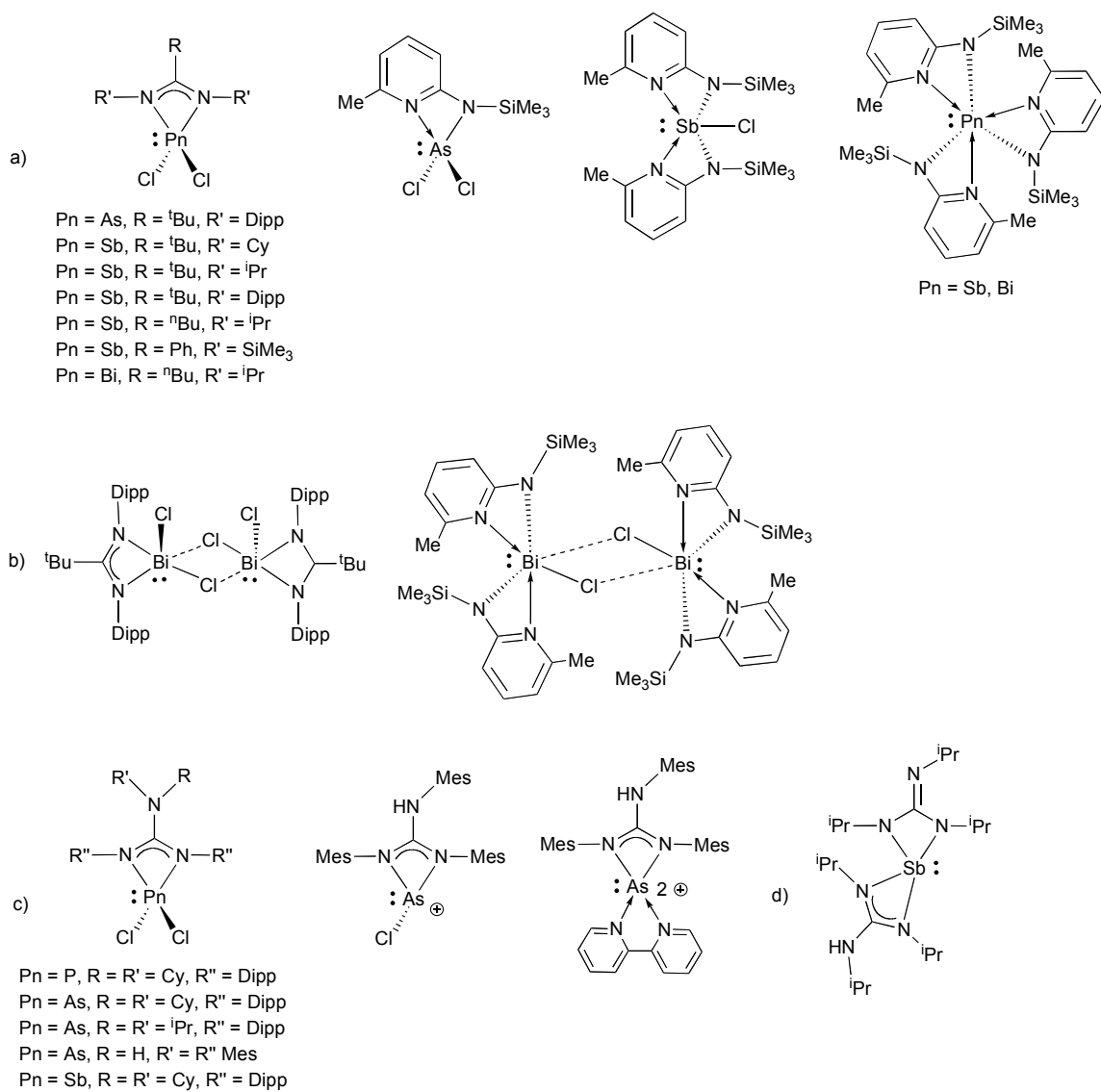


Chart 4.3: Literature examples of (a) monomeric (monoanionic)amidinate, (b) dimeric (monoanionic)amidinate, (c) (monoanionic)guanidinate, and (d) (dianionic)guanidinate ligands.

In this context, this chapter reports the first synthesis and comprehensive characterization of a series of diaminochlorophosphines supported by homo- and heteroleptic (dianionic)guanidates. The reactivity of the model compound tris(Mes)guanidinato chlorophosphine (Mes = 2,4,6-trimethylphenyl) has been studied extensively. We have explored the tendency of these compounds to retain the halogen and therefore the reluctance to form the “free” NHP. A base-stabilized NHP however

was easily accessible and computational[†] analysis has provided insight on this rather counterintuitive result and gave valuable data on the nature of the electronics about the phosphorus atom, and why these particular systems are resistant to halide abstraction. Novel chemically instigated carbodiimide elimination was observed in conjunction with metal coordination, resulting in the first structurally characterized metal complex with a cationic iminophosphine ligand. A study between diaminochlorophosphine and a gentle one-electron reductant was explored to give the clean synthesis of the reductively coupled product featuring a dimeric structure with μ -*N,N'* bridging guanidates and a P–P bond. Upon investigating the thermal stability of the tris(Mes)guanidinato chlorophosphine we discovered the thermally induced ejection of carbodiimide and subsequent insertion of chloro(imino)phosphine into the P–N bond of the initial diaminochlorophosphine resulting in a new ring expansion product with a μ -*N,N'* bridging guanidate and a μ -bridging N-Mes. This ring expansion chemistry is extremely rare within P(III)–N chemistry. These observations collectively give a deeper perception on the nature and reactivity of diaminochlorophosphines constrained in a four-membered ring.

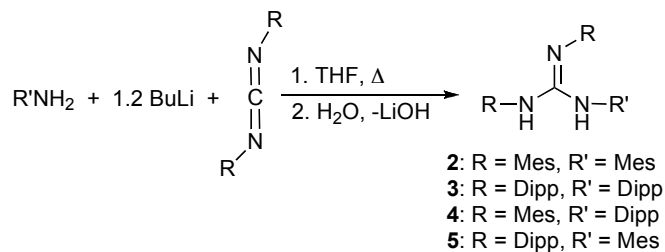
4.2 Results and discussion

4.2.1 Synthesis

Synthesis of *N,N',N''*-tris(*aryl*)guanidines (**2-5**, *aryl* = Mes and Dipp) followed the literature procedure of Boéré *et al.*⁴⁶ Preparations were accomplished by refluxing *N,N'*-bis(R)carbodiimide and lithium (R')anilide in THF for 2 h, the addition of water, gave either the homoleptic guanidines **2** and **3** (R = R' = Mes for **2**; R = R' = Dipp for **3**) or the heteroleptic guanidines **4** and **5** (R = Mes; R' = Dipp for **4**; R = Dipp; R' = Mes for **5**; Scheme 4.1). Upon removal of THF, compounds **4** and **5** deposited as wax like materials on the sides of the flask. Further recrystallization from hexanes produced white powders, which were sampled for analysis by proton NMR spectroscopy. Spectra of the isolated materials demonstrated dynamic behaviour indicative of sterically bulky guanidines.⁴⁶ These phenomena have been documented elsewhere (for **3**)⁴⁶ using variable temperature

[†] Computational analyses were completed by Mikko M. Hänninen and Heikki M. Tuononen at University of Jyväskylä, Finland.

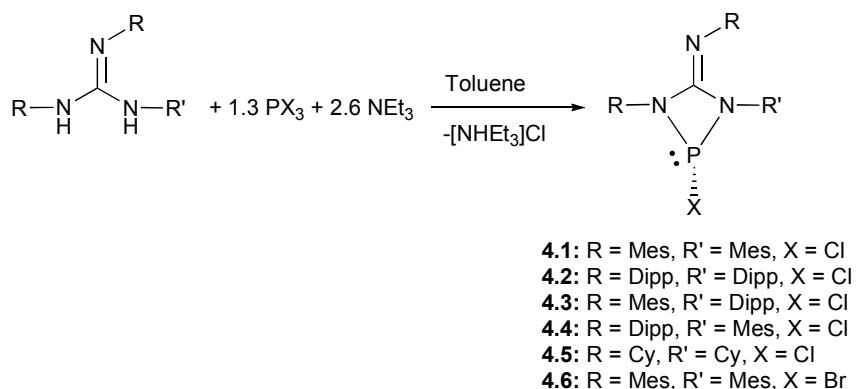
NMR spectroscopy and will not be discussed further. Single crystals of **2**, **4** and **5** were obtained and subsequent X-ray diffraction studies confirmed the synthesis of the guanidines in good to low yields (73, 58 and 33 %, respectively; see Figure 4.5). Synthesis of *N,N',N''*-tris(cyclohexyl)guanidine (**6**) followed the reported facile procedure of Richeson *et al.* where cyclohexylamine and *N,N'*-dicyclohexylcarbodiimide are combined and heated at 90 °C in hexane in a pressure tube for two days.⁴⁷



Scheme 4.1: Synthetic route for *N,N',N''*-tris(*aryl*)guanidines (**2-5**).

The sequential addition of PCl_3 and NEt_3 to a toluene solution of *N,N',N''*-tris(*aryl*)guanidine (**2-5**) or *N,N',N''*-tris(cyclohexyl)guanidine (**6**) (Scheme 4.2) in a 1.3:2.6:1 stoichiometry at room temperature generated copious amounts of white precipitate. Aliquots of the reaction mixture were sampled every hour and analyzed by $^{31}\text{P}\{^1\text{H}\}$ NMR spectroscopy, which in all cases showed the emergence of signals ($\delta_{\text{P}} = 178\text{--}181$) shifted upfield from PCl_3 ($\delta_{\text{P}} = 220$), consistent with the chemical shifts reported for diaminochlorophosphines (*cf.* $\delta_{\text{P}} = 102\text{--}210$).^{25,29,48-51} A distinct difference in reaction completion times emerged based on the steric bulk of the ligands; when the steric demand was increased, reaction times were correspondingly longer from 1 (**2,4-6**) to 12 (**3**) hours. Upon no further change in the $^{31}\text{P}\{^1\text{H}\}$ NMR spectra, the reaction mixtures were filtered or centrifuged. Removal of the volatiles of the supernatant *in vacuo* gave light yellow powders in all cases. Further washing of the powders with CH_3CN yielded white powders, which were sampled for multinuclear NMR spectroscopic analysis, where the $^{31}\text{P}\{^1\text{H}\}$ NMR spectra showed only a single peak identical to that observed for their respective reaction mixtures, with the exception of **4.3**. The initial reaction mixture of **4.3** taken after 1 h showed the emergence of two peaks ($\delta_{\text{P}} = 178$ and 181) with equal intensities, no change was observed in the $^{31}\text{P}\{^1\text{H}\}$ NMR

spectrum after continuing to monitor the reaction for 24 h. The purified product had a single resonance ($\delta_p = 181$). The proton NMR spectrum of crude **4.3** supported the conclusion that two products were present based on the extra resonances observed when compared to a spectrum of pure **4.3** at $\delta_p = 181$. Presumably the products at $\delta_p = 178$ and 181 were the symmetric and asymmetric chelating guanidinate, respectively (Chart 4.4). Single crystals of the product with a phosphorus chemical shift of 181 ppm were grown, which confirmed an asymmetric chelating guanidinate (Chart 4.4b). In an attempt to isomerize to one product, an aliquot of the reaction mixture was transferred to an NMR tube and heated at 90 °C overnight. The $^{31}\text{P}\{^1\text{H}\}$ NMR spectrum revealed that two peaks were still present in approximately the same ratio, but that the resonances had now shifted downfield approximately 30 ppm to $\delta_p = 210.9$ and 211.1. There were no observable N–H peaks in the ^1H NMR spectra of **4.1–4.5** and the IR spectra of the solids lacked N–H vibrations in the range of $\nu = 3100\text{--}3500\text{ cm}^{-1}$.^{44,52} Given these data, the compounds were assigned as the diaminochlorophosphines **4.1–4.5** isolated in low to good yields. X-ray quality crystals were grown from samples of the bulk powders for **4.1–4.4** and subsequent X-ray diffraction experiments confirmed the synthesis of the strained, four-membered, cyclic diaminochlorophosphines (Figure 4.6).



Scheme 4.2: General method for synthesizing halophosphines with (dianionic)guanidinate ligands.

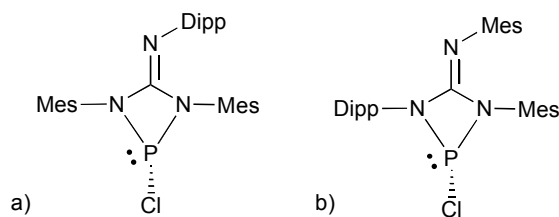


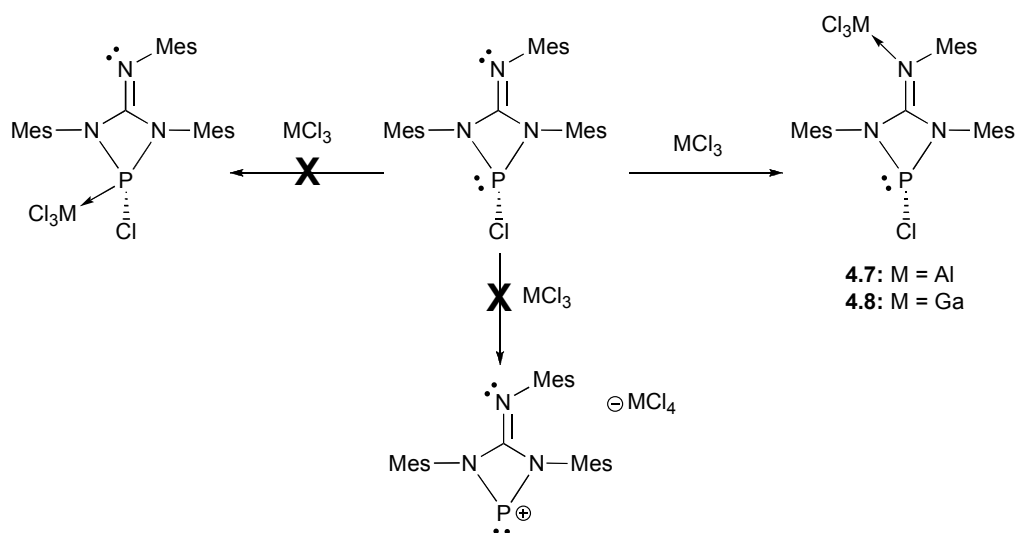
Chart 4.4: (a) Symmetric and (b) asymmetric chelating guanidates for **4.3**.

4.2.2 Reactivity

Given the strained nature of these ring systems, we surmised that conversion to the NHP would generate highly reactive cationic phosphorus centres. This transformation was attempted using several metathetical reagents, including a variety of triflate salts (EOTf; E = Me₃Si, Ag, Na, Li). A stoichiometric amount of Me₃SiOTf was added to CH₂Cl₂ solutions of **4.1-4.5** and reaction mixtures were monitored by ³¹P{¹H} NMR spectroscopy. At room temperature for **4.1-4.4** no change was detected over the course of 7 days, even after the addition of excess amounts of Me₃SiOTf. Identical reaction mixtures were heated to 100 °C in toluene and monitored by ³¹P{¹H} NMR spectroscopy, which showed the slow evolution of multiple products, with one peak downfield of the diaminochlorophosphines at δ_P = 211, indicative of the generation of the phosphetidine Cl₂P₂N₂Mes₂ (*vide infra*).⁴⁹ Analogous results were observed using the sources of metal triflates with **4.1** over 7 days at 100 °C. Only compound **4.1** was employed as a model system in subsequent reactivity studies given the simplicity of its solution ¹H NMR spectrum. In the case of **4.5** many signals were observed in the ³¹P{¹H} NMR spectrum after the addition of Me₃SiOTf, which was an indication that several products were produced.

Given the difficulty associated with removing chloride from the diaminochlorophosphines, we looked to the bromo- derivatives, as heavier halides generally undergo more facile metathesis.⁵³ The bromophosphine **4.6** (Figure 4.7) was synthesized in a similar manner to **4.1** (Scheme 4.2) and subjected to identical metathesis conditions. Again no reaction or multiple products were observed, none of which corresponded to a downfield chemical shift expected of an NHP in the ³¹P{¹H} NMR spectra.

Given the puzzling failure of the salt metathesis routes, the Lewis acids AlCl_3 and GaCl_3 were employed as halide abstracting reagents for **4.1**. These reactions were also monitored by $^{31}\text{P}\{^1\text{H}\}$ NMR spectroscopy and revealed the formation of single products with upfield chemical shifts ($\Delta\delta_{\text{P}} \approx 10$, Table 4.1). The volatiles were removed *in vacuo* and the bulk powders were redissolved in CDCl_3 to obtain the ^1H NMR spectra, which in both cases showed sharp peaks indicating that there was no longer a slow exchange process on the NMR time scale, and furthermore that symmetry within the molecule had been lost. Given the upfield chemical shift in the $^{31}\text{P}\{^1\text{H}\}$ NMR spectra and the lack of symmetry noted in the ^1H NMR spectra, it was hypothesized that halide abstraction was not effected, rather a Lewis acid (AlCl_3 , GaCl_3)/Lewis base (N or P) adduct was formed (Scheme 4.3). Single crystals suitable for X-ray diffraction studies were obtained for the product containing AlCl_3 and the solid-state structure confirmed an $\text{N} \rightarrow \text{Al}$ adduct of AlCl_3 from the exocyclic nitrogen of the guanidinate ligand (**4.7**, Figure 4.7). Although suitable single crystals for X-ray diffraction studies could not be grown for the GaCl_3 adduct (**4.8**) an identical structure was assigned based on identical ^1H NMR spectra and similar chemical shifts in the $^{31}\text{P}\{^1\text{H}\}$ NMR spectra.



Scheme 4.3: Lewis acid/Lewis base adduct formation of **4.7** and **4.8**.

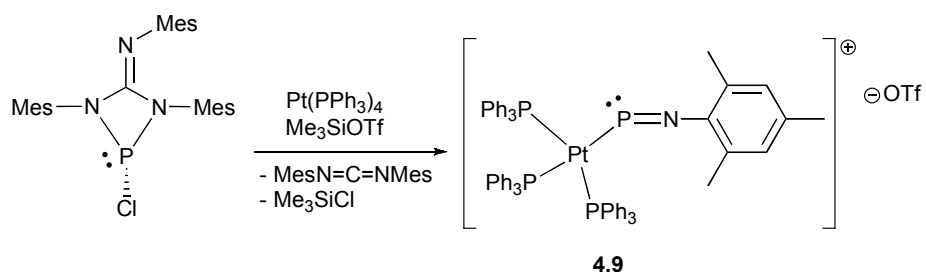
Given the production of **4.7** and **4.8**, two stoichiometric equivalents of AlCl_3 were added to a CH_2Cl_2 solution of **4.1** at rt, where it was envisaged that the exocyclic nitrogen

could be blocked and the second Lewis acid would be free to abstract the chloride ion. After 24 h **4.7** was completely consumed and two phosphorus resonances at $\delta_p = 165$ and 184 were observed. The volatiles were removed *in vacuo* and an orange powder was isolated. A sample of the powder was redissolved in CDCl_3 and a ^1H NMR spectrum of the crude material was obtained, which confirmed the presence of multiple products none of which could be isolated separately.

It should be noted that while halide abstraction with these four-membered diaminochlorophosphines appear to be non-trivial, the analogous reaction of those with unsaturated five-membered rings are generally facile.^{28,54-58} One major difference between these two species is the additional stabilization gained from the delocalization of a 6π -electron system in the case of the five-membered ring, contrary to the 4π -electrons present in the four-membered ring. While aromaticity is not a necessity for the isolation of NHPs^{25,34,35,37,38,48} and has been found to be a weak factor in their stabilization,⁵⁶ the lack thereof in our four-membered diaminochlorophosphines may be a contributing factor to the difficulty in halide abstraction.

Given that the isolation of the free NHP was proving to be a difficult feat, an attempt was made to trap the desired phosphonium cation by reaction with a Pt(0) metal centre (Scheme 4.4), of which several examples with NHP as ancillary ligands are known.^{26,27} The 1:1:1 stoichiometric reaction of **4.1**, $\text{Pt}(\text{PPh}_3)_4$, and Me_3SiOTf was monitored by $^{31}\text{P}\{^1\text{H}\}$ NMR spectroscopy. Combining **4.1** and $\text{Pt}(\text{PPh}_3)_4$ resulted in an orange solution, which had a change in the $^{31}\text{P}\{^1\text{H}\}$ NMR spectrum from a singlet to a downfield triplet with Pt satellites for the phosphorus atom of **4.1** (P_{Cl}) and an upfield doublet with Pt satellites for coordinated PPh_3 (P_{PPh_3}), also free PPh_3 was observed. The splitting pattern was indicative of an AX_2 spin system. The addition of Me_3SiOTf caused a colour change to red and an aliquot sampled for $^{31}\text{P}\{^1\text{H}\}$ NMR spectroscopy showed an upfield shift for the triplet of P_{Cl} , which had broadened out significantly. The volatiles were removed *in vacuo* yielding a red waxy material that became a powder after agitation in hexanes. A sample of the bulk material was used for ^1H NMR spectroscopy, analysis of the spectrum showed the presence of two products (Figure 4.1), one of which was identified as free *N,N'*-bis(Mes)carbodiimide. The other product could be isolated in pure

form from repeated recrystallizations (x2) from DCM/hexanes at $-30\text{ }^{\circ}\text{C}$. X-ray diffraction studies revealed that the phosphorus containing product was actually the iminophosphine complex of $\text{Pt}(\text{PPh}_3)_3$, **4.9** (Figure 4.8).[‡] Although there has been a previous report of cationic iminophosphines acting as ancillary ligands for $\text{Ni}(0)$ and $\text{Pt}(0)$, no solid-state structures have been obtained.⁵⁹



Scheme 4.4: Using $\text{Pt}(0)$ as a trapping agent.

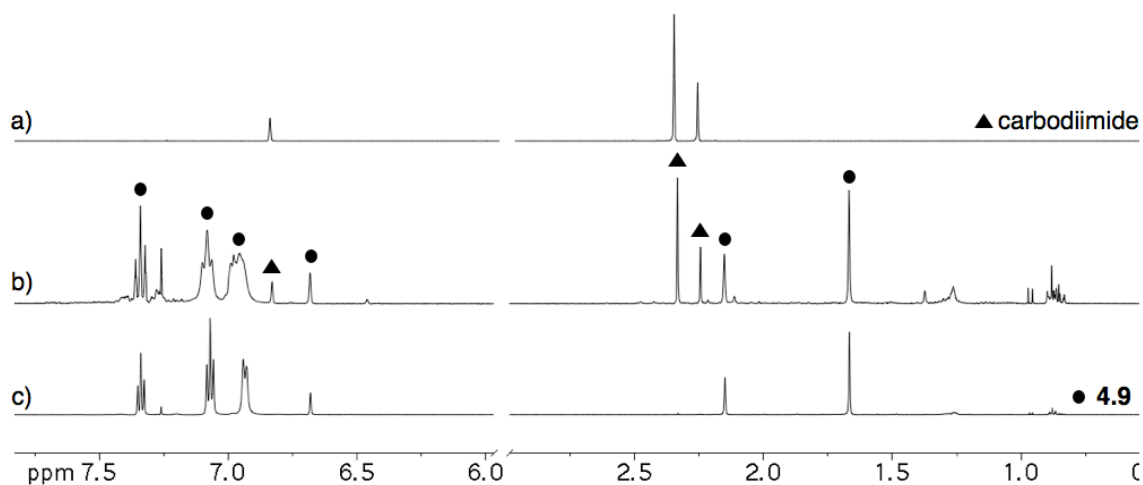
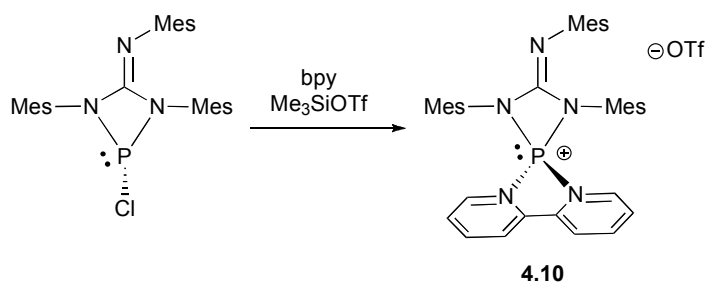


Figure 4.1: Stacked plot of the ^1H NMR spectra for (a) pure N,N' -bis(Mes)carbodiimide, (b) crude **4.9**, and (c) purified **4.9**.

[‡] Several solvents and techniques were attempted for the crystallization of **4.9** and **4.10**, and while X-ray quality single crystals suitable for diffraction studies were grown and the data collected, a highly disordered anion was present in each, which could not be modeled appropriately. The solid-state structures of the cations, confirming the identity and connectivity are presented in Figures 4.8 and 4.7, respectively.

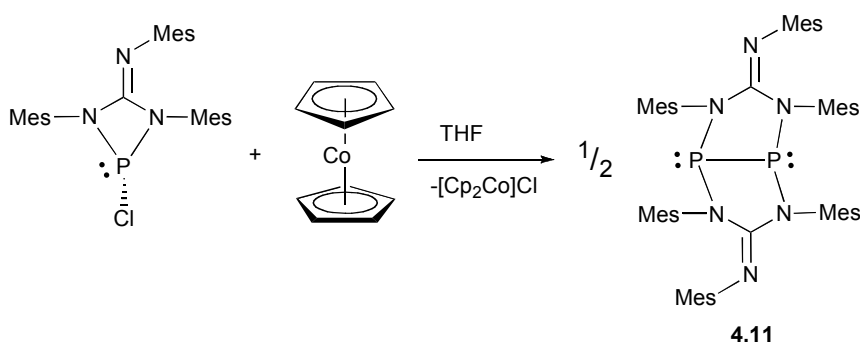
Similar to previous work reported by our group,⁴⁴ we sought to employ a Lewis base to help support the coordinatively unsaturated phosphonium centre. In this regard, one equivalent of 2,2'-bipyridine (bpy) was added to **4.1** followed by the addition of Me₃SiOTf (Scheme 4.5). The colour of the solution changed from colourless to yellow. The ³¹P{¹H} NMR spectrum showed an upfield shift ($\Delta\delta_P = 75$) from **4.1**, as well as a shift corresponding to the starting material, showing no change in intensity between 3 and 24 h. A proton NMR spectrum was collected after removing the volatiles *in vacuo* and showed four resonances corresponding to coordinated bpy, and four resonances for free bpy. The product was purified by redissolving in CH₂Cl₂ and adding hexanes to give an oil, which became a powder after drying *in vacuo*. Multinuclear NMR spectroscopy of the purified material showed a single resonance in the ³¹P{¹H} NMR spectrum at $\delta_P = 106$ and the loss of peaks corresponding to free bpy in the ¹H NMR spectrum. Single crystals were grown and a solid-state structure was obtained, which confirmed that bpy and a dianionic ligand were coordinated to the phosphorus atom to give the base-stabilized cation, **4.10** (Figure 4.7).[‡]



Scheme 4.5: Synthesis of base-stabilized cationic **4.10**.

Jones *et al.* attempted to reduce a dichlorophosphine supported by a bulky (monoanionic)guanidinate with KC₈, anticipating a diphosphene, however the result was many non-isolable phosphorus containing products.³⁹ In this context, we investigated the reactivity of **4.1** with the one-electron reducing agent cobaltocene (Cp₂Co). The 1:1 stoichiometric reaction of **4.1** and Cp₂Co in THF at room temperature (Scheme 4.6) produced copious amounts of green precipitate ([Cp₂Co]Cl; $\delta_H = 5.9$) and monitoring the reaction by ³¹P{¹H} NMR spectroscopy revealed the production of a single product at $\delta_P = 59$ ($\Delta\delta_P = 123$). The reaction was complete after 48 h, at which time the green

precipitate was separated from the solution by centrifugation, the volatiles were removed from the supernatant *in vacuo*, and washing the product with CH₃CN yielded a white powder. The ¹H NMR spectrum of the white powder in CDCl₃ at room temperature had four signals in the *aryl* region and five methyl resonances, however if the sample was cooled to -50 °C, six *aryl* and nine methyl signals were observed. X-ray diffraction studies revealed that reductive coupling had occurred, resulting in a dimeric structure with μ -*N,N'* bridging guanidinate for **4.11** (Figure 4.9).



Scheme 4.6: Redox reaction for the synthesis of **4.11**.

The thermal stability of the cyclic four-membered diaminochlorophosphines (**4.1-4.4**) was investigated given the multiple instances of a peak emerging at $\delta_P \approx 211$ upon heating of these species. This was accomplished by heating a toluene solution of **4.1** at 90 °C overnight to deduce what had occurred. Resembling the attempted isomerization of **4.3** and halide abstraction of **4.1-4.4**, a 30 ppm downfield chemical shift was noted in the ³¹P{¹H} NMR spectrum after 2 days at 90 °C, giving a singlet at $\delta_P = 211$. The product was waxy after the volatiles were removed *in vacuo*, but became a white powder after stirring in pentane for 5 min. Decanting the supernatant and drying the powder under reduced pressure yielded pure product as evidenced by ¹H NMR spectroscopy, which showed a drastically simplified spectrum (Figure 4.2). X-ray diffraction studies revealed that the product was indeed the dichlorodiazadiphosphetidine, **4.12** (Figure 4.9). The proposed route from **4.1** to **4.12** is by elimination of *N,N'*-bis(Mes)carbodiimide resulting in a chloro(2,4,6-trimethylphenylimino)phosphine (MesNPCl), which dimerizes to give a dichlorodiazadiphosphetidine.⁶⁰ An analogous dichlorodiazadiazetidine, [$\{2-(6\text{-Me})\text{C}_5\text{H}_3\text{N}\}\text{NAsCl}\}_2$], has been observed by the thermal elimination of Me₃SiCl from

[{2-(6-Me)C₅H₃N}NSiMe₃]AsCl₂.⁴² The thermally induced removal of a carbodiimide fragment from guanidinato molecular species has been comprehensively studied by Barry *et al.* and is a known pathway in their thermal decomposition.^{61,62} While **4.12** was the major product from heating **4.1**, there was a minor product at $\delta_P = 140$. This species could be isolated from collecting the CH₃CN washes of **4.12**. Single crystals suitable for X-ray diffraction studies revealed that the minor product was actually a dinuclear compound featuring a μ -*N,N'* bridging guanidinate and a bridging N–Mes (Scheme 4.7), **4.13** (Figure 4.9). Heating a NMR tube charged with **4.1** in a CDCl₃ solution at 90 °C overnight in an oil bath also produces **4.13** in nearly quantitative yields (92%) according to the ³¹P{¹H} NMR spectrum. Possible routes for the ring expansion are proposed as either: (a) ring opening of **4.1** to dimerize with MesNPCl; or, (b) insertion of *N,N'*-bis(Mes)carbodiimide into a P–N bond of **4.12** (Scheme 4.8). To elucidate the likely reaction pathway this reaction was monitored by ³¹P{¹H} NMR spectroscopy where a spectrum was collected every hour for 43 h (Figure 4.3). It was determined that **4.12** was a short-lived intermediate in the reaction when CDCl₃ was used as the solvent (Figure 4.3), as the reaction appeared to be solvent dependent.[‡] Regardless if the route followed proposed mechanism (a) or (b), a 1:1 stoichiometric ratio of **4.13** and carbodiimide should be observed in the ¹H NMR spectrum of the crude material upon the completion of the reaction, which is indeed the case (Figure 4.4). Given that the reaction between isolated **4.12** and *N,N'*-bis(Mes)carbodiimide (Scheme 4.8b, Eq. 4.2c) in various stoichiometries (1:1, 1:2, 1:5), solvents and temperatures (toluene (90 °C), xylene (140 °C) and CDCl₃ (90 °C)) gave no change in the signals observed within the ³¹P{¹H} NMR spectra, it was deduced that the mechanism most likely follows route (a). This is similar to the Lewis acid induced oligomerization observed by Burford *et al.*, where an iminophosphine, in equilibrium with the corresponding phosphetidine, is formally inserted into a phosphazane.⁶³

[‡] It was observed experimentally that **4.13** was produced in significantly higher yields and shorter time if CDCl₃ was used as the solvent compared to toluene. However, no further solvent dependency experiments were conducted.

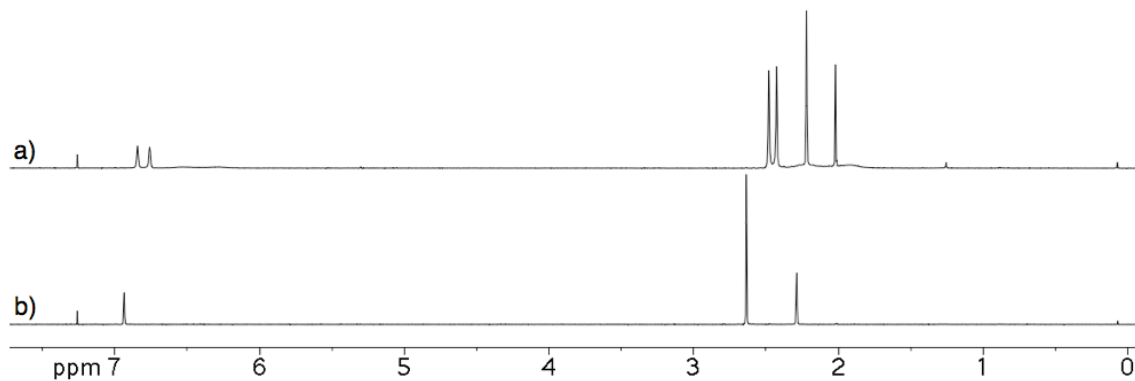
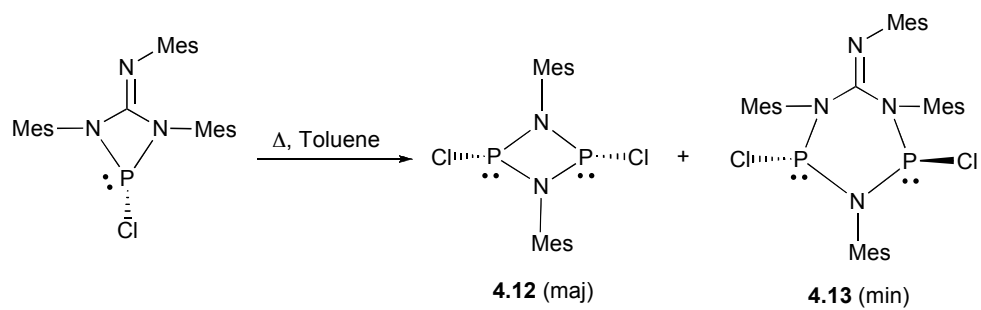
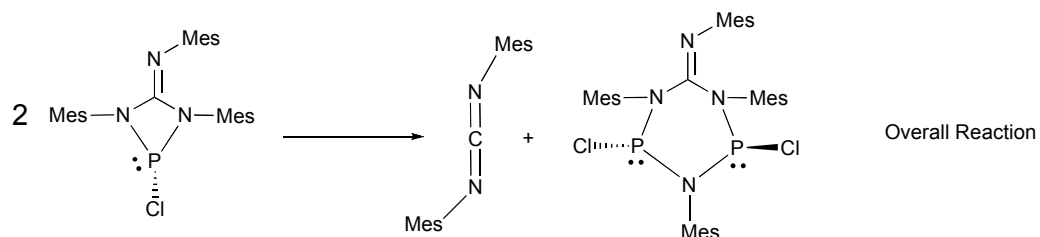
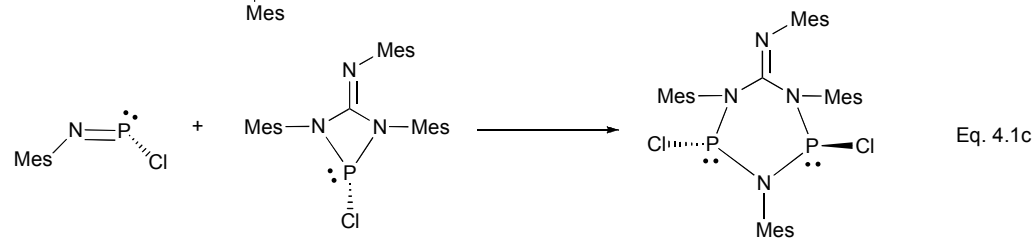
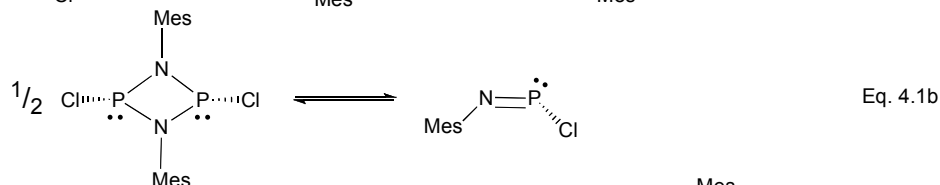
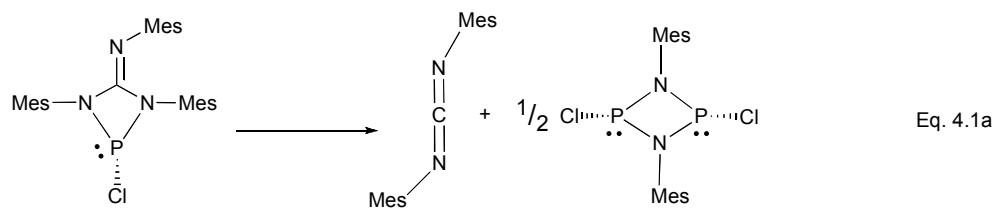


Figure 4.2: Stacked plot of the ^1H NMR spectra for (a) 4.1 and (b) 4.12.

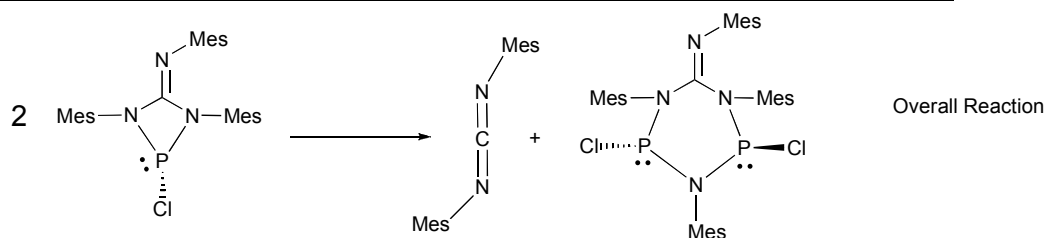
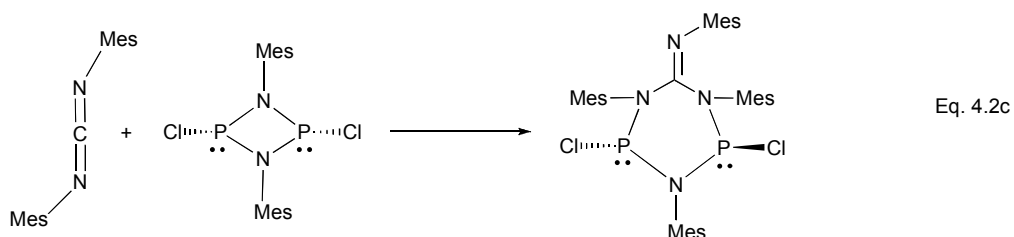
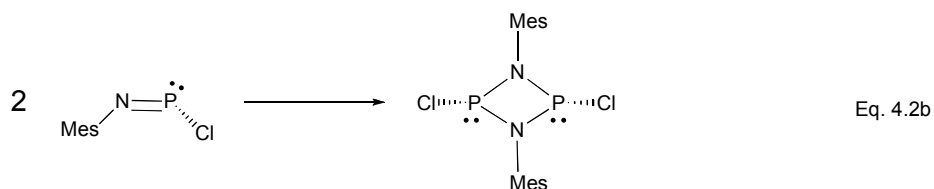
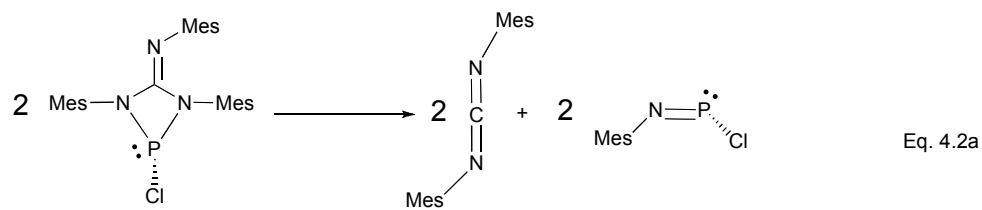


Scheme 4.7: Carbodiimide elimination and ring expansion producing 4.12 and 4.13.



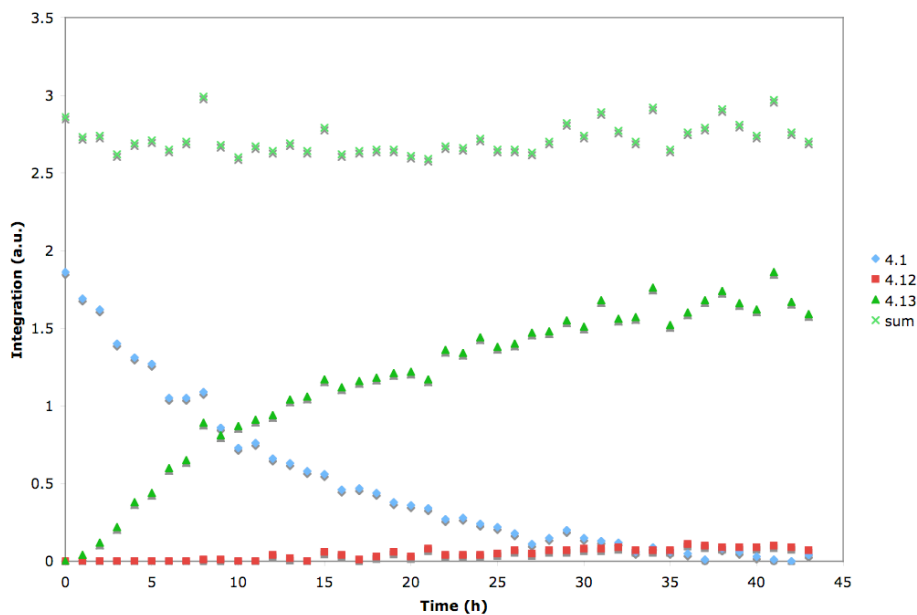
Scheme 4.8a: Proposed route to **4.13** by insertion of MesNPCl.

Reaction pathway for the insertion of MesNPCl into a P–N bond of **4.1**. Following the individual steps: (Eq. 4.1a) the thermal ejection of carbodiimide from **4.1** to give phosphetidine **4.12**; (Eq. 4.1b) monomer/dimer equilibrium of **4.12** and MesNPCl; and, (Eq. 4.1c) the insertion of MesNPCl into a P–N bond of **4.1** to give **4.13**. Overall, the reaction starts with two equivalents of **4.1** and ends with equal equivalents of carbodiimide and **4.13**.

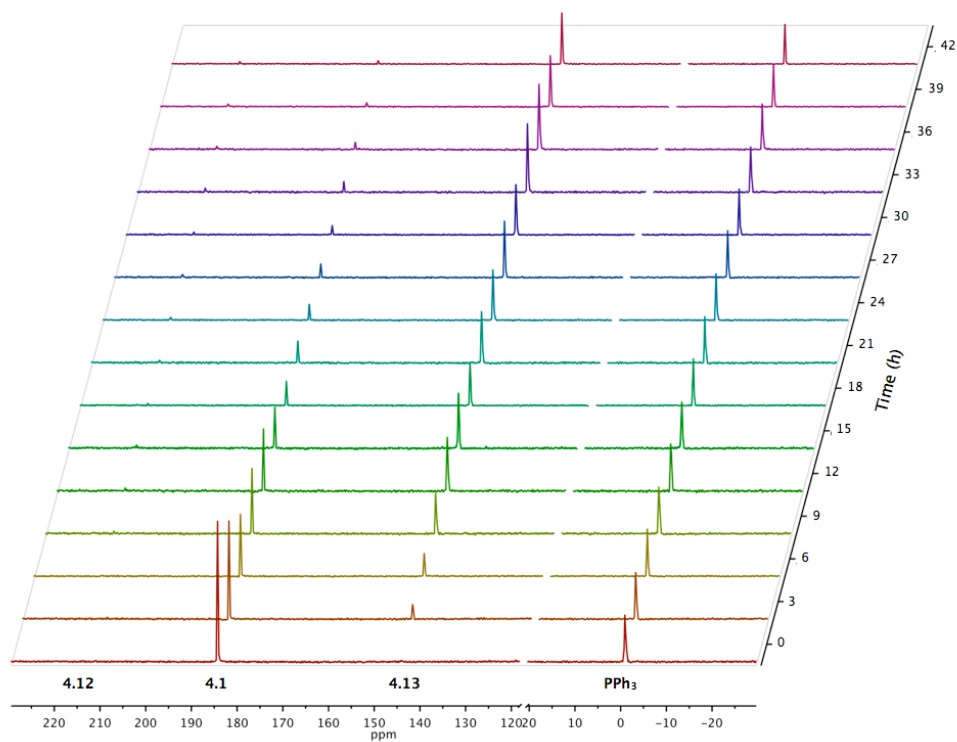


Scheme 4.8b: Proposed route to **4.13** by insertion of carbodiimide.

Reaction pathway for the insertion of carbodiimide into a P–N bond of **4.12**. Following the individual steps: (Eq. 4.2a) the thermal ejection of carbodiimide from **4.1** to give MesNPCl; (Eq. 4.2b) dimerization of MesNPCl to **4.12**; and, (Eq. 4.2c) the insertion of carbodiimide into a P–N bond of **4.12** to give **4.13**. Overall, the reaction starts with two equivalents of **4.1** and ends with equal equivalents of carbodiimide and **4.13**.



a)



b)

Figure 4.3: (a) Plot of the integration of δ_p **4.1**, **4.12**, and **4.13** relative to normalized PPh_3 and the sum of the integrations as a function of time. (b) Stacked plot of $^{31}\text{P}\{^1\text{H}\}$ NMR spectra for monitoring the production of **4.13** from **4.1** in CDCl_3 .

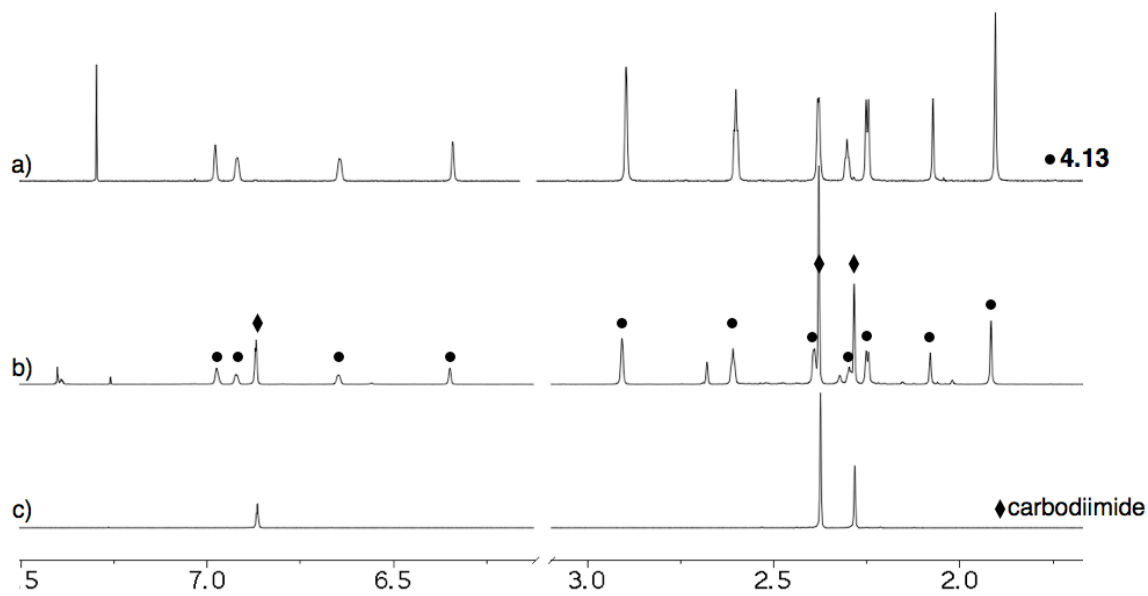


Figure 4.4: Stack plot of ¹H NMR spectra for (a) pure **4.13**, (b) crude completed ring expansion, and (c) pure *N,N'*-bis(Mes)carbodiimide.

4.2.3 X-ray crystallographic studies

Selected bond lengths (Å) and bond angles (°) of compounds characterized by single crystal X-ray diffraction studies are given in Tables 4.1-4.3. Refinement details are summarized in Tables 4.4 and 4.5.

Solid-state structures of **2**, **4** and **5** were obtained by X-ray diffraction studies and are shown in Figure 4.5. Due to the low quality data obtained from the best of the examined crystals for **5**, the metrical parameters will not be discussed. However, the solution and refinement of the structure confirmed the identity and atom connectivity in **5**. The key metrical parameters of **2** and **4** are that the central carbon atom, C(1), has a trigonal planar geometry ($\Sigma_{\text{ang}} = 360$ and 361° , respectively), a localized double bond (C(1)–N(3) 1.314(3) and 1.287(2) Å, respectively), and two C–N single bonds (C(1)–N(1) 1.364(3) and 1.376(2); and C(1)–N(2) 1.426(3) and 1.375(2)). The *aryl* substituents of compounds **2**, **4** and **5** give these molecules a propeller-type shape.

Single crystals suitable for X-ray diffraction studies were grown for compounds **4.1-4.4** and **4.6** by various techniques and solvent combinations. The solid-state

structures of **4.1-4.4** (Figure 4.6) and **4.6** (Figure 4.7) are analogous and were all crystallized in the monoclinic $P2_1/c$ space group. In all cases, the coordination of the guanidinate ligand to phosphorus is κ^2-N,N' chelating, which generates a strained four-membered ring. The N–P–N bond angles range from $75.73(7)$ – $78.61(7)^\circ$, which are on the smaller end of the scale compared to other similar four-membered rings derived from chelating nitrogen-based ligands on phosphorus (*cf.* 70.66 – 120.72° , mean[§] = 87.21°).⁶⁴ The metrical parameters of the guanidinate ligands further confirmed its dianionic nature in **4.1-4.4** and **4.6**. The C–N_{endo} bond lengths within the ring are consistent with carbon-nitrogen single bonds C(1)–N(1) $1.403(2)$ – $1.437(2)$ Å and C(1)–N(2) $1.410(3)$ – $1.477(2)$ Å (*cf.* 1.42 (avg) Å)⁴⁷ while the C–N_{exo} bond lengths are representative of a carbon-nitrogen double bond C(1)–N(3) $1.249(3)$ – $1.261(2)$ Å (*cf.* 1.28 Å).⁴⁷ The exocyclic nitrogen N(3) has a stereochemically active lone pair and the *aryl* substituent on N(3) in **4.3** and **4.4** resides on the side of the endocyclic nitrogen bearing the substituent with the least bulk to minimize steric interactions in the case of the heteroleptic guanidinate. The expected trigonal planar geometry is observed about C(1) ($\Sigma_{\text{ang}} = 360^\circ$) and a pyramidal geometry about P(1) ($\Sigma_{\text{ang}} = 280.8$ – 287.2°). Short P(1)–Cl(1) bonds are noted for **4.1-4.4** with bond lengths ranging from $2.0476(7)$ – $2.1141(7)$ Å. This is contrary to the characteristically long P–Cl bonds commonly observed for 6π aromatic cyclic diaminochlorophosphines in the larger five-membered ring, attributed to the hyperconjugation of $\pi(\text{C}_2\text{N}_2)$ – $\sigma^*(\text{P}-\text{Cl})$ (*e.g.* 2.24 – 2.70 Å).^{50,56,65} The P–Cl bond lengths are even shorter than acyclic $(\text{NMe}_2)_2\text{PCl}$ ($2.180(4)$).⁶⁶ A possible reason for the failed metathesis reactions is the strong phosphorus-halide bond, reflected in the short P–X (X = Cl, Br ($2.2936(10)$ Å, *cf.* 2.43 – 2.95 Å)^{28,53,55}) bond distance for **4.1-4.4** and **4.6**.

[§] Average result of a query in the CSD for the N–P–N angle of four-membered rings featuring chelating N-based ligands. Accessed 9 November 2011.

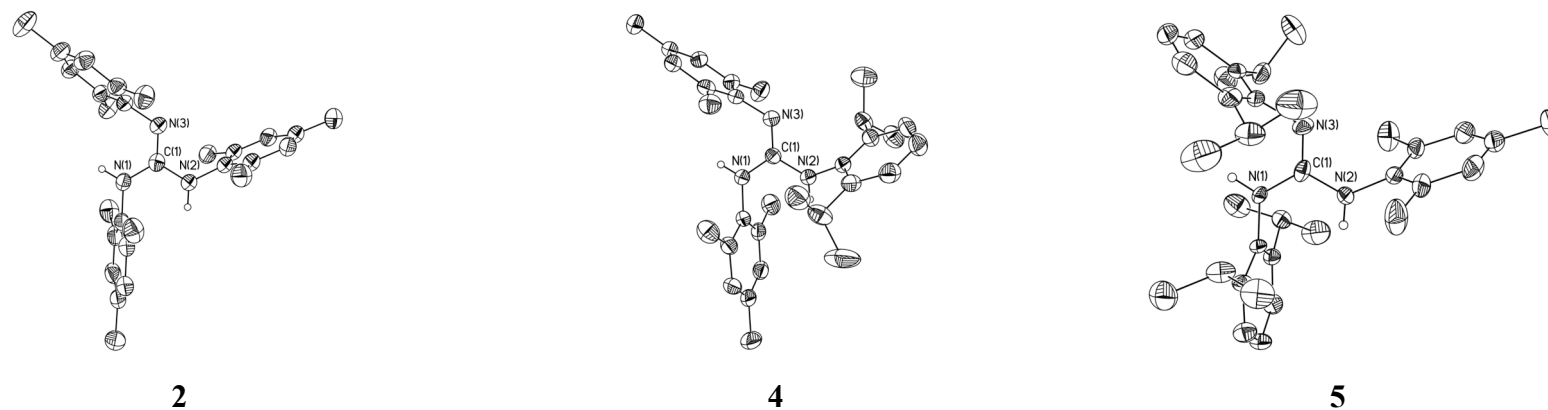
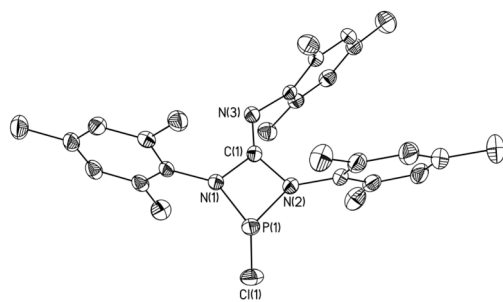


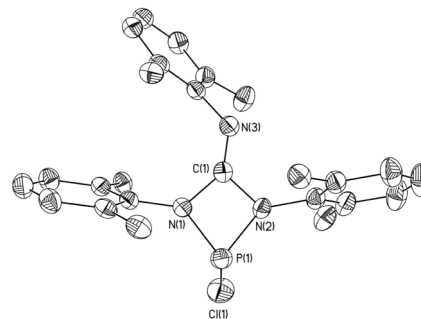
Figure 4.5: Solid-state structures of **2**, **4**, and **5**. Ellipsoids are drawn to 50% probability.

Table 4.1: Selected bond lengths (Å) and bond angles (°) for **2** and **4**.

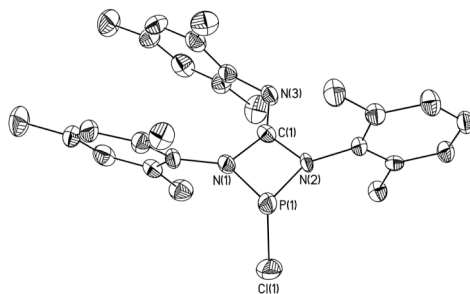
Bond	Compound	
	2	4
C(1)–N(1)	1.364(3)	1.376(2)
C(1)–N(2)	1.426(3)	1.375(2)
C(1)–N(3)	1.314(3)	1.287(2)
N(1)–C(1)–N(2)	117.08(18)	114.50(14)
N(1)–C(1)–N(3)	122.71(18)	125.75(15)
N(2)–C(1)–N(3)	120.21(19)	120.73(15)



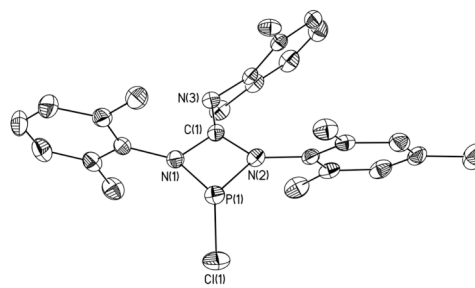
4.1



4.2

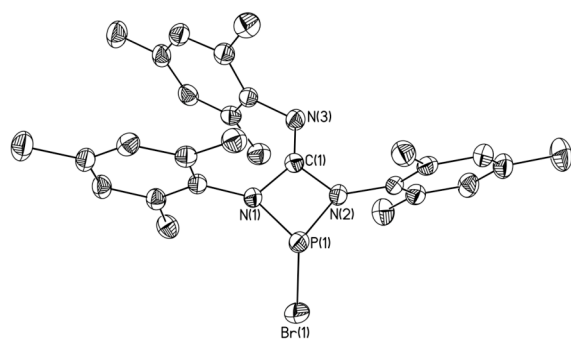


4.3

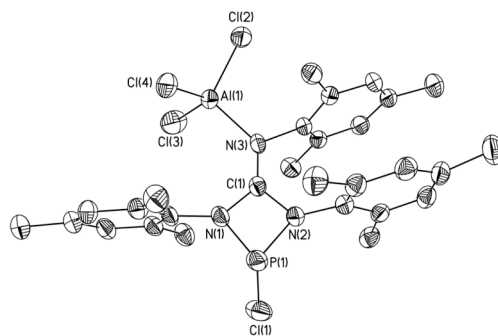


4.4

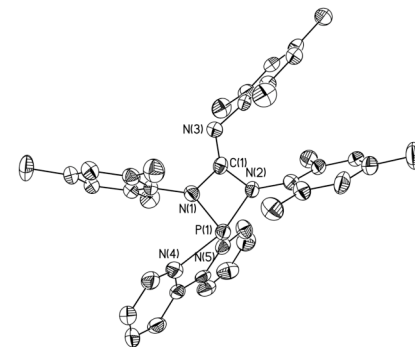
Figure 4.6: Solid-state structures of **4.1-4.4**. Ellipsoids are drawn to 50% probability. The methyl groups on the ⁱPr substituents, and the hydrogen atoms have been omitted for clarity.



4.6



4.7



4.10

Figure 4.7: Solid-state structures of **4.6**, **4.7**, **4.10**. Ellipsoids are drawn to 50% probability. The hydrogen atoms and the triflate anion (**4.10**) have been omitted for clarity.

Table 4.2: Selected bond lengths (Å) and bond angles (°) for **4.1-4.4**, **4.6** and **4.7**.

Compound	4.1	4.2	4.3	4.4	4.6	4.7
Bond	X = Cl	X = Cl	X = Cl	X = Cl	X = Br	X = Cl
P(1)–N(1)	1.7081(14)	1.716(2)	1.717(5)	1.7592(15)	1.722(2)	1.742(3)
P(1)–N(2)	1.7235(15)	1.707(2)	1.690(4)	1.7193(15)	1.711(2)	1.743(3)
C(1)–N(1)	1.403(2)	1.427(3)	1.418(7)	1.437(2)	1.427(3)	1.375(4)
C(1)–N(2)	1.420(2)	1.410(3)	1.433(7)	1.477(2)	1.411(3)	1.398(4)
C(1)–N(3)	1.252(2)	1.249(3)	1.256(7)	1.261(2)	1.255(4)	1.304(4)
P(1)–X(1)	2.1141(7)	2.0936(10)	2.095(3)	2.0476(7)	2.2936(10)	2.0603(15)
N(1)–P(1)–N(2)	75.73(7)	75.88(9)	76.1(2)	78.61(7)	75.97(11)	74.24(12)

The solid-state structure of **4.7** (Figure 4.7) confirmed the atom connectivity of N(3) to Al(1) with a bond length of 1.936(3) Å, which is in the typical range found for other AlCl₃ adducts.^{67,68} Compared to **4.1**, **4.7** has shortened C(1)–N(1), C(1)–N(2) and P(1)–Cl(1) bond lengths and an elongated C(1)–N(3) bond (Table 4.1). The Al–Cl bond lengths have also elongated from 2.068(4) Å in AlCl₃ to 2.1132(16)–2.1304(13) Å in **4.7**.⁶⁹ Endocyclic N(1) has a trigonal planar geometry with the $\Sigma_{\text{ang}} = 359.9^\circ$, while for N(2) $\Sigma_{\text{ang}} = 349.8^\circ$. The Mes substituent on N(3) residing above, thus causes a slight pyramidalization of N(2) to decrease steric interactions.

The refined solid-state structure of **4.9** contained a highly disordered triflate anion that could not be resolved, which resulted in a large amount of unaccounted electron density and therefore the metrical parameters cannot be discussed with confidence. Nevertheless the isotropic solid-state structure of the cationic fragment is shown in Figure 4.8, which confirms the identity and atom connectivity of the cation. The bent geometry at P(1) suggests that there is a stereochemically active non-bonding lone pair present, which gives rise to three possibilities for describing the bonding within **4.9** (Chart 4.5); (i) a metal-phosphide bond;^{25,27} (ii) a metalla-phosphine bond in which the Pt–P may be represented as a $M \rightarrow L$ donor-acceptor bond,³² where L is an iminophosphenium; and, (iii) a metalla-phosphine bond ($M \rightarrow L$), where L is a monophosphadiazonium. The Pt geometry appears to be a distorted tetrahedron with bond angles ranging from 99.9–117.6° and has a Pt–P⁺ bond length of 2.17 Å. The P–N bond is 1.45 Å, which could be indicative of a high degree of triple bond character (*cf.* P–N = 1.495(4) in CIPNMes* and 1.476 in [P≡NH]⁺)⁷⁰ and the N–C bond is 1.36 Å, which is between that of a single and double bond. The bond lengths about nitrogen suggest that there is electron delocalization within the iminophosphenium, which is consistent with the linear geometry. These bond lengths, bond angles and geometry descriptions are consistent with a bonding model that is between that of ii) and iii). Given the uncertainty of the metrical parameters, these bond lengths and bond angles are more qualitative descriptions for **4.9**.

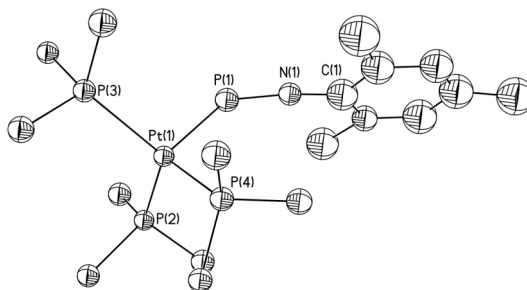


Figure 4.8: Isotropic solid-state structure of cation **4.9**. Ellipsoids are drawn to 30% probability.

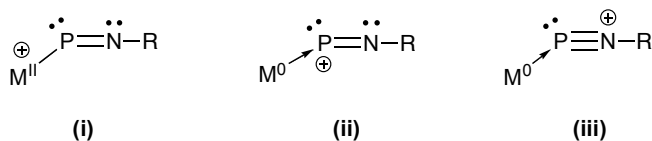


Chart 4.5: Possible bonding descriptions of **4.9**.

The most notable structural change of **4.1** upon its reaction with Cp_2Co to form **4.11** (Figure 4.9) is the switching of the coordination mode of the guanidinate ligand from κ^2 - N,N' chelating to μ - N,N' bridging. The dianionic nature of the ligand is retained in the bridging mode, as indicated by the carbon-nitrogen bond lengths. The P(1)–P(2) bond length is 2.2251(14) Å, which is similar to an analogous structure with μ - N,N' bridging ureas (P–P 2.222(2) Å),⁷¹ and consistent with typical P–P single bond lengths^o (*cf.* 2.21 Å).⁶⁴ Unlike the planar $\text{As}_2\text{N}_4\text{C}$ bicyclic fragment in the (monoanionic)guanidinate-bridged diarsene ($[\text{As}_2\{\mu\text{-(ArN)}_2\text{-CR}\}_2]$; Ar = Dipp; R = $\text{N}(\text{C}_6\text{H}_{11})_2$, N^iPr_2 , $t\text{Bu}$),³⁹ **4.11** has a puckered arrangement of the two five-membered $\text{P}_2\text{N}_2\text{C}$ rings, where the two planes are 100.4° to each other (Figure 4.9). The molecular geometry about the phosphorus atoms is trigonal pyramidal with a stereochemically active lone pair of electrons indicative of an AX_3E electron pair geometry.

^o Mean value observed for P–P single bonds in literature based on a CSD search on 21 November 2011.

Compound **4.12** has an analogous structure (Figure 4.9) to dihalodiazadiphosphetidines ((XPNR)₂; X = Cl, R = Ph⁷², Dipp⁴⁹; R = Dmp⁷³, X = Br, Cl) previously reported with the chlorines arranged in a *cis* fashion and the *aryl* substituents oriented in a perpendicular fashion (74.6° avg.) to the P–N–P–N plane. The four-membered ring in **4.12** deviates from planarity by 0.0571 Å.

The solid-state structure of **4.13** revealed that a ring expansion of **4.1** had occurred (Figure 4.9). This was most likely the result of a monomeric chloro(imino)phosphine unit inserting into a P–N bond in **4.1**.⁶³ Upon ring expansion the coordination of the guanidinate ligand changes from κ^2 -*N,N'* chelating to μ -*N,N'* bridging and retains its dianionic charge as indicated by the C(1)–N bond lengths (C(1)–N(1) 1.411(3) Å, C(1)–N(2) 1.416(3) Å, C(1)–N(3) 1.270(3) Å; Table 4.3). The P(1)–Cl(1) and P(2)–Cl(2) bond lengths are 2.1228(11) and 2.1290(12) Å, respectively, and are significantly longer than in **4.1**. Unlike the phosphetidine **4.12**, the chlorine atoms in **4.13** are in a *trans* conformation and the ring is puckered with a mean deviation from the plane of 0.1425 Å, compared to nearly planar **4.12** with a mean deviation from the plane of 0.0571 Å. The P–N bonds range from 1.688(2)–1.704(2) Å, which are shorter than **4.1** (1.7081(14)–1.7235(15) Å) and longer than that of a monomeric chloro(imino)phosphine (P–N 1.495(4) Å for Cl–P=N–Mes*, Mes*=2,4,6-tri-*tert*-butylphenyl).⁷⁰

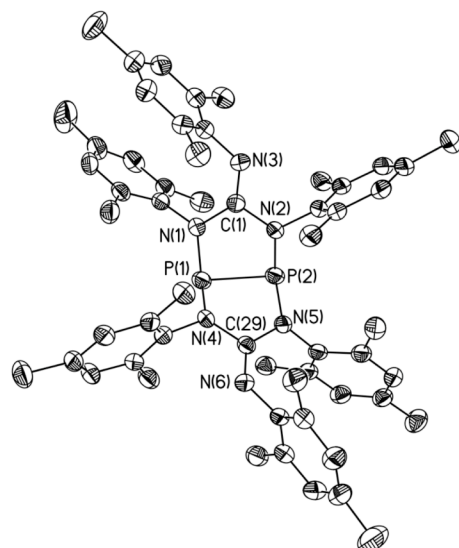
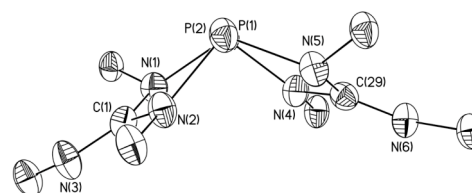
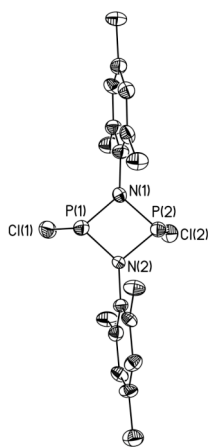
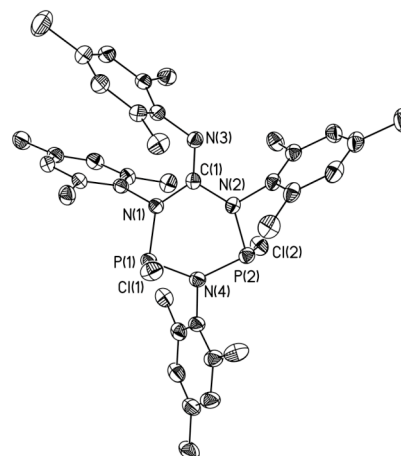
**4.11****4.11** along P-P bond**4.12****4.13**

Figure 4.9: Solid-state structures of **4.11-4.13**. Ellipsoids are drawn to 50% probability. Hydrogen atoms and solvates have been omitted for clarity. The view along the P-P bond of **4.11** has all but the *ipso* carbons removed from the Mes substituents for simplicity.

Table 4.3: Selected bond lengths (Å) and bond angles (°) for **4.11-4.13**.

Compound	4.11	4.12	4.13
Bond			
P(1)–N(1)	1.725(3)	1.705(4)	1.696(2)
P(1)–N(4)	1.725(3)	1.694(4)	1.688(2)
P(2)–N(n)	n = 2; 1.729(3)	n = 1; 1.711(4)	n = 2; 1.701(2)
P(2)–N(n)	n = 5; 1.721(3)	n = 2; 1.705(4)	n = 4; 1.704(2)
P(1)–Cl(1)	–	2.110(2)	2.1228(11)
P(2)–Cl(2)	–	2.1112(19)	2.1290(12)
C(1)–N(1)	1.419(5)	–	1.411(3)
C(1)–N(2)	1.409(4)	–	1.416(3)
C(1)–N(3)	1.265(5)	–	1.270(3)
C(29)–N(4)	1.415(4)	–	–
C(29)–N(5)	1.424(4)	–	–
C(29)–N(6)	1.266(4)	–	–
P(1)–P(2)	2.2251(14)	–	–
N(1)–C(1)–N(2)	111.7(3)	–	114.7(2)
N(4)–C(29)–N(5)	110.9(3)	–	–
N(1)–P(1)–N(n)	n = 4; 108.28(15)	n = 2; 82.0(2)	n = 4; 101.36(10)
N(2)–P(2)–N(n)	n = 5; 108.67(15)	n = 1; 81.47(19)	n = 4; 100.52(10)
N(1)–P(1)–Cl(1)	–	103.86(17)	101.68(8)
N(n)–P(1)–Cl(1)	–	n = 2; 104.23(16)	n = 4; 101.13(9)
N(n)–P(2)–Cl(2)	–	n = 1; 104.37(16)	n = 4; 100.17(8)
N(2)–P(2)–Cl(2)	–	103.00(16)	105.86(8)
P(1)–N(n)–P(2)	–	n = 1; 97.4(2)	n = 4; 128.25(12)
P(1)–N(2)–P(2)	–	98.1(2)	–

Table 4.4: X-ray details for **2**, **4**, **4.1-4.4**.

Compound	2	4	4.1	4.2	4.3	4.4
empirical formula	C ₂₈ H ₃₅ N ₃	C ₃₁ H ₄₁ N ₃	C ₂₈ H ₃₃ Cl ₁ N ₃ P ₁	C ₃₇ H ₅₁ Cl ₁ N ₃ P ₁	C ₃₁ H ₃₉ Cl ₁ N ₃ P ₁	C ₃₄ H ₄₅ Cl ₁ N ₃ P ₁
FW (g/mol)	413.59	455.67	477.99	604.23	520.07	562.15
crystal system	Trigonal	Monoclinic	Monoclinic	Monoclinic	Monoclinic	Monoclinic
space group	$R\bar{3}$	$P2_1/c$	$P2_1/c$	$P2_1/c$	$P2_1/c$	$P2_1/c$
<i>a</i> (Å)	37.575(5)	12.679(3)	8.6540(5)	15.829(3)	20.468(2)	10.744(2)
<i>b</i> (Å)	37.575(5)	15.506(3)	26.8867(14)	11.199(2)	9.2821(10)	15.331(3)
<i>c</i> (Å)	8.9153(18)	16.460(6)	12.6400(6)	24.175(8)	15.5195(18)	22.699(6)
α (deg)	90	90	90	90	90	90
β (deg)	90	123.40(2)	115.843(3)	125.42(2)	92.061(4)	118.03(2)
γ (deg)	120	90	90	90	90	90
<i>V</i> (Å ³)	10901(3)	2701.6(13)	2646.9(2)	3492.3(15)	2946.6(6)	3300.3(12)
<i>Z</i>	18	4	4	4	4	4
<i>D_c</i> (mg m ⁻³)	1.134	1.120	1.199	1.149	1.172	1.131
<i>R</i> _{int}	0.0190	0.0255	0.0787	0.0578	0.0827	0.0756
<i>R</i> 1[<i>I</i> > 2σ(<i>I</i>)] ^a	0.0683	0.0681	0.0422	0.055	0.0894	0.0371
<i>wR</i> 2(<i>F</i> ²) ^a	0.2062	0.1789	0.1035	0.1687	0.2347	0.1026
GOF (<i>S</i>) ^a	1.098	1.097	1.016	1.069	1.126	1.029

^a $R1(F[I > 2(I)]) = \sum || |F_o| - |F_c| || / \sum |F_o|$; $wR2(F^2 [all data]) = [w(F_o^2 - F_c^2)^2]^{1/2}$; $S(all data) = [w(F_o^2 - F_c^2)^2 / (n - p)]^{1/2}$ (*n* = no. of data; *p* = no. of parameters varied; $w = 1/[\sigma^2(F_o^2) + (aP)^2 + bP]$ where $P = (F_o^2 + 2F_c^2)/3$ and *a* and *b* are constants suggested by the refinement program.

Table 4.5: X-ray details for **4.6**, **4.7**, and **4.11-4.13**.

Compound	4.6	4.7	4.11	4.12	4.13
empirical formula	C ₂₈ H ₃₃ Br ₁ N ₃ P ₁	C ₂₈ H ₃₃ Al ₁ Cl ₄ N ₃ P ₁	C ₅₆ H ₆₆ N ₆ P ₁	C ₁₈ H ₂₂ Cl ₂ N ₂ P ₂	C ₂₉ H ₉₄ Cl ₆ N ₁₀ P ₄
FW (g/mol)	522.45	611.32	885.09	399.22	1520.22
crystal system	Monoclinic	Monoclinic	Monoclinic	Monoclinic	Triclinic
space group	<i>P2₁/c</i>	<i>P2₁/c</i>	<i>P2₁/c</i>	<i>P2₁</i>	<i>P</i> $\bar{1}$
<i>a</i> (Å)	8.6103(17)	14.544(3)	15.278(3)	7.5319(15)	11.562(2)
<i>b</i> (Å)	14.299(3)	13.657(3)	21.301(4)	15.796(3)	13.418(3)
<i>c</i> (Å)	21.572(4)	17.327(7)	21.126(7)	8.8077(18)	14.712(3)
α (deg)	90	90	90	90	65.35(3)
β (deg)	91.13(3)	119.39(2)	133.195(17)	109.64(3)	78.17(3)
γ (deg)	90	90	90	90	88.20(3)
<i>V</i> (Å ³)	2655.4(9)	2998.7(15)	5012(2)	986.9(3)	2026.6(7)
<i>Z</i>	4	4	4	2	1
<i>D_c</i> (mg m ⁻³)	1.307	1.354	1.173	1.343	1.246
<i>R</i> _{int}	0.0305	0.0534	0.0609	0.1306	0.1067
<i>R</i> 1[<i>I</i> > 2σ <i>I</i>] ^a	0.0533	0.0557	0.0788	0.0642	0.0606
<i>wR</i> 2(<i>F</i> ²) ^a	0.1424	0.1887	0.23	0.1078	0.1461
GOF (<i>S</i>) ^a	1.056	1.083	1.105	0.983	1.01

^a $R1(F[I > 2(I)]) = \sum || |F_o| - |F_c| || / \sum |F_o|$; $wR2(F^2 [all data]) = [w(F_o^2 - F_c^2)^2]^{1/2}$; $S(all data) = [w(F_o^2 - F_c^2)^2 / (n - p)]^{1/2}$ (n = no. of data; p = no. of parameters varied; $w = 1/[\sigma^2(F_o^2) + (aP)^2 + bP]$ where $P = (F_o^2 + 2F_c^2)/3$ and a and b are constants suggested by the refinement program.

4.2.4 Computational studies[†]

To shed light on the resistance of compounds **4.1-4.6** to halide abstraction, the electronic structures of diaminochlorophosphines **4.5** and **4.14-4.17** (Chart 4.6) were analyzed using density functional theory (DFT) by determining their charge distributions, orbital structures and relative P–Cl bond energies. For comparison, similar calculations were also performed for chlorophosphines incorporated in four- (P–N–Si–N) and five-membered (P–N–C=C–N) rings **4.18-4.21**, which are known to undergo facile metathesis.

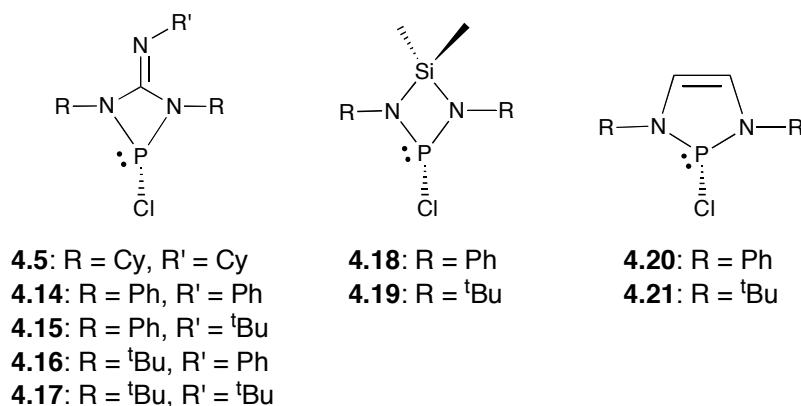


Chart 4.6: Compounds studied computationally.

Table 4.6 lists the atomic partial charges for the studied chlorophosphines as obtained from the natural population analysis (NPA) of their Kohn-Sham electron densities.⁷⁴ It is necessary to stress that the absolute values of the calculated charges have no physical meaning and it is only their relative magnitudes which yield useful information about structure-induced changes in the electron distribution. The atomic partial charges of phosphorus and carbon in **4.5** and **4.14-4.17** display only small variations, which is in contrast to those calculated for nitrogen and chlorine. These both show a more distinct dependence on the electron withdrawing/donating nature of *N*-substituents, most notably the all-Ph derivative **4.14** has the least charge concentrated on the electronegative elements within the molecular framework, thereby yielding the least polar P–Cl bond. In contrast, the *N*-alkyl substituted variants **4.5**, **4.16** and **4.17** display a less uniform charge distribution and consequently a more ionic P^{δ+}–Cl^{δ-} interaction.

These results pinpoint *N*-alkyl derivatives of the target chlorophosphines as the most favorable candidates for halide abstraction. The increased reactivity of the cyclohexyl derivative **4.5** towards Me₃SiOTf was also observed experimentally (*vide supra*).

A comparison of charge distributions calculated for **4.5** and **4.14-4.17** with those of compounds for which halide abstraction is reported to take place reveals, as expected, that the P–Cl interaction is significantly more ionic in the latter systems. The currently characterized chlorophosphines **4.18-4.21** display equal and roughly 0.10 units greater charge separation within the P–Cl bond as compared to the identically *N*-substituted species with a P–N–C–N backbone (see Table 4.6). Consequently, chlorophosphines with a P–N–C–N backbone appear, by their nature, to be resilient to salt metathesis. To analyze the origin of this phenomenon in detail, we turned our attention to the frontier orbital structure of the corresponding NHPs.

Table 4.6: Atomic partial charges (δ) as obtained from the natural population analysis of the studied chlorophosphines.

Compound	P	Cl	N	C / Si	$\Delta\delta(\text{P-Cl})^b$
4.5	1.15	-0.36	-0.71 ^a	0.59	1.51
4.14	1.16	-0.32	-0.68 ^a	0.6	1.48
4.15	1.16	-0.33	-0.71 ^a	0.59	1.49
4.16	1.18	-0.37	-0.73 ^a	0.61	1.56
4.17	1.17	-0.38	-0.74 ^a	0.61	1.55
4.18	1.19	-0.38	-1.09	1.98	1.57
4.19	1.23	-0.45	-1.17	2.02	1.68
4.20	1.17	-0.42	-0.68	-0.08	1.58
4.21	1.2	-0.53	-0.71	-0.09	1.72

^a Average values. ^b Absolute charge difference.

Figure 4.10 shows the lowest unoccupied molecular (Kohn-Sham) orbitals (LUMOs) and orbital energies of NHPs with different backbones but identical *N*-substituents. This orbital is of particular interest in the study of the nature of bonding in equivalent chlorophosphines as it interacts directly with an electron pair from the halide anion to form the P–Cl bond. Although the overall morphology of the orbitals in Figure 4.10 is rather similar, a π -type molecular orbital (MO) with a major contribution from the

p_z atomic orbital (AO) of phosphorus and a smaller admixture of AOs from the two flanking nitrogen nuclei, their orbital energies are vastly different with the LUMO of our target cations residing by far the lowest. Frontier MO theory based arguments predict that NHPs based on the P–N–C–N backbone should be the best electron acceptors in the series and form the most covalent P–X bonds. The observed differences in the charge distributions of the investigated halophosphines can therefore be correlated with the differing orbital characteristics of the corresponding NHPs. This holds not only for systems shown in Figure 4.10 but also for other chlorophosphines examined in the current work (Table 4.7). In addition, we note that the morphology of the LUMO is consistent with the possibility to affect the details of the P–Cl interaction by changing the exocyclic substituents from σ - (alkyl) to π -type (aryl).

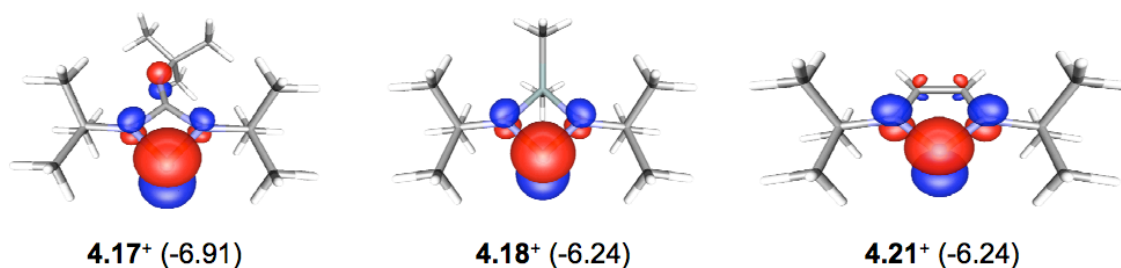


Figure 4.10: Lowest unoccupied molecular orbitals of the studied *N*-heterocyclic phosphines and their orbital energies (eV, in parenthesis).

Table 4.7: LUMO energies (in eV) of 4.5^+ and 4.14^+ - 4.21^+ .

Cation	E(LUMO)
4.5^+	-6.96
4.14^+	-7.30
4.15^+	-7.24
4.16^+	-7.18
4.17^+	-6.91
4.18^+	-6.24
4.19^+	-6.69
4.20^+	-6.31
4.21^+	-5.91

Given that our target cations appear to be much better electron acceptors than other known NHPs, the details of the P–X interaction in the corresponding halophosphines should be inferable not only from atomic partial charges but also from calculated bond strengths. We examined the nature of the P–Cl bond in compounds **4.5** and **4.14–4.17** with the help of energy decomposition analysis (EDA) which partitions the bonding interaction between a cationic NHP and a chloride anion into physically meaningful components (see Table 4.8).⁷⁵ It should be noted here that the instantaneous interaction energy (E_{int}) given by the EDA is not (the negative of) bond dissociation energy, which takes into account the energy gained from relaxation of the fragment geometries upon bond breaking. However, when comparing bonding trends across multiple similar systems, the snapshot-type picture given by the EDA procedure is sufficient.

Table 4.8: Results from energy decomposition analyses of P–Cl bonding in the studied chlorophosphines.^a

Compound	E_{Pauli}	$E_{\text{elstat}}^{\text{b}}$	$E_{\text{orb}}^{\text{b}}$	E_{int}
4.5	947	-875 (57%)	-651 (43%)	-580
4.14	1065	-941 (56%)	-754 (44%)	-630
4.15	1021	-924 (56%)	-717 (44%)	-621
4.16	909	-883 (58%)	-628 (42%)	-602
4.17	910	-870 (58%)	-619 (42%)	-579
4.18	654	-726 (64%)	-402 (36%)	-475
4.19	869	-827 (60%)	-551 (40%)	-509
4.20	774	-801 (62%)	-511 (38%)	-539
4.21	932	-873 (58%)	-639 (42%)	-580

^a Energies are reported in kJ mol^{-1} . ^b Percentage of total attractive interactions given in parenthesis

Table 4.8 lists the calculated EDA interaction energies along with their division into individual contributions from Pauli repulsion (E_{Pauli}) and electrostatic (E_{elstat}) and orbital interactions (E_{orb}). The trend in E_{int} values confirms that the P–Cl bond is markedly stronger in all chlorophosphines with a P–N–C–N backbone as compared to systems previously reported to undergo salt metathesis. The only exception are the fully alkyl substituted **4.5** and **4.17** whose interaction energy equals that of **4.21**. This is in

accord with experimental observations, which demonstrated the increased reactivity of **4.5** over other halophosphines studied in the present work. Changes in the percentage of E_{orb} from the total attractive interactions ($E_{\text{orb}} + E_{\text{elstat}}$) show that as the P–Cl interaction weakens it also becomes more electrostatic in nature. These results are fully in accord with the picture gleaned from the calculated charge distributions and LUMO energies. A correlation analysis on the calculated P–Cl charge difference (Table 4.6) and the percentage of covalent (orbital-type) character in the P–Cl bond (Table 4.8) yields a linear relationship with a correlation coefficient $R^2 = 0.93$ (Figure 4.11a). An equally good linear regression (Figure 4.11b) is obtained if the LUMO energies of NHPs are plotted against the EDA interaction energies (Table 4.8).

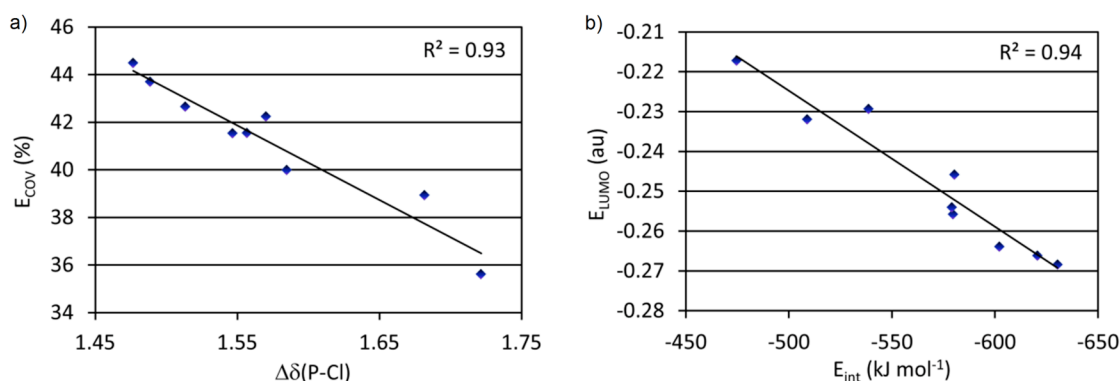


Figure 4.11: Correlation between (a) the covalent contribution and the charge difference in the P–Cl bond of the studied chlorophosphines, and (b) correlation between the LUMO energies of the studied NHPs and the EDA P–Cl interaction energies of the studied chlorophosphines.

Investigation of the unoccupied orbitals of the studied chlorophosphines offers a rationale for the role of bpy in capturing the targeted NHP as a base-stabilized cation. As shown in Figure 4.12 for **4.14**, both of its two lowest unoccupied orbitals have suitable morphologies to accept electron density from a coordinating Lewis base. A geometry optimization for **4.14** with bpy was ran and led to the formation of an adduct with a slightly (0.05 Å) longer P–Cl bond as compared to **4.14**. This is consistent with the antibonding nature of the orbitals in Figure 4.12, which in turn implies a weakened P–Cl interaction in the adduct. Consequently, an EDA calculation conducted for the bpy

complex of **4.14** yields a P–Cl interaction energy of -482 kJ mol^{-1} which is significantly less than that obtained for free **4.14** and similar to that found for chlorophosphines with either P–N–Si–N or P–N–C=C–N backbones (Table 4.8).

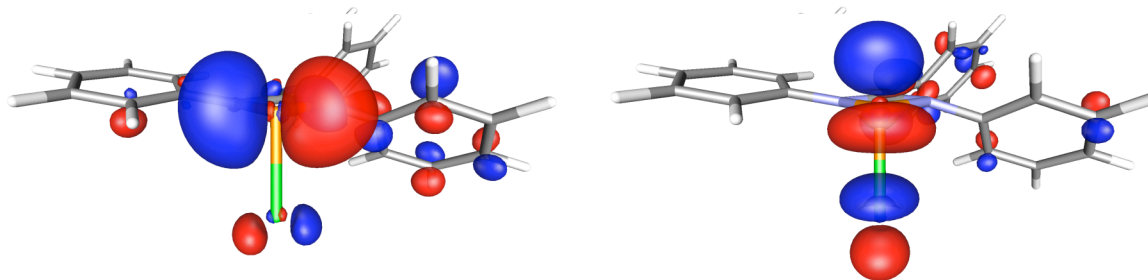


Figure 4.12: Two of the lowest unoccupied molecular orbitals of **4.14**.

The collective results from computational investigations enable us to conclude that the exceptionally good electron acceptor properties of the target NHP cations render the corresponding halophosphines reluctant to halide abstraction, unless there is additional stabilization from a Lewis base. The P–X bonds are not only stronger but also more covalent than in analogous systems known to undergo salt metathesis. Consequently, triflate-based reagents show no or only limited reactivity with **4.1-4.5**, most likely simply due to increased energy required to break the P–Cl bond. reactivity of diaminochlorophosphines constrained in a four-membered ring.

4.3 Conclusion

In summary, **4.1-4.6** represent the first examples of *N*-heterocyclic halophosphines supported by (dianionic)guanidinate ligands. The experimentally observed reluctance to form the corresponding *N*-heterocyclic phosphonium cations was rationalized by computational studies. Analysis of the charge distributions, orbital structures and relative P–Cl bond energies of the computationally studied compounds give corroborating evidence of the strong P–X bond and strong Lewis acidity of the cationic species. Reactivity studies of **4.1** demonstrate the high degree of strain induced by the four-membered ring, which leads to chemically and thermally induced carbodiimide elimination, as well as a novel ring expansion by insertion of chloro(imino)phosphine

into a P–N bond of **4.1**. These results demonstrate the electronic nature and alluring reactivity of diaminochlorophosphines restricted in a four-membered ring.

4.4 Experimental section

General synthetic and crystallography experimental details can be found in Appendix 1.

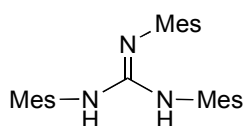
4.4.1 Synthesis

General synthesis for guanidine.

After cooling a THF solution (15 mL) of aniline to 0 °C, *n*-butyllithium (*n*BuLi) was added to the cooled solution and stirred for 20 min. The yellow solution was allowed to warm to room temperature (rt). A THF solution (6 mL) of carbodiimide was added to the solution *via* cannula transfer causing the solution to turn orange. The reaction mixture was refluxed for 2 h. After cooling to rt, H₂O (1.5 mL) was added dropwise, resulting in a white precipitate from the dark orange solution. The reaction mixture was dried over MgSO₄ and filtered.

Specific procedures for guanidines.

Compound 2



Prepared from 2,4,6-trimethylaniline (0.680 mL, 4.84 mmol), *n*-BuLi (1.6 M in hexanes, 3.60 mL, 5.76 mmol) and *N,N'*-bis(Mes)carbodiimide (1.35 g, 4.86 mmol). Concentrating the

orange filtrate by rotary evaporation yielded an orange solid, which was washed with CH₃CN (2 x 3 mL). The white product was dried *in vacuo*. X-ray quality colourless crystals were obtained from a CH₂Cl₂ solution layered with hexanes after three weeks at -20 °C.

Yield 73% (1.46 g, 3.53 mmol);

d.p.: 245-248 °C;

¹H NMR: δ 6.92 (s, 2H, *m*-CH), 6.83 (s, 2H, *m*-CH), 6.86 (s, 2H, *m*-CH), 4.97 (s, 1H, NH), 4.72 (s, 1H, NH), 2.37 (s, 6H, *o*-CH₃), 2.34 (s, 6H, *o*-CH₃), 2.26 (s, 9H, *p*-CH₃), 2.22 (s, 6H, *o*-CH₃);

$^{13}\text{C}\{^1\text{H}\}$ NMR: δ 146.2, 144.3, 137.7, 136.5, 136.4, 133.3, 132.3, 130.9, 130.9, 129.6, 129.2, 128.9, 21.1, 20.9, 18.9, 18.8;

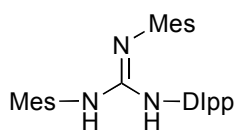
FT-IR (cm^{-1} (ranked intensity)): 544(9), 693(11), 778(13), 849(2), 947(15), 1032(8), 1152(10), 1224(5), 1291(7), 1311(12), 1474(6), 1646(1), 2917(3), 3360(4), 3392(14);

FT-Raman (cm^{-1} (ranked intensity)): 235(8), 278(14), 424(6), 504(12), 582(2), 1162(13), 1246(11), 1308(5), 1379(4), 1480(10), 1609(3), 1647(9), 2859(15), 2918(1), 3005(7);

HRMS: $\text{C}_{28}\text{H}_{35}\text{N}_3$ calcd (found) 413.2831 (413.2848);

Elemental Analysis (%): calcd for $\text{C}_{28}\text{H}_{35}\text{N}_3$ C 81.31, H 8.53, N 10.16; found C 80.44, H 8.25, N 10.00.

Compound 4



Prepared from 2,6-diisopropylaniline (90%, 2.30 mL, 11.0 mmol), $n\text{-BuLi}$ (2.0 M in cyclohexane, 6.60 mL, 13.2 mol) and N,N' -bis(Mes)carbodiimide (3.06 g, 11.0 mmol). The filtrate was dried by rotary evaporation, resulting in an orange wax. Recrystallization from hexanes at $-30\text{ }^\circ\text{C}$ yielded a white powder. X-ray quality colourless crystals were obtained from a concentrated CH_3CN solution after 8 days at $-20\text{ }^\circ\text{C}$.

Yield: 58% (2.90 g, 6.36 mmol);

m.p.: 146-149 $^\circ\text{C}$;

^1H NMR: δ 7.33-7.10 (3H, *aryl*), 7.00-6.86 (4H, *aryl*), 5.00 (br, 1H, *NH*), 4.78-4.71 (3s, 1H, *NH*), 3.63-3.37 (m, 2H, $\text{CH}(\text{CH}_3)_2$), 2.41 (d, 3H, $\text{CH}(\text{CH}_3)_2$, $^3J_{\text{H-H}} = 4.8$), 2.37 (d, 3H, $\text{CH}(\text{CH}_3)_2$, $^3J_{\text{H-H}} = 6.0$), 2.30 (s, 3H, CH_3), 2.25 (s, 3H, CH_3), 1.39 (d, 3H, $\text{CH}(\text{CH}_3)_2$, $^3J_{\text{H-H}} = 6.8$), 1.35 (d, 3H, $\text{CH}(\text{CH}_3)_2$, $^3J_{\text{H-H}} = 7.2$), 1.11 (m, 3H, CH_3);

$^{13}\text{C}\{^1\text{H}\}$ NMR: δ 148.3, 147.2, 146.9, 146.4, 145.5, 144.4, 144.2, 144.0, 141.2, 137.8, 137.6, 136.6, 136.5, 136.3, 133.5, 133.3, 133.2, 132.3, 132.2, 130.9, 129.7, 129.6, 129.2, 129.1, 128.9, 127.9, 123.9, 123.4, 123.0, 122.4, 28.5, 28.1, 25.1, 24.0, 23.5, 22.5, 21.1, 20.9, 18.8, 18.6;

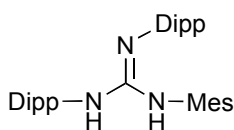
FT-IR (cm^{-1} (ranked intensity)): 551(10), 693(11), 757(6), 799(8), 863(4), 1034(12), 1104(13), 1151(14), 1222(9), 1292(7), 1378(15), 1473(5), 1650(1), 2963(2), 3399(3);

FT-Raman (cm⁻¹(ranked intensity)): 142(5), 236(14), 266(13), 572(3), 689(12), 883(15), 1159(10), 1255(8), 1306(6), 1381(4), 1444(11), 1608(2), 1650(7), 2867(9), 2919(1);

HRMS: C₃₁H₄₁N₃ calcd (found) 455.3300 (455.3298);

Elemental analysis (%): calcd for C₃₁H₄₁N₃ C 81.71, H 9.07, N 9.22; found C 81.23, H 9.28, N 9.28.

Compound 5



Prepared from 2,4,6-trimethylaniline (1.40 mL, 9.96 mmol), ^tBuLi (2.0 M in cyclohexane, 6.00 mL, 12.0 mmol) and *N,N'*-bis(Dipp)carbodiimide (3.58 g, 9.87 mmol). The filtrate was dried by rotary evaporation, resulting in an orange wax. Recrystallization from hexanes at -30 °C yielded a white powder. X-ray quality colourless crystals were obtained from a concentrated CH₃CN solution after 5 days at -20 °C.

Yield: 33% (1.61 g, 3.23 mmol);

m.p.: 156-160 °C;

¹H NMR: δ 7.33-7.11 (5H, *aryl*), 7.01-6.86 (3H, *aryl*), 5.00 (s, 1H, NH), 4.74 (br, 1H, NH), 3.64-3.36 (m, 4H, CH(CH₃)₂), 2.42 (s, 2H, CH₃), 2.36 (s, 2H, CH₃), 2.29 (s, 3H, CH₃), 2.25 (d, 2H, CH(CH₃)₂, ³J_{H-H} = 9.2), 1.38-1.04 (24H, CH₃);

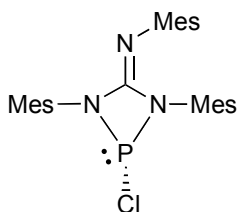
¹³C{¹H} NMR: δ 148.4, 148.3, 147.4, 147.3, 147.2, 146.3, 145.6, 144.2, 143.9, 141.5, 141.1, 137.8, 136.8, 136.4, 133.8, 133.5, 132.8, 132.5, 132.2, 131.7, 130.9, 129.7, 129.0, 128.9, 127.9, 127.7, 124.1, 123.8, 123.5, 123.1, 123.0, 122.5, 28.9, 28.8, 28.6, 28.5, 28.4, 28.0, 25.8, 25.3, 24.8, 24.1, 23.6, 23.1, 23.0, 22.2, 21.0, 20.8, 18.5, 18.3;

FT-IR (cm⁻¹(ranked intensity)): 764(5), 800(8), 849(7), 935(10), 1059(15), 1109(9), 1255(13), 1295(6), 1361(11), 1383(14), 1493(4), 1586(12), 1647(1), 2962(2), 3409(3);

FT-Raman (cm⁻¹(ranked intensity)): 147(6), 275(8), 445(14), 574(3), 676(9), 884(15), 1046(13), 1108(11), 1261(4), 1308(10), 1382(12), 1444(5), 1588(2), 2866(7), 2917(1);

HRMS: C₃₄H₄₇N₃ calcd (found) 497.3770 (497.3771)

Elemental analysis (%): calcd for C₃₄H₄₇N₃ C 82.04, H 9.52, N 8.44; found C 81.93, H 9.47, N 8.46.

Compound **4.1**^Ω

To a toluene solution (30 mL) of **2** (2.64 g, 6.39 mmol), PCl₃ (0.720 mL, 8.25 mmol) and NEt₃ (2.30 mL, 16.5 mmol) were added sequentially. The cloudy reaction mixture was stirred at rt for 2.5 h. The reaction mixture was cannula transferred to a Schlenk filter frit and the yellow filtrate was dried *in vacuo* to give a yellow powder.

The powder was dissolved in CH₂Cl₂ (2 mL) and CH₃CN (5 mL) was added with vigorous stirring to precipitate a white powder. The suspension was centrifuged and the yellow solution decanted. This process was repeated and the decanted solutions were combined and placed in the freezer (-30 °C) for 30 min, during which, more white powder precipitated. The solution was decanted and the powder was dissolved in CH₂Cl₂ (2 mL) and added to those collected by centrifugation. The volatiles were removed *in vacuo* to give **4.1** as a white powder. Single crystals suitable for X-ray diffraction experiments were grown by diffusion of CH₃CN into a concentrated CH₂Cl₂ solution of the bulk material at -30 °C for 4 weeks.

Yield: 69% (2.11 g, 4.42 mmol);

m.p.: 143-146 °C;

¹H NMR (-30 °C): δ 6.87 (s, 2H, *aryl*), 6.77 (s, 2H, *aryl*), 6.57 (s, 1H, *aryl*), 6.24 (s, 1H, *aryl*), 2.49 (s, 6H, CH₃), 2.41 (s, 6H, CH₃), 2.26 (s, 3H, CH₃), 2.22 (s, 6H, CH₃), 2.02 (s, 3H, CH₃), 1.88 (s, 3H, CH₃);

¹³C{¹H} NMR (-30 °C): δ 144.8 (d, ²J_{13C-P} = 6.0), 138.5, 138.3, 137.8, 135.9 (br), 131.3, 130.0, 129.2, 128.9 (d, ²J_{13C-P} = 5.3), 128.0, 127.7 (d, ³J_{13C-P} = 3.7), 127.3, 127.2, 21.1, 20.7, 20.3, 19.9 (br), 19.1, 18.4;

³¹P{¹H} NMR: δ 181 (s);

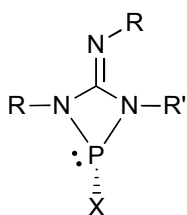
FT-IR (cm⁻¹(ranked intensity)): 448(6), 562(8), 682(10), 714(15), 756(11), 849(4), 948(14), 986(3), 1173(13), 1263(2), 1312(9), 1480(5), 1608(12), 1720(1), 2915(7);

^Ω Attempts to obtain HRMS for **4.1-4.6** were unsuccessful and only the protonated form of their ligands (compounds **2-6**) could be observed in the spectrum. Low temperature NMR spectroscopy was used in acquiring the ¹H and ¹³C{¹H} NMR spectra for compounds **4.1-4.6** (-30 °C) and **4.11** (-50 °C). At room temperature the resonances were broad due to dynamic processes.

FT-Raman (cm^{-1} (ranked intensity)): 120(9), 193(11), 225(14), 253(7), 391(15), 448(8), 574(1), 1008(12), 1347(5), 1381(6), 1485(10), 1610(3), 1716(4), 2916(2), 3018(13);

Elemental analysis (%): calcd for $\text{C}_{28}\text{H}_{33}\text{N}_3\text{P}_1\text{Cl}_1$ C 70.35, H 6.96, N 8.79; found C 69.32, H 7.18, N 8.65.

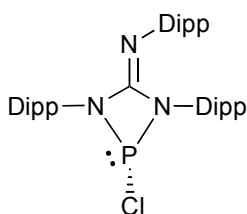
General synthesis for halophosphine.



To a toluene solution (20 mL) of guanidine (**2-6**), 1.3 and 2.6 equivalents of PX_3 ($\text{X} = \text{Cl}, \text{Br}$) and NEt_3 were added, respectively in a sequential fashion. The reaction mixture was left to stir at rt overnight, during which time the solution became cloudy. Volatiles were removed *in vacuo* giving an off-white solid, which was resuspended in THF. The white solid was removed by centrifugation, and the liquid was concentrated *in vacuo* to give an off-white solid. The product was washed with CH_3CN (2 x 4 mL), decanting the coloured solution each time. The product was dried *in vacuo* to give a white solid.

Specific procedures for halophosphines.

Compound **4.2**^Ω



Prepared from **3** (0.749 g, 1.39 mmol), PCl_3 (0.160 mL, 1.83 mmol) and NEt_3 (0.500 mL, 3.59 mmol). X-ray quality colourless crystals were obtained from a concentrated CH_2Cl_2 solution after four weeks at $-20\text{ }^\circ\text{C}$.

Yield: 72% (0.601 g, 0.997 mmol);

m.p.: 127-130 $^\circ\text{C}$;

$^1\text{H NMR}$ ($-30\text{ }^\circ\text{C}$): δ 7.30 (t, 2H, *aryl*, $^3J_{\text{H-H}} = 7.6$), 7.22 (d, 2H, *aryl*, $^3J_{\text{H-H}} = 7.6$), 7.13 (m, 2H, *aryl*), 7.00 (d, 1H, *aryl*, $^3J_{\text{H-H}} = 7.6$), 6.81 (t, 1H, *aryl*, $^3J_{\text{H-H}} = 7.6$), 6.61 (d, 1H, *aryl*, $^3J_{\text{H-H}} = 7.6$), 3.42 (m, 4H, $\text{CH}(\text{CH}_3)_2$), 3.31 (br sept, 1H, $\text{CH}(\text{CH}_3)_2$), 2.47 (br sept, 1H, $\text{CH}(\text{CH}_3)_2$), 1.41 (d, 6H, $\text{CH}(\text{CH}_3)_2$, $^3J_{\text{H-H}} = 6.4$), 1.32 (d, 6H, $\text{CH}(\text{CH}_3)_2$, $^3J_{\text{H-H}} = 6.8$), 1.26 (d, 6H, $\text{CH}(\text{CH}_3)_2$, $^3J_{\text{H-H}} = 6.8$), 1.18 (m, 9H, $\text{CH}(\text{CH}_3)_2$), 0.86 (d, 6H, $\text{CH}(\text{CH}_3)_2$, $^3J_{\text{H-H}} = 6.4$), 0.56 (d, 6H, $\text{CH}(\text{CH}_3)_2$, $^3J_{\text{H-H}} = 6.0$);

$^{13}\text{C}\{^1\text{H}\}$ NMR (-30 °C): δ 149.5, 147.5, 141.3 (d, $^2J_{13\text{C-P}} = 5.6$), 140.0, 138.5, 137.4, 130.6 (d, $^2J_{13\text{C-P}} = 4.8$), 128.8, 124.1, 124.0, 123.4, 123.0, 121.2, 30.1, 30.0, 28.9, 28.2, 27.4, 27.3, 23.6, 23.3, 22.9, 22.6, 22.4;

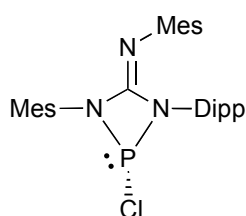
$^{31}\text{P}\{^1\text{H}\}$ NMR: δ 180 (s);

FT-IR (cm^{-1} (ranked intensity)): 527(15), 674(11), 752(8), 786(4), 984(3), 1121(10), 1219(7), 1260(5), 1323(9), 1363(14), 1386(12), 1438(6), 1588(13), 1717(1), 2965(2);

FT-Raman (cm^{-1} (ranked intensity)): 137(6), 279(9), 451(13), 887(5), 1048(15), 1104(12), 1252(14), 1299(10), 1353(8), 1443(4), 1589(1), 1718(3), 2867(7), 2909(2), 3062(11);

Elemental analysis (%): calcd for $\text{C}_{37}\text{H}_{51}\text{N}_3\text{P}_1\text{Cl}_1$ C 73.55, H 8.51, N 6.95; found C 72.69, H 8.66, N 6.90.

Compound 4.3 $^{\Omega}$



Synthesized from **4** (1.10 g, 2.42 mmol), PCl_3 (0.270 mL, 3.12 mmol) and NEt_3 (0.87 mL, 6.25 mmol). X-ray quality colourless crystals were obtained after three days from a concentrated hexanes solution at -20 °C.

Yield: 35% (0.436 g, 0.837 mmol);

m.p.: 142-146 °C;

^1H NMR (-30 °C): δ 7.38 (t, 1H, *aryl*, $^3J_{\text{H-H}} = 7.6$), 7.30 (d, 1H, *aryl*, $^3J_{\text{H-H}} = 7.6$), 7.26 (d, 1H, *aryl*, $^3J_{\text{H-H}} = 7.6$), 6.76 (s, 1H, *aryl*), 6.58 (s, 1H, *aryl*), 6.54 (s, 1H, *aryl*), 6.25 (s, 1H, *aryl*), 3.81 (sept, 1H, CHCH_3 , $^3J_{\text{H-H}} = 6.4$), 3.42 (sept, 1H, CHCH_3 , $^3J_{\text{H-H}} = 6.8$), 2.49 (s, 3H, CH_3), 2.27 (s, 3H, CH_3), 2.21 (s, 3H, CH_3), 2.15 (s, 3H, CH_3), 2.02 (s, 3H, CH_3), 1.90 (s, 3H, CH_3), 1.38 (m, 9H, CHCH_3), 1.32 (d, 3H, CHCH_3 , $^3J_{\text{H-H}} = 6.8$);

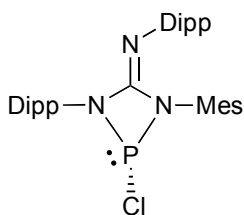
$^{13}\text{C}\{^1\text{H}\}$ NMR (-30 °C): δ 150.2, 148.1, 145.5 (d, $^2J_{13\text{C-P}} = 5.9$), 138.4, 137.6, 137.1, 134.6, 131.4, 130.2, 129.2, 129.1 (d, $^2J_{13\text{C-P}} = 2.8$), 128.95, 128.9, 128.6, 128.1, 127.8, 127.3, 124.4, 123.9, 29.5 (d, $J_{13\text{C-P}} = 4.2$), 28.8, 25.8, 25.5 (d, $J_{13\text{C-P}} = 4.8$), 24.6, 24.3, 21.0, 20.7, 20.1 (d, $J_{13\text{C-P}} = 9.9$), 19.8, 19.1, 18.3;

$^{31}\text{P}\{^1\text{H}\}$ NMR: δ 181 (s);

FT-IR (cm⁻¹(ranked intensity)): 462(4), 561(13), 681(10), 714(15), 767(9), 803(5), 846(12), 985(6), 1227(11), 1266(2), 1317(8), 1466(7), 1608(14), 1698(1), 2963(3);

FT-Raman (cm⁻¹(ranked intensity)): 97(15), 143(7), 226(6), 461(8), 575(2), 1009(14), 1316(10), 1358(5), 1455(9), 1590(12), 1609(4), 1701(3), 2863(11), 2917(1), 2964(13).

Compound 4.4^Ω



Synthesized from **5** (0.750 g, 1.51 mmol), PCl₃ (0.171 mL, 1.96 mmol) and NEt₃ (0.550 mL, 3.92 mmol). X-ray quality colourless crystals were obtained after two weeks from a concentrated CH₂Cl₂/Et₂O solution at -20 °C.

Yield: 61% (0.520 g, 0.925 mmol);

m.p.: 138-141 °C;

¹H NMR (-30 °C): δ 7.43 (t, 1H, *aryl*, ³J_{H-H} = 7.6), 7.34 (d, 1H, *aryl*, ³J_{H-H} = 7.6), 7.30 (d, 1H, *aryl*, ³J_{H-H} = 7.6), 6.92 (d, 1H, *aryl*, ³J_{H-H} = 7.2), 6.78 (s, 1H, *aryl*), 6.75 (t, 1H, *aryl*, ³J_{H-H} = 7.6), 6.53 (d, 1H, *aryl*), 6.51 (s, 1H, *aryl*), 3.80 (sept, 1H, CH(CH₃)₂, ³J_{H-H} = 6.8), 3.39 (m, 2H, CH(CH₃)₂), 2.94 (sept, 1H, CH(CH₃)₂, ³J_{H-H} = 6.4), 2.47 (s, 3H, CH₃), 2.15 (s, 3H, CH₃), 2.13 (s, 3H, CH₃), 1.41 (m, 9H, CH(CH₃)₂), 1.35 (d, 3H, CH(CH₃)₂, ³J_{H-H} = 6.4), 1.32 (d, 3H, CH(CH₃)₂, ³J_{H-H} = 6.8), 0.95 (m, 6H, CH(CH₃)₂), 0.83 (d, 3H, CH(CH₃)₂, ³J_{H-H} = 6.4);

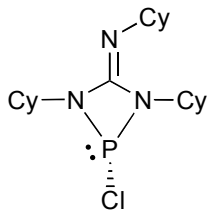
¹³C{¹H} NMR (-30 °C): δ 150.7, 148.4, 142.7 (d, ²J_{13C-P} = 5.6), 139.7, 138.6, 138.3, 137.1, 137.0, 134.4, 130.3, 129.5 (d, ²J_{13C-P} = 4.0), 129.0, 128.95, 128.9, 124.2, 123.6, 122.7, 121.6, 120.6, 29.5 (d, J_{13C-P} = 2.9), 29.0, 28.9, 28.4, 26.5 (d, J_{13C-P} = 8.0), 26.4, 25.2, 24.9, 24.1, 23.9, 21.2, 21.0, 20.5, 19.8 (d, J_{13C-P} = 10.9), 19.2;

³¹P{¹H} NMR: δ 179 (s);

FT-IR (cm⁻¹(ranked intensity)): 432(11), 461(9), 558(15), 675(12), 754(5), 782(7), 883(14), 986(4), 1268(3), 1317(8), 1362(13), 1465(6), 1587(10), 1705(1), 2965(2);

FT-Raman (cm⁻¹(ranked intensity)): 109(9), 200(14), 462(8), 578(5), 625(11), 887(7), 1011(13), 1259(10), 1319(12), 1360(4), 1448(6), 1590(2), 1708(3), 2925(1), 3065(15);

Elemental analysis (%): calcd for C₃₄H₄₅N₃P₁Cl₁ C 72.64, H 8.07, N 7.47; found C 71.97, H 8.06, N 7.37.

Compound 4.5^Ω

Prepared from **6** (0.550 g, 1.80 mmol), PCl₃ (0.200 mL, 2.34 mmol), NEt₃ (0.650 mL, 4.68 mmol).

Yield: 31% (0.206 g, 0.558 mmol);

m.p.: 75-78 °C;

¹H NMR (-30 °C): δ 3.53-3.35 (m, 3H, CH), 2.10-2.01 (m, 4H, CH₂), 1.82-1.14 (m, 26H, CH₂);

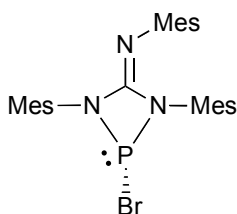
¹³C{¹H} NMR (-30 °C): δ 145.6, 55.9, 54.5, 51.4, 35.5, 35.3, 33.6, 33.5, 33.4, 32.1, 31.8, 25.61, 25.56, 25.4, 25.2, 25.1, 25.0;

³¹P{¹H} NMR: δ 182 (s);

FT-IR (cm⁻¹(ranked intensity)): 433(7), 655(3), 699(8), 725(14), 839(10), 890(9), 988(4), 1109(13), 1148(12), 1215(5), 1298(11), 1361(15), 1449(6), 1704(2), 2930(1);

FT-Raman (cm⁻¹(ranked intensity)): 85(8), 143(14), 216(6), 430(10), 659(13), 728(12), 811(7), 1027(9), 1253(11), 1347(15), 1444(4), 1702(3), 2854(2), 2887(5), 2938(1);

Elemental analysis (%): calcd for C₁₉H₃₃N₃P₁Cl₁ C 61.69, H 8.99, N 11.36; found C 61.35, H 9.26, N 11.17.

Compound 4.6^Ω

2 (0.928 g, 2.24 mmol), PCl₃ (0.270 mL, 2.87 mmol), NEt₃ (0.810 mL, 5.81 mmol). Single crystals suitable for X-ray diffraction experiments were grown by diffusion of CH₃CN into a concentrated CH₂Cl₂ solution of the bulk material at -30 °C for 3 days.

Yield: 70% (0.815 g, 1.56 mmol);

m.p.: 117-123 °C;

¹H NMR (-30 °C): δ 6.88 (s, 2H, aryl), 6.79 (br s, 2H, aryl), 6.61 (s, 1H, aryl), 6.26 (s, 1H, aryl), 2.49 (s, 6H, CH₃), 2.47 (br s, 6H, CH₃), 2.29 (s, 3H, CH₃), 2.24 (s, 6H, CH₃), 2.04 (s, 3H, CH₃), 1.89 (s, 3H, CH₃);

$^{13}\text{C}\{^1\text{H}\}$ NMR (-30 °C): δ 144.1 (d, $^2J_{13\text{C-P}} = 5.13$ Hz), 138.2, 137.8, 135.6, 131.4, 129.8, 129.4, 129.0, 127.9, 127.8, 127.3, 21.1, 20.7, 20.3, 19.9, 19.8, 19.3, 18.3;

$^{31}\text{P}\{^1\text{H}\}$ NMR: δ 200 (s);

FT-IR (cm^{-1} (ranked intensity)): 414(15), 559(7), 674(11), 756(9), 803(14), 849(6), 951(12), 983(3), 1268(2), 1315(8), 1374(13), 1478(4), 1609(10), 1698(1), 2916(5);

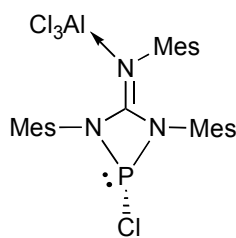
FT-Raman (cm^{-1} (ranked intensity)): 97(8), 147(4), 177(15), 207(12), 240(9), 324(7), 413(13), 570(2), 1010(14), 1358(6), 1379(11), 1489(10), 1610(3), 1700(1), 2918(5);

Elemental analysis (%): calcd for $\text{C}_{28}\text{H}_{33}\text{N}_3\text{P}_1\text{Br}_1$ C 64.37, H 6.37, N 8.04; found C 64.06, H 6.42, N 7.93.

General synthesis for 4.7-4.8.

To a CH_2Cl_2 solution (5 mL) of **4.1**, a CH_2Cl_2 solution (3 mL) of MCl_3 (M = Al, Ga) was added slowly with stirring. In all cases the reaction mixtures turned yellow. The reactions were stirred at rt for 3 h, during which time the yellow colour became less intense. The volatiles were removed *in vacuo* to give slightly yellow powders.

Compound 4.7



Compound **4.7** was prepared from **4.1** (0.196 g, 0.409 mmol) and AlCl_3 (0.0550 g, 0.412 mmol). The crude product was purified by liquid diffusion of hexane into a concentrated CH_2Cl_2 solution of the bulk powder at -30 °C for 48 h. This gave a microcrystalline white powder. X-ray quality crystals were obtained from slow evaporation

of a concentrated CH_2Cl_2 solution of the bulk powder at rt for a two week period.

Yield: 53% (0.129 g, 0.211 mmol);

d.p.: 160-164 °C;

^1H NMR: δ 7.02 (s, 1H, *aryl*), 7.00 (s, 1H, *aryl*), 6.76 (s, 1H, *aryl*), 6.68 (s, 1H, *aryl*), 6.52 (s, 1H, *aryl*), 6.19 (s, 1H, *aryl*), 2.72 (s, 3H, CH_3), 2.64 (s, 3H, CH_3), 2.55 (s, 3H, CH_3), 2.51 (d, 3H, CH_3 $J_{\text{H-P}} = 2.0$), 2.35 (s, 3H, CH_3), 2.20 (s, 3H, CH_3), 2.11 (s, 3H, CH_3), 2.07 (s, 6H, CH_3);

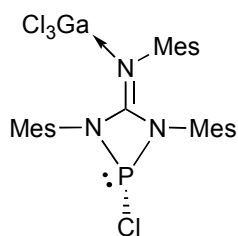
$^{13}\text{C}\{^1\text{H}\}$ NMR: δ 160.8 (d, $^2J_{13\text{C-P}} = 9.95$), 140.8, 140.0, 139.0, 138.8, 137.7, 137.3, 136.6, 135.3, 133.6, 133.3, 130.5, 130.2, 130.0, 129.6, 129.0, 128.5, 127.3, 21.4, 21.3 (d, $J_{13\text{C-P}} = 7.34$), 21.0, 20.9, 20.8, 20.7, 20.6, 20.3, 19.2;

$^{31}\text{P}\{^1\text{H}\}$ NMR: δ 171 (s);

FT-IR (cm⁻¹(ranked intensity)): 412(14), 429(9), 471(11), 505(2), 661(6), 711(10), 748(4), 855(3), 885(15), 981(8), 1195(12), 1282(5), 1352(13), 1555(1), 2922(7);

FT-Raman (cm⁻¹(ranked intensity)): 186(7), 221(9), 283(10), 430(8), 495(5), 574(2), 661(13), 1018(14), 1321(12), 1352(4), 1386(6), 1482(11), 1609(3), 2925(1), 3024(15).

Compound 4.8



Compound **4.8** was synthesized from **4.1** (0.250 g, 0.523 mmol) and GaCl₃ (0.0929 g, 0.528 mmol). The crude product was purified by redissolving in CH₂Cl₂ and precipitating white solids by the addition of hexanes with rapid stirring. The solution was decanted and the white product was dried *in vacuo*.

Yield: 66% (0.227 g, 0.347 mmol);

d.p.: 171-179 °C;

^1H NMR: δ 7.02 (s, 1H, *aryl*), 7.01 (s, 1H, *aryl*), 6.75 (s, 1H, *aryl*), 6.68 (s, 1H, *aryl*), 6.51 (s, 1H, *aryl*), 6.20 (s, 1H, *aryl*), 2.73 (s, 3H, CH₃), 2.65 (s, 3H, CH₃), 2.53 (s, 3H, CH₃), 2.51 (d, 3H, CH₃ $J_{\text{H-P}}$ = 2.4), 2.35 (s, 3H, CH₃), 2.20 (s, 3H, CH₃), 2.07 (virtual d, 9H, CH₃);

$^{13}\text{C}\{^1\text{H}\}$ NMR: δ 159.7 (d, $^2J_{13\text{C-P}}$ = 10.3), 140.8, 139.9, 139.0, 138.8, 137.9, 137.4, 136.5, 135.3, 133.4, 133.3, 130.7, 130.1 (d, $^3J_{13\text{C-P}}$ = 3.32), 130.06, 129.6, 129.4, 129.0, 128.4, 127.0 (d, $^3J_{13\text{C-P}}$ = 1.81), 21.4, 21.2 (d, $J_{13\text{C-P}}$ = 3.22), 21.0, 20.9, 20.8, 20.7, 20.6, 20.1, 19.2;

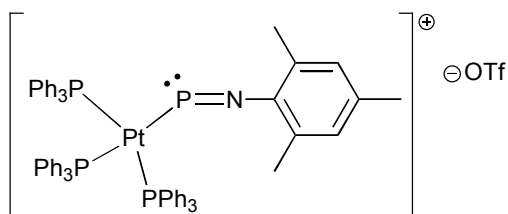
$^{31}\text{P}\{^1\text{H}\}$ NMR: δ 173 (s);

FT-IR (cm⁻¹(ranked intensity)): 463(15), 493(2), 552(5), 657(9), 705(14), 750(7), 855(3), 980(8), 1280(4), 1321(10), 1352(12), 1477(6), 1560(1), 1611(13), 2921(11);

FT-Raman (cm⁻¹(ranked intensity)): 199(6), 241(13), 360(4), 388(11), 493(7), 573(2), 657(15), 1017(12), 1321(10), 1352(5), 1385(8), 1482(9), 1609(3), 2924(1), 3023(14);

Elemental analysis (%): calcd for C₂₈H₃₃N₃P₁Cl₄Ga₁ C 51.41, H 5.09, N 6.42; found C 50.95, H 5.31, N 6.32.

Compound 4.9



A CH_2Cl_2 solution (8 mL) of **4.1** (0.353 g, 0.739 mmol) was added to solid $\text{Pt}(\text{PPh}_3)_4$ (0.914 g, 0.734 mmol) to give a clear orange solution. After stirring at rt for 45 min Me_3SiOTf was added and the colour changed instantly to dark

red. The volatiles were removed after stirring at rt for 30 min resulting in a waxy brown product. Washing the product with hexanes (3 x 5 mL) yielded a brown powder. The bulk material was dissolved in CH_2Cl_2 (3 mL) and stirred vigorously as hexanes (8 mL) were added leading to the precipitation of brown powder. The supernatant was decanted and discarded and the bulk material once again dissolved in CH_2Cl_2 (3 mL) and set up for recrystallization by layering hexanes (6 mL) and keeping at $-30\text{ }^\circ\text{C}$ for 4 days.

Yield: 56% (0.528 g, 0.408 mmol);

d.p.: 87-92 $^\circ\text{C}$;

^1H NMR: δ 7.34 (t, 9H, *aryl*, $^3J_{\text{H-H}} = 8.0$), 7.07 (t, 18H, *aryl*, $^3J_{\text{H-H}} = 8.0$), 6.94 (d, 18H, *aryl*, $^3J_{\text{H-H}} = 8.0$), 6.68 (s, 2H, *aryl*), 2.15 (s, 3H, CH_3), 1.67 (s, 6H, CH_3);

$^{13}\text{C}\{^1\text{H}\}$ NMR: δ 133.5, 131.0, 129.0, 128.9, 21.6, 19.2;

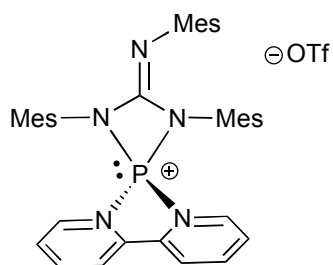
$^{31}\text{P}\{^1\text{H}\}$ NMR: δ 147 (br t), 23 (d, $^2J_{\text{P-P}} = 65$, $^1J_{\text{P-195Pt}} = 3990$);

$^{19}\text{F}\{^1\text{H}\}$ NMR: δ -78.3 (s);

FT-IR (cm^{-1} (ranked intensity)): 418(12), 516(2), 637(7), 694(1), 744(5), 853(13), 998(14), 1030(6), 1092(9), 1147(10), 1222(15), 1272(3), 1435(4), 1480(8), 3054(11);

FT-Raman (cm^{-1} (ranked intensity)): 97(8), 244(4), 313(13), 415(11), 618(15), 1001(2), 1029(10), 1075(12), 1094(9), 1302(7), 1382(14), 1492(1), 1585(6), 1605(3), 3059(5);

Elemental analysis (%): calcd for $\text{C}_{64}\text{H}_{56}\text{F}_3\text{N}_1\text{O}_3\text{P}_4\text{Pt}_1\text{S}_1$ C 59.35, H 4.36, N 1.08; found C 59.04, H 4.42, N 1.07.

Compound **4.10**

To a CH₂Cl₂ solution (5 mL) of **4.1** (0.396 g, 0.828 mmol) was added a CH₂Cl₂ solution (2 mL) of 2,2'-bipyridine (0.131 g, 0.837 mmol) and Me₃SiOTf (150 μL, 0.829 mmol). The previously colourless solution turned yellow after the addition of Me₃SiOTf and was allowed to stir at rt for 3.5 h before removing the volatiles *in vacuo* to give an orange waxy product. Washing the product with hexanes (2 x 5 mL) produced an orange powder. The powder was redissolved in CH₂Cl₂ (3 mL) and hexanes (6 mL) were added to produce an oil. The supernatant was decanted and the oil dried to give an orange powder. This process was repeated three times.

Yield: 72% (0.447 g, 0.597 mmol);

d.p.: 128-133 °C;

¹H NMR: δ 9.22 (d, 2H, *bpy*, ³*J*_{H-H} = 8.0), 8.59 (br d, 2H, *bpy*), 8.50 (t, 2H, *bpy*, ³*J*_{H-H} = 8.0), 7.64 (br t, 2H, *bpy*), 2.76 (br s, 6H, CH₃), 2.21 (s, 6H, CH₃), 2.06 (s, 3H, CH₃), 1.99 (s, 3H, CH₃), 1.82 (br s, 6H, CH₃), 1.77 (s, 3H, CH₃);

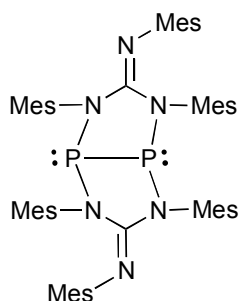
¹³C{¹H} NMR: δ 146.6 (d, ²*J*_{13C-P} = 5.0), 145.1, 144.6, 139.8, 138.1, 136.6, 136.1, 132.0, 131.3, 130.0, 128.8, 128.1, 127.8, 127.6 (d, ²*J*_{13C-P} = 4.0), 125.8 (d, ²*J*_{13C-P} = 5.0), 21.4, 21.0, 20.7, 19.8, 18.7, 18.5;

³¹P{¹H} NMR: δ 106 (s);

¹⁹F {¹H} NMR: δ -78.6 (s);

FT-IR (cm⁻¹(ranked intensity)): 476(14), 517(8), 564(12), 637(3), 724(13), 770(7), 854(10), 988(15), 1031(2), 1155(5), 1260(1), 1478(6), 1613(11), 1695(4), 2921(9);

FT-Raman (cm⁻¹(ranked intensity)): 85(2), 394(14), 570(4), 633(13), 770(9), 1016(7), 1251(15), 1304(11), 1331(3), 1384(12), 1497(8), 1563(10), 1608(1), 1694(6), 2922(5).

Compound **4.11**^Ω

A THF (3mL) solution of Cp₂Co (0.429 g, 2.27 mmol) was added to a colourless THF (3 mL) solution of **4.1** (1.08 g, 2.25 mmol). The reaction mixture turned a dark brown colour and after stirring for 48 h at rt copious amounts of green precipitate were visible. The green precipitate was separated by centrifugation and the dark solution was decanted and dried *in vacuo* to give an off-white solid. The product was washed with CH₃CN (2 x 6 mL) to remove remaining Cp₂Co and the suspension was centrifuged. The solid white product was dissolved in CH₂Cl₂ (3 mL) and precipitated with the addition of CH₃CN, the solution was decanted and discarded, and this process was repeated once more. After the second precipitation the vial was placed in the freezer (-30 °C) for 45 min, the slightly coloured solution was discarded and the white precipitate was dried *in vacuo*. X-ray quality crystals were grown at -30 °C from the liquid diffusion of CH₃CN into a concentrated CH₂Cl₂ solution of the bulk material over a one-week period.

Yield: 61% (0.612 g, 0.692 mmol);

d.p.: 310-320 °C;

¹H NMR (-50 °C): δ 6.95 (s, 2H, *aryl*), 6.80 (s, 2H, *aryl*), 6.63 (s, 2H, *aryl*), 6.42 (s, 2H, *aryl*), 6.10 (s, 2H, *aryl*), 5.96 (s, 2H, *aryl*), 2.82 (s, 6H, CH₃), 2.44 (s, 6H, CH₃), 2.39 (s, 6H, CH₃), 2.30 (s, 6H, CH₃), 2.22 (s, 6H, CH₃), 2.06 (s, 6H, CH₃), 1.98 (s, 6H, CH₃), 1.52 (s, 6H, CH₃), 1.48 (s, 6H, CH₃);

¹³C{¹H} NMR (-50 °C): δ 146.2 (t, ²J_{13C-P} = 6.0), 142.2, 138.4, 138.2, 137.3 (br), 136.8, 135.8 (br), 134.5, 130.2 (br), 129.6 (br), 129.2, 128.3 (br), 128.1, 126.8 (t, ²J_{13C-P} = 7.2), 125.6, 21.8, 21.3 - 20.8 (br), 20.6, 20.2 (br), 19.0 (d, J_{13C-P} = 2.6), 18.7 (br);

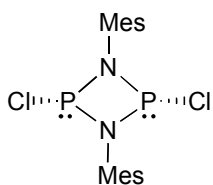
³¹P{¹H} NMR: δ 59 (s);

FT-IR (cm⁻¹(ranked intensity)): 532(10), 562(7), 604(14), 719(5), 747(9), 848(6), 949(11), 1005(3), 1188(12), 1232(2), 1308(15), 1375(13), 1477(4), 1642(1), 2915(8);

FT-Raman (cm⁻¹(ranked intensity)): 108(9), 243(14), 403(15), 430(10), 474(6), 531(11), 576(5), 968(12), 1019(13), 1220(8), 1307(4), 1381(7), 1609(1), 1660(3), 2915(2);

Elemental analysis (%): calcd for $C_{56}H_{66}N_6P_2$ C 75.99, H 7.52, N 9.49; found C 75.67, H 7.44, N 9.47.

Compound 4.12



Compound **4.1** (0.540 g, 1.13 mmol) was dissolved in toluene (6 mL) and heated to 90 °C for 48 h. The solvent was removed *in vacuo* giving a colourless waxy material, which became a powder after stirring in pentane for 5 min. The solvent was decanted and the white powder was dried *in vacuo*. The product was further purified by recrystallization from slow diffusion of CH_3CN into a concentrated CH_2Cl_2 solution of the bulk material at -35 °C. Single crystals suitable for X-ray diffraction studies were grown in a similar fashion after 11 days in the freezer.

Yield: 34% (0.0766 g, 0.192 mmol);

m.p.: 178-182 °C;

1H NMR: δ 6.94 (s, 4H, *aryl*), 2.64 (s, 12H, CH_3), 2.29 (s, 6H, CH_3);

$^{13}C\{^1H\}$ NMR: δ 138.3, 138.1, 132.0, 129.8, 21.1, 19.6;

$^{31}P\{^1H\}$ NMR: δ 211 (s);

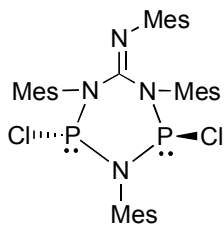
FT-IR (cm^{-1} (ranked intensity)): 408(2), 485(5), 511(7), 558(3), 600(10), 716(14), 896(1), 1035(13), 1158(9), 1218(6), 1263(11), 1308(15), 1375(12), 1476(4), 2916(8);

FT-Raman (cm^{-1} (ranked intensity)): 181(14), 221(2), 379(3), 405(11), 486(10), 543(12), 577(4), 632(8), 984(15), 1274(6), 1317(1), 1386(9), 1482(13), 1612(5), 2920(7);

HRMS: $C_{18}H_{22}N_2Cl_2P_2^+$ calcd (found) 398.0635(398.0622);

Elemental analysis (%): calcd for $C_{18}H_{22}Cl_2N_2P_2$ C 54.15, H 5.55, N 7.02; found C 53.97, H 5.51, N 6.92.

Compound 4.13



In a pressure tube **4.1** (0.543 g, 1.14 mmol) was dissolved in $CDCl_3$ (3 mL) and heated in an oil bath at 90 °C overnight. The solvent was removed *in vacuo*, producing a wax-like colourless product. This was washed with pentane (6 mL), which produced a white powder. The suspension was centrifuged and the decanted solution was transferred to a vial and kept in the freezer (-35 °C) for 1 h. The centrifuged white solid

was dissolved in CH₂Cl₂, transferred to a vial and dried *in vacuo* to give a sticky white solid. Resuspension of the solid in pentane followed by decanting the pentane and drying the solid *in vacuo* produced a fine white powder. More white precipitate was isolated by keeping the decanted pentane -30 °C for 2 h. The precipitate was isolated by decanting the supernatant and drying *in vacuo* to give a white powder, which was combined with the previous isolated product. Single crystals suitable for X-ray diffraction studies were grown from a concentrated CH₃CN solution of the bulk material at -30 °C for two weeks.

Yield: 31% (0.239 g, 0.352 mmol);

m.p.: 204-209 °C;

¹H NMR: δ 6.94 (br s, 2H, *aryl*), 6.88 (br s, 2H, *aryl*), 6.61 (br s, 2H, *aryl*), 6.30 (br s, 2H, *aryl*), 2.86 (s, 6H, CH₃), 2.56 (br s, 6H, CH₃), 2.35 (br s, 6H, CH₃), 2.27 (br s, 3H, CH₃), 2.22 (s, 3H, CH₃), 2.21 (s, 3H, CH₃), 2.04 (s, 3H, CH₃), 1.87 (s, 6H, CH₃);

¹³C{¹H} NMR: δ 141.9, 138.8, 138.7138.0, 137.9, 137.8, 137.7, 136.7, 136.6, 136.1, 135.9, 131.2, 130.2, 129.9, 129.0, 127.8, 126.7, 21.5, 21.4, 21.0, 20.9, 20.6, 20.5, 20.4, 19.7;

³¹P{¹H} NMR: δ 140 (s);

FT-IR (cm⁻¹(ranked intensity)): 452(3), 563(9), 600(11), 722(15), 853(5), 950(7), 981(10), 1056(4), 1140(14), 1183(8), 1222(1), 1475(6), 1608(12), 1649(2), 2919(13);

FT-Raman (cm⁻¹(ranked intensity)): 86(6), 204(7), 396(14), 421(8), 443(10), 511(15), 580(4), 1058(11), 1307(5), 1381(9), 1535(13), 1610(2), 1652(3), 2921(1), 3007(12);

HRMS: C₃₇H₄₄N₄Cl₂P₂⁺ calcd (found) 676.2418 (676.2413);

Elemental analysis (%): calcd for C₃₇H₄₄N₄Cl₂P₂ C 65.58, H 6.54, N 8.27; found C 65.81, H 6.94, N 8.15.

4.4.2 Computational details[†]

All calculations were done with the program packages Turbomole 6.3⁷⁶ and ADF 2010.2.⁷⁷ Geometries of the studied systems were optimized using the PBE1PBE density functional⁷⁸⁻⁸¹ in combination with the def2-TZVP basis sets.^{82,83} The nature of stationary points found was assessed by calculating full Hessian matrices at the respective level of theory. Partial atomic charges were calculated with the natural population analysis (NPA) as implemented in Turbomole 6.3.⁷⁴ The nature of phosphorus-chlorine

interaction in the studied chlorophosphines was inspected with the energy decomposition analysis (EDA) procedure⁷⁵ as implemented in ADF 2010.2.⁸⁴⁻⁸⁶ The analyses were performed at the PBE1PBE/def2-TZVP optimized geometries using the PBE1PBE density functional in together with the all electron Slater-type TZP basis sets.⁸⁷ The program gOpenMol was used for all visualizations of molecular structures and Kohn-Sham orbitals.^{88,89}

4.5 References

- (1) Spikes, G. H.; Fettingner, J. C.; Power, P. P. *J. Am. Chem. Soc.* **2005**, *127*, 12232.
- (2) Peng, Y.; Brynda, M.; Ellis, B. D.; Fettingner, J. C.; Rivard, E.; Power, P. P. *Chem. Commun.* **2008**, 6042.
- (3) Li, J.; Schenk, C.; Goedecke, C.; Frenking, G.; Jones, C. *J. Am. Chem. Soc.* **2011**, *133*, 18622.
- (4) Power, P. P. *Acc. Chem. Res.* **2011**, *44*, 627.
- (5) Peng, Y.; Guo, J.-D.; Ellis, B. D.; Zhu, Z.; Fettingner, J. C.; Nagase, S.; Power, P. P. *J. Am. Chem. Soc.* **2009**, *131*, 16272.
- (6) Peng, Y.; Ellis, B. D.; Wang, X.; Power, P. P. *J. Am. Chem. Soc.* **2008**, *130*, 12268.
- (7) Zhu, Z.; Wang, X.; Peng, Y.; Lei, H.; Fettingner, J. C.; Rivard, E.; Power, P. P. *Angew. Chem. Int. Ed.* **2009**, *48*, 2031.
- (8) Khan, S.; Michel, R.; Dieterich, J. M.; Mata, R. A.; Roesky, H. W.; Demers, J.-P.; Lange, A.; Stalke, D. *J. Am. Chem. Soc.* **2011**, *133*, 17889.
- (9) Welch, G. C.; Juan, R. R. S.; Masuda, J. D.; Stephan, D. W. *Science* **2006**, *314*, 1124.
- (10) Stephan, D. W.; Erker, G. *Angew. Chem. Int. Ed.* **2010**, *49*, 46.
- (11) Dureen, M. A.; Lough, A.; Gilbert, T. M.; Stephan, D. W. *Chem. Commun.* **2008**, 4303.
- (12) Mömning, C. M.; Otten, E.; Kehr, G.; Fröhlich, R.; Grimme, S.; Stephan, D. W.; Erker, G. *Angew. Chem. Int. Ed.* **2009**, *48*, 6643.
- (13) Ménard, G.; Stephan, D. W. *J. Am. Chem. Soc.* **2010**, *132*, 1796.
- (14) Chase, P. A.; Welch, G. C.; Jurca, T.; Stephan, D. W. *Angew. Chem. Int. Ed.* **2007**, *46*, 8050.
- (15) Chase, P. A.; Jurca, T.; Stephan, D. W. *Chem. Commun.* **2008**, 1701.
- (16) Spies, P.; Schwendemann, S.; Lange, S.; Kehr, G.; Fröhlich, R.; Erker, G. *Angew. Chem. Int. Ed.* **2008**, *47*, 7543.
- (17) Sumerin, V.; Schulz, F.; Atsumi, M.; Wang, C.; Nieger, M.; Leskelä, M.; Repo, T.; Pyykkö, P.; Rieger, B. *J. Am. Chem. Soc.* **2008**, *130*, 14117.

- (18) Wang, H.; Fröhlich, R.; Kehr, G.; Erker, G. *Chem. Commun.* **2008**, 5966.
- (19) Jana, A.; Schulzke, C.; Roesky, H. W. *J. Am. Chem. Soc.* **2009**, *131*, 4600.
- (20) Präsang, C.; Stoelzel, M.; Inoue, S.; A]Meltzer, A.; Driess, M. *Angew. Chem. Int. Ed.* **2010**, *49*, 10002.
- (21) Payraastre, C.; Madaule, Y.; Wolf, J. G.; Kim, T. C.; Mazières, M.-R.; Wolf, R.; Sanchez, M. *Heteroat. Chem.* **1992**, *3*, 157.
- (22) Burford, N.; Cameron, T. S.; Ragogna, P. J. *J. Am. Chem. Soc.* **2001**, *123*, 7947.
- (23) Burford, N.; Ragogna, P. J. *J. Chem. Soc., Dalton Trans.* **2002**, 4307.
- (24) Cowley, A. H.; Kemp, R. A. *Chem. Rev.* **1985**, *85*, 367.
- (25) Abrams, M. B.; Scott, B. L.; Baker, R. T. *Organometallics* **2000**, *19*, 4944.
- (26) Hardman, N. J.; Abrams, M. B.; Pribisko, M. A.; Gilbert, T. M.; Martin, R. L.; Kubas, G. J.; Baker, R. T. *Angew. Chem. Int. Ed.* **2004**, *43*, 1955.
- (27) Caputo, C. A.; Jennings, M. C.; Tuononen, H. M.; Jones, N. D. *Organometallics* **2009**, *28*, 990.
- (28) Caputo, C. A.; Brazeau, A. L.; Hynes, Z.; Price, J. T.; Tuononen, H. M.; Jones, N. D. *Organometallics* **2009**, *28*, 5261.
- (29) Spinney, H. A.; Yap, G. P. A.; Korobkov, I.; DiLabio, G.; Richeson, D. S. *Organometallics* **2006**, *25*, 3541.
- (30) Montemayor, R. G.; Sauer, D. T.; Fleming, S. S.; Bennett, D. W.; Thomas, M. G.; Parry, R. W. *J. Am. Chem. Soc.* **1978**, *100*, 2231.
- (31) Nakazawa, H.; Yamaguchi, Y.; Mizuta, T.; Miyoshi, K. *Organometallics* **1995**, *14*, 4173.
- (32) Burck, S.; Daniels, J.; Gans-Eichler, T.; Gudat, D.; Nättinen, K.; Nieger, M. Z. *Anorg. Allg. Chem.* **2005**, *631*, 1403.
- (33) Burford, N.; Dyker, C. A.; Decken, A. *Angew. Chem. Int. Ed.* **2005**, *44*, 2364.
- (34) Holthausen, M. H.; Weigand, J. J. *J. Am. Chem. Soc.* **2009**, *131*, 14210.
- (35) Holthausen, M. H.; Richter, C.; Hepp, A.; Weigand, J. J. *Chem. Commun.* **2010**, 46, 6921.
- (36) Weigand, J. J.; Feldman, K.-O.; Henne, F. D. *J. Am. Chem. Soc.* **2010**, *132*, 16321.

- (37) Scherer, O. J.; Schnabl, G. *Chem. Ber.* **1976**, *109*, 2996.
- (38) Niecke, E.; Kröher, R. *Angew. Chem. Int. Ed. Engl.* **1976**, *15*, 692.
- (39) Green, S. P.; Jones, C.; Jin, G.; Stasch, A. *Inorg. Chem.* **2007**, *46*, 8.
- (40) Ergezinger, C.; Weller, F.; Dehnicke, K. *Z. Naturforsch., B: Chem. Sci.* **1988**, *43*, 1119.
- (41) Raston, C. L.; Skelton, B. W.; Tolhurst, V.-A.; White, A. H. *Polyhedron* **1998**, *17*, 935.
- (42) Raston, C. L.; Skelton, B. W.; Tolhurst, V.-A.; White, A. H. *J. Chem. Soc., Dalton Trans.* **2000**, 1279.
- (43) Lyhs, B.; Schulz, S.; Westphal, U.; Bläser, D.; Boese, R.; Bolte, M. *Eur. J. Inorg. Chem.* **2009**, 2247.
- (44) Brazeau, A. L.; Nikouline, A. S.; Ragogna, P. J. *Chem. Commun.* **2011**, *47*, 4817.
- (45) Bailey, P. J.; Gould, R. O.; Harmer, C. N.; Pace, S.; Steiner, A.; Wright, D. S. *Chem. Commun.* **1997**, 1161.
- (46) Boéré, R. E.; Boéré, R. T.; Masuda, J.; Wolmershäuser, G. *Can. J. Chem.* **2000**, *78*, 1613.
- (47) Tin, M. K. T.; Yap, G. P. A.; Richeson, D. S. *Inorg. Chem.* **1998**, *37*, 6728.
- (48) Caputo, C. A.; Price, J. T.; Jennings, M. C.; McDonald, R.; Jones, N. D. *Dalton Trans.* **2008**, 3461.
- (49) Burford, N.; Cameron, T. S.; Conroy, K. D.; Ellis, B.; Macdonald, C. L. B.; Ovans, R.; Phillips, A. D.; Ragogna, P. J.; Walsh, D. *Can. J. Chem.* **2002**, *80*, 1404.
- (50) Burck, S.; Gudat, D.; Nättinen, K.; Nieger, M.; Niemeyer, M.; Schmid, D. *Eur. J. Inorg. Chem.* **2007**, 5112.
- (51) Denk, M. K.; Gupta, S.; Ramachandran, R. *Tetrahedron Lett.* **1996**, *37*, 9025.
- (52) Pavia, D. L.; Lampman, G. M.; Kriz, G. S. *Introduction to Spectroscopy*; 2nd ed.; Saunders College Publishing: Orlando, 1996.
- (53) Burck, S.; Gudat, D.; Nieger, M.; Benkö, Z.; Nyulászi, L. *Z. Anorg. Allg. Chem.* **2009**, *635*, 245.
- (54) Reeske, G.; Cowley, A. H. *Inorg. Chem.* **2007**, *46*, 1426.
- (55) Dube, J. W.; Farrar, G. J.; Norton, E. L.; Szekely, K. L. S.; Cooper, B. F. T.; Macdonald, C. L. B. *Organometallics* **2009**, *28*, 4377.

- (56) Gudat, D.; Haghverdi, A.; Hupfer, H.; Nieger, M. *Chem. Eur. J.* **2000**, *6*, 3414.
- (57) Carmalt, C. J.; Lomeli, V.; McBurnett, B. G.; Cowley, A. H. *Chem. Commun.* **1997**, 2095.
- (58) Denk, M. K.; Gupta, S.; Lough, A. J. *Eur. J. Inorg. Chem.* **1999**, 41.
- (59) Niecke, E.; Nixon, J. F.; Wenderoth, P.; Passos, B. F. T.; Nieger, M. *J. Chem. Soc., Chem. Commun.* **1993**, 846.
- (60) Lehmann, M.; Schulz, A.; Villinger, A. *Struct. Chem.* **2011**, *22*, 35.
- (61) Coyle, J. P.; Johnson, P. A.; DiLabio, G. A.; Barry, S. T.; Müller, J. *Inorg. Chem.* **2010**, *49*, 2844.
- (62) Ziffle, L. C.; Kenney, A. P.; Barry, S. T.; Müller, J. *Polyhedron* **2008**, *27*, 1832.
- (63) Burford, N.; Cameron, T. S.; Conroy, K. D.; Ellis, B.; Lumsden, M.; Macdonald, C. L. B.; McDonald, R.; Philips, A. D.; Ragogna, P. J.; Schurko, R. W.; Walsh, D.; Wasylishen, R. E. *J. Am. Chem. Soc.* **2002**, *124*, 14012.
- (64) Bruno, I. J.; Cole, J. C.; Edgington, P. R.; Kessler, M.; Macrae, C. F.; McCabe, P.; Pearson, J.; Taylor, R. *Acta Crystallogr., Sect. B: Struct. Sci* **2002**, *58*, 389.
- (65) Gudat, D. *Acc. Chem. Res.* **2010**, *43*, 1307.
- (66) Zaripov, N. M.; Naumov, V. A.; Tuzova, L. L. *Phosphorus* **1974**, *4*, 179.
- (67) Grant, D. F.; Killean, R. C. G.; Lawrence, J. L. *Acta Crystallogr., Sect. B: Struct. Sci* **1969**, *B25*, 377.
- (68) Thomas, F.; Bauer, T.; Schulz, S.; Nieger, M. *Z. Anorg. Allg. Chem.* **2003**, *629*, 2018.
- (69) Timoshkin, A. Y.; Suvorov, A. V.; Bettinger, H. F.; Schaefer, H. F. *J. Am. Chem. Soc.* **1999**, *121*, 5687.
- (70) Niecke, E.; Nieger, M.; Reichert, F. *Angew. Chem. Int. Ed.* **1988**, *27*, 1715.
- (71) Roesky, H. W.; Zamankhan, H.; Sheldrick, W. S.; Cowley, A. H.; Mehrotra, S. K. *Inorg. Chem.* **1981**, *20*, 2910.
- (72) Chen, H.-J.; Haltiwanger, R. C.; Hill, T. G.; Thompson, M. L.; Coons, D. E.; Norman, A. D. *Inorg. Chem.* **1985**, *24*, 4725.
- (73) Burford, N.; Conroy, K. D.; Landry, J. C.; Ragogna, P. J.; Ferguson, M. J.; McDonald, R. *Inorg. Chem.* **2004**, *43*, 8245.
- (74) Reed, A. E.; Weinstock, R. B.; Weinhold, F. *J. Chem. Phys.* **1985**, *83*, 735.

- (75) Bickelhaupt, F. M.; Baerends, E. J. In *Rev. Comput. Chem.*; Lipkowitz, K. B., Boyd, D. B., Eds.; Wiley-VCH: New York, 2000; Vol. 15, p 1.
- (76) TURBOMOLE V6.3 2011, a development of University of Karlsruhe and Forschungszentrum Karlsruhe GmbH, 1989-2007, TURBOMOLE GmbH, since 2007; available from <http://www.turbomole.com>.
- (77) ADF2010, SCM, Theoretical Chemistry, Vrije Universiteit, Amsterdam, The Netherlands, <http://www.scm.com>.
- (78) Perdew, J. P.; Burke, K.; Ernzerhof, M. *Phys. Rev. Lett.* **1996**, *77*, 3865.
- (79) Perdew, J. P.; Burke, K.; Ernzerhof, M. *Phys. Rev. Lett.* **1997**, *78*, 1396.
- (80) Perdew, J. P.; Ernzerhof, M.; Burke, K. *J. Chem. Phys.* **1996**, *105*, 9982.
- (81) Adamo, C.; Barone, V. *J. Chem. Phys.* **1999**, *10*, 6158.
- (82) Weigend, F.; Häser, M.; Patzelt, H.; Ahlrichs, R. *Chem. Phys. Lett.* **1998**, *294*, 143.
- (83) Weigend, F.; Ahlrichs, R. *Phys. Chem. Chem. Phys.* **2005**, *7*, 3297.
- (84) Morokuma, K. *J. Chem. Phys.* **1971**, *55*, 1236.
- (85) Kitaura, K.; Morokuma, K. *Int. J. Quantum Chem* **1976**, *10*, 325.
- (86) Ziegler, T.; Rauk, A. *Theoret. Chim. Acta* **1977**, *46*, 1.
- (87) van Lenthe, E.; Baerends, E. J. *J. Comput. Chem.* **2003**, *24*, 1142.
- (88) Laaksonen, L. *J. Mol. Graphics* **1992**, *10*, 33.
- (89) Bergman, D. L.; Laaksonen, L.; Laaksonen, A. *J. Mol. Graphics Modell.* **1997**, *15*, 301.

Chapter 5

5 Reactions of trichloropnictogens with a bulky guanidinate ligand^ϕ

5.1 Introduction

New directions in low valent, cationic main group chemistry involve the following two key objectives; (a) identifying new ways to apply electronic and steric stress to the p-block element centre such that unprecedented bonding arrangements can be identified; and, (b) discovering applications for these molecules, which are considered to be in highly unusual environments. To promote the former, new or unconventional ligands and their main group complexes are being developed, and these efforts have resulted in significant discoveries in structure, bonding and reactivity.¹⁻⁶

An emerging avenue of investigation has been to synthesize and isolate molecules with main group polycations, where one can envision localizing the high degree of positive charge on the central element. This has been achieved for Group 16 (S, Se, Te)⁷ and for the electron deficient boron.⁸⁻¹⁰ Rare examples from other groups within the p-block have emerged,^{5,6,11-13} where most of these involve phosphorus as a dicationic centre.^{2,14-16} We have been working to merge the areas of novel ligand synthesis, highly charged main group cations, and new reactivity by utilizing the guanidinate class of ligands, as they have been shown to act as versatile supports for metals spanning the periodic table.¹⁷ While there have been several examples of monoanionic guanidinate stabilized group 15(III) dihalides (See Chart 4.3) from the groups of Jones,¹⁸ Dehnicke,¹⁹ Raston,^{20,21} Schulz,²² and Coles,²³ there has only been one structurally characterized Group 15(III) complex featuring a dianionic guanidinate.²⁴ Despite the extensive use of guanidinate ligands, there are surprisingly no reports of these frameworks in cationic

^ϕ A portion of this work is published in Brazeau, A. L.; Nikouline, A. S.; Ragonna, P. J. *Chem. Commun.* **2011**, 47, 4817. Reproduced by permission of The Royal Society of Chemistry (RSC). See Appendix 2.2.

pnictenium compounds, which could have new and exciting reactivity towards small molecules arising from the highly strained four-membered ring system.

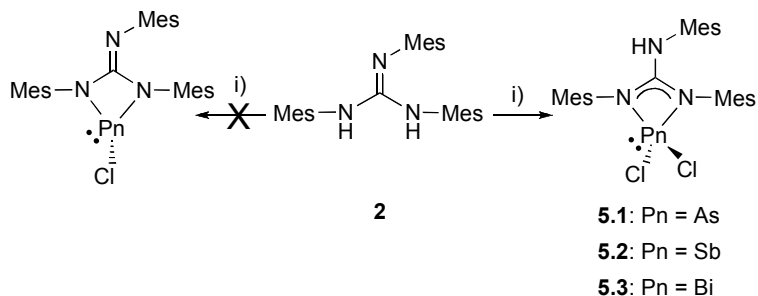
In this context, this chapter focuses on using a bulky trisubstituted guanidine to synthesize neutral and cationic arsenic, antimony and bismuth (in the +3 oxidation state) complexes and dicationic arsenic(III) and antimony(III) complexes. This is the first report of both guanidinate stabilized pnictenium (Pn = As, Sb, Bi) cations and an arsetidinium dication, which was trapped using 2,2'-bipyridine (bpy).

5.2 Results and discussion

5.2.1 Synthesis

The reaction of **2**, PnCl₃ (Pn = As, Sb, Bi), and NEt₃ in a 1:1:2 stoichiometry at room temperature was anticipated to give the corresponding diaminochloropnictine supported by a dianionic guanidinate ligand (**5.1-5.3**, Scheme 5.1). Analysis of the product by ¹H NMR spectroscopy after removal of the ammonium chloride salt by-product, revealed the presence of an N-H proton ($\delta_{\text{H}} = 5.60$ (As, Sb) and 5.18 (Bi) in CDCl₃) suggesting that the chelating ligand was not doubly deprotonated. A corroborating N-H vibration was observed in the FT-IR spectrum ($\nu = 3321$ (As), 3331(Sb) and 3338 (Bi) cm⁻¹) of the isolated powders. The purification of **5.3** was not trivial. The reaction produced an insoluble black material and [HNEt₃]Cl, guanidine (**2**) and an unknown product were observed in the ¹H NMR spectrum of the crude material. The guanidine was removed by stirring the crude product in hexane overnight, and the ammonium salt could be removed by CH₃CN washes (3 x 4 mL). This led to the isolation of the yellow unknown product. The yellow powder, unlike the isolated white powders of **5.1** and **5.2**, was confirmed to be pure **5.3** by elemental analysis. Single crystals for **5.1** and **5.2** were grown from the bulk powders and subsequent X-ray diffraction studies revealed that the products were the dichloroarsine and dichlorostibine complexes, respectively (Figure 5.2). Since only monodeprotonation was being effected, various bases were otherwise employed (e.g. *N*-methyl morpholine, lithium diisopropylamide and *n*-butyllithium). In the case of Pn = As, neither the dehydrohalogenation or salt metathesis routes gave the dianionic product. The isolation

of **5.1-5.3** was contrary to the analogous phosphorus chemistry (Chapter 4), which under identical conditions gives the diaminochlorophosphine supported by a dianionic guanidinate backbone.



Scheme 5.1: Anticipated and observed (**5.1-5.3**) reactivity of **2** with PnCl_3 and NEt_3 ; i) PnCl_3 , 2 eq NEt_3 .

Compounds **5.1-5.3** were used as precursors to the corresponding pnictenium cation *via* halide abstraction using a stoichiometric amount of Me_3SiOTf (Scheme 5.2). After the reaction, removal of the volatiles produced white (Pn = As, Sb) and yellow (Pn = Bi) powders. Multinuclear NMR spectroscopy in CD_3CN revealed a downfield shift in the ^1H NMR spectrum of the amine proton at $\delta_{\text{H}} = 8.09$ (As; *cf.* $\delta_{\text{H}} = 7.29$ in **5.1**) and 7.12 (Sb; *cf.* $\delta_{\text{H}} = 6.50$ in **5.2**), and an ionic triflate was observed in the $^{19}\text{F}\{^1\text{H}\}$ NMR spectrum ($\delta_{\text{F}} = -78.8$ and -79.5 , respectively; *cf.* MeOTf $\delta_{\text{F}} = -75.4$; $[\text{NOct}_4]\text{OTf}$ $\delta_{\text{F}} = -79.0$). The synthesis of the bismuthenium cation was not as facile as the As and Sb analogues. A ^1H NMR spectrum was acquired after removal of the volatiles, revealing the presence of at least two products (Figure 5.1a). This mixture was dissolved in CH_2Cl_2 and hexane was added with vigorous stirring in an attempt to purify a single product by precipitation, however an oil was produced. The volatiles were removed *in vacuo* for both the supernatant and oil to produce yellow solids in each case. The ^1H NMR spectrum of the material that was an oil (Figure 5.1b), still contained two products, but with now different ratios. The spectrum of the major product had a singlet at $\delta_{\text{H}} = 5.31$ ($\Delta\delta_{\text{H}} = 0.13$) for the N–H resonance and peaks corresponding to the Mes groups in the range of $\delta_{\text{H}} = 2.0\text{-}2.8$ and $6.4\text{-}7.0$. Some of the Mes peaks were broad at room temperature, which was also observed in the As and Sb analogue, and is thought to be the

expected bismuthenium product **5.6**. Pure **5.6** has not yet been isolated for a full comprehensive characterization. After washing the yellow solid from the supernatant with Et₂O (3 x 3 mL), a white solid was isolated. The ¹H NMR spectrum of the white solid (Figure 5.1c) had one resonance indicative of an acidic N–H bond at δ_H = 7.06, and peaks corresponding to Mes groups were observed, this matched the minor product in the previously described ¹H NMR spectrum. The ¹⁹F{¹H} NMR spectrum had a single peak at δ_F = -79.0. This product is most likely a guanidinium (cationic ligand) cation with a triflate anion. X-ray quality single crystals of the arsenium salt **5.4** were grown at room temperature by vapour diffusion of Et₂O into a concentrated CH₃CN solution of the bulk powder (Figure 5.2). Although single crystals could not be obtained in the case of Pn = Sb, an analogous structure was assigned based on the comprehensive characterization to give **5.5**.

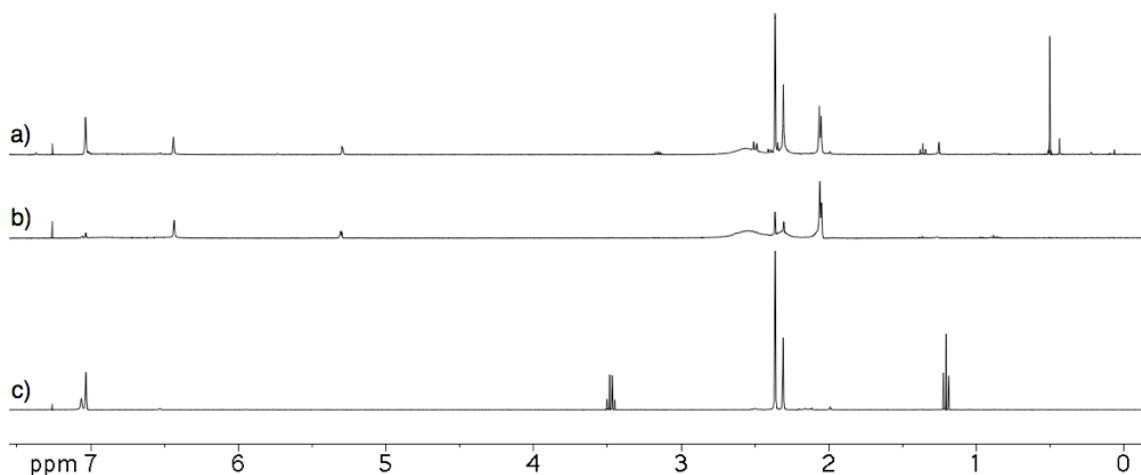
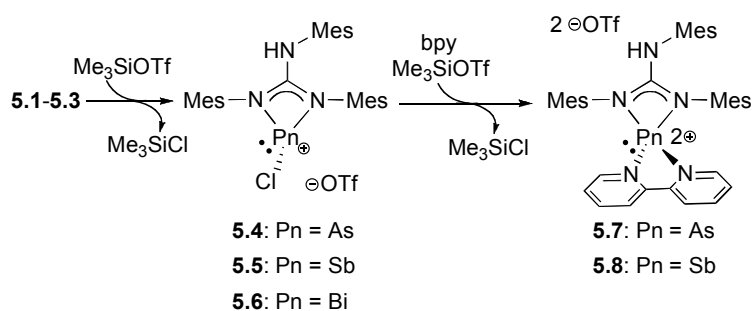


Figure 5.1: Stacked plot of the ¹H NMR spectra for **5.6**: (a) crude; (b) yellow; and (c) white material.

Using an excess amount of Me₃SiOTf with **5.1-5.3** also yielded the removal of a single chloride ion. However, if the reaction of **5.4** or **5.5** was carried out with a stoichiometric equivalent of Me₃SiOTf in the presence of bpy (Scheme 5.2), an instantaneous colour change from colourless to yellow was observed for both Pn = As and Sb and a yellow powder was obtained after removal of the volatiles *in vacuo*. The ¹H NMR spectrum of the redissolved solid in CD₃CN displayed sharp resonances

corresponding to both the bpy and guanidinate fragments residing in unsymmetrical environments in the case of arsenic, and an upfield shift of the amine proton to $\delta_{\text{H}} = 7.61$ ($\Delta\delta_{\text{H}} = 0.48$ ppm). Broad resonances were observed in the ^1H NMR spectra for antimony, even at -30 °C. The $^{19}\text{F}\{^1\text{H}\}$ NMR spectra had a single peak for ionic triflate at $\delta_{\text{F}} = -78.9$ and -79.5 , for As and Sb, respectively. X-ray quality crystals of the arsenic analogue were grown by room temperature vapour diffusion of Et_2O into a concentrated CH_3CN solution of the bulk material over two days. X-ray diffraction experiments confirmed that the product contained a base-stabilized dicationic arsenic centre supported by the monoanionic guanidinate as well as bpy with two triflate anions (**5.7**, Figure 5.2). Solid-state structures were not obtained in the case of antimony, an analogous dicationic structure **5.8** was assigned based on the comprehensive characterization.



Scheme 5.2: Synthesis of mono- (**5.4-5.6**) and dicationic (**5.7-5.9**) Pn(III) complexes.

5.2.2 X-ray crystallography

Compounds **5.1**, **5.2**, **5.4** and **5.7** have been studied by X-ray diffraction studies. All hydrogen atoms are placed in calculated positions. Selected metrical parameters are summarized in Table 5.1 and refinement details are given in Table 5.2.

Distorted seesaw molecular geometries with a stereochemically active lone pair on the central pnictogen were observed in the solid-state for compounds **5.1**, **5.2**, **5.4** and **5.7**. In the case of **5.1**, **5.2** and **5.7** the axial Pn–N (Pn = As, Sb) and Pn–X (X = Cl, N) bonds were all longer than their equatorial counterparts, consistent with AX_4E electron pair geometries.¹⁸ The N(1)–Pn(1)–N(2) angle varied from $60.13(12)$ – $67.51(14)^\circ$ in the four compounds. Trigonal planar geometries were found about C(1), N(1) and N(3)

indicative of electron delocalization within the four atom N₃C backbone. There was a slight pyramidalization found at N(2) ($\Sigma_{\text{angles}} = 347.2$ (**5.1**), 352.9 (**5.2**), 350.1 (**5.4**) and 346.9° (**5.7**)) to minimize steric interactions of the Mes substituent located on exocyclic N(3). Electron delocalization was also evident by the intermediate C–N bond lengths in the crystallized compounds (1.320(5)–1.373(6) Å) compared to a C–N single (1.47 Å) and double bond (1.28 Å)²⁵, the latter being that of an exocyclic C–N bond length in a dianionic guanidinate complex.

In compounds **5.4** and **5.7** the triflate anion is weakly coordinating in the solid-state (As(1)⋯O(1) 2.363(3) Å (**5.4**), As(1)⋯O(2A) 2.938(4) Å (**5.7**), $\Sigma_{\text{vdW(As-O)}} = 3.30$ Å²⁶). The corresponding triflate S–O bonds in **5.4** were crystallographically inequivalent with a range of bond lengths from 1.396(5)–1.446(3) Å, indicating a significant cation-anion interaction in the solid-state. The length of the As–O bond was however significantly longer than that of a triflate covalently bound to As (1.987(2) for *N*-(trifluoromethylsulfonatodimethylsilyl)-*N*-(*m*-terphenyl)trifluoromethylsulfonatomethylarsane).²⁷ On the contrary, the S–O bonds in **5.7** were of similar length (1.440(4)–1.446(4) Å) and the weakly coordinated triflate is thus best described as an electrostatic interaction in the solid state.

The solid-state structure of **5.7** shows a bound bpy substituent to arsenic with elongated axial and equatorial As–N bonds. Given a dative bonding model for this compound (Figure 5.4b) it can be considered as a base-stabilized dicationic arsetidinium, the first observation of such a species.

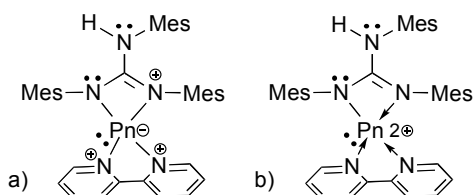
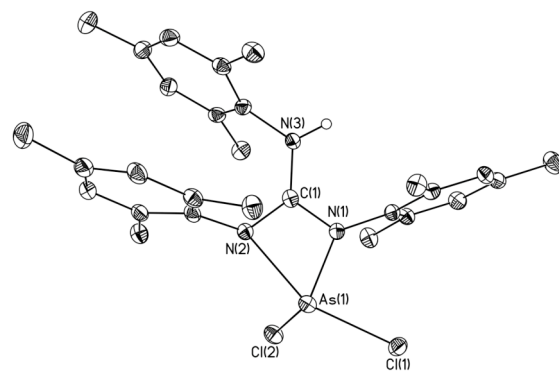
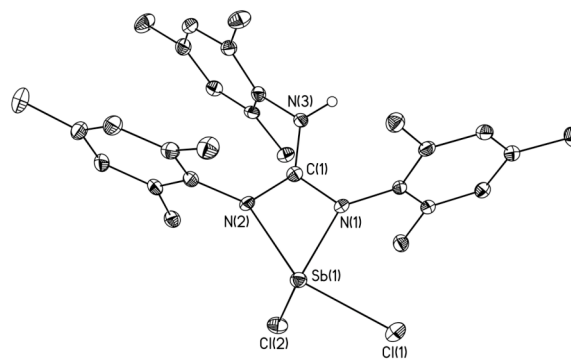


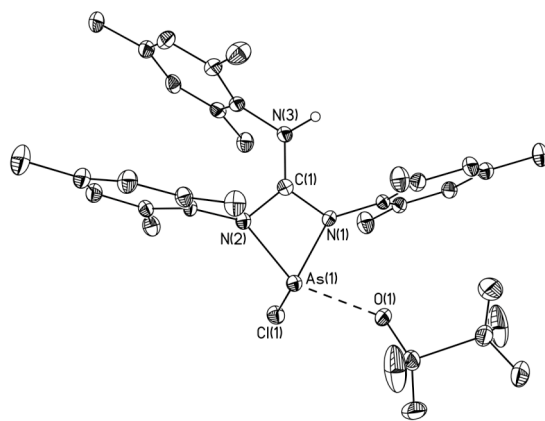
Figure 5.4: (a) Lewis structure and (b) dative bonding models for **5.7** and **5.8**.



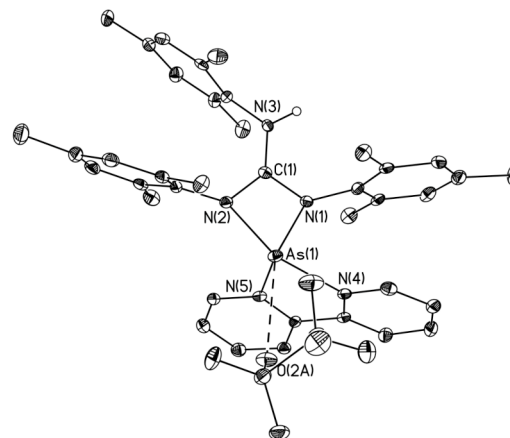
5.1



5.2



5.4



5.7

Figure 5.2: Solid-state structures of **5.1**, **5.2**, **5.4** and **5.7**. Ellipsoids are drawn to 30% probability. Non-essential hydrogen atoms, solvates and non-interacting anions are removed for clarity.

Table 5.1: Selected bond lengths (Å) and bond angles (°) for compounds **5.1**, **5.2**, **5.4** and **5.7**.

Compound	5.1 [§]	5.2 [§]	5.4	5.7
Bond	Pn = As	Pn = Sb	Pn = As	Pn = As
C(1)–N(1)	1.345(5)	1.361(5)	1.343(5)	1.373(6)
C(1)–N(2)	1.322(5)	1.320(5)	1.345(5)	1.335(6)
C(1)–N(3)	1.348(5)	1.364(5)	1.320(5)	1.324(6)
Pn(1)–N(1)	1.897(3)	2.104(3)	1.891(3)	1.872(4)
Pn(1)–N(2)	2.202(3)	2.296(3)	1.979(3)	2.086(4)
As(1)–N(4)	–	–	–	2.141(4)
As(1)–N(5)	–	–	–	1.985(4)
Pn(1)–Cl(1)	2.3460(12)	2.4848(12)	2.1894(13)	–
Pn(1)–Cl(2)	2.2105(11)	2.3845(13)	–	–
N(1)–C(1)–N(2)	109.7(3)	111.1(3)	106.3(3)	106.0(4)
N(1)–Pn(1)–N(2)	63.77(12)	60.13(12)	67.51(14)	65.99(16)
As(1)···O	–	–	2.363(3)	2.938(4)

§ Metrical parameters for only one of the two molecules in the asymmetric unit are given.

Table 5.2: Refinement details for compounds **5.1**, **5.2**, **5.4** and **5.7**.

Compound	5.1	5.2	5.4	5.7
Empirical formula	C ₅₇ H ₆₈ As ₂ Cl ₆ N ₆	C ₅₈ H ₇₁ Cl ₄ N ₇ Sb ₂	C ₂₉ H ₃₄ As ₁ Cl ₁ F ₃ N ₃ O ₃ S ₁	C ₄₁ H ₄₄ As ₁ Cl ₂ F ₆ N ₅ O ₆ S ₂
FW (g/mol)	1199.71	1251.52	672.02	1026.75
Crystal system	Monoclinic	Triclinic	Triclinic	Monoclinic
Space group	<i>P</i> 2 ₁ / <i>c</i>	<i>P</i> $\bar{1}$	<i>P</i> $\bar{1}$	<i>C</i> 2/ <i>c</i>
<i>a</i> (Å)	8.5877(17)	8.7040(17)	8.4795(17)	46.542(6)
<i>b</i> (Å)	24.885(5)	17.247(3)	11.348(2)	11.8257(13)
<i>c</i> (Å)	13.608(3)	20.299(4)	17.240(3)	17.160(2)
α (deg)	90	92.42(3)	88.43(3)	90
β (deg)	98.80(3)	101.77(3)	79.28(3)	109.257(5)
γ (deg)	90	98.22(3)	70.44(3)	90
<i>V</i> (Å ³)	2873.9(10)	2944.5(10)	1534.8(5)	8916.1(18)
<i>Z</i>	2	2	2	8
<i>D_c</i> (mg m ⁻³)	1.386	1.412	1.454	1.530
<i>R</i> _{int}	0.0373	0.0533	0.0444	0.1722
<i>R</i> 1[<i>I</i> > 2σ <i>I</i>] ^a	0.0598	0.0411	0.0599	0.0601
<i>wR</i> 2(<i>F</i> ²) ^a	0.1508	0.1103	0.1581	0.1351
GOF (<i>S</i>) ^a	1.067	1.052	1.083	0.986

^a $R1(F[I > 2(I)]) = \sum ||F_o| - |F_c|| / \sum |F_o|$; $wR2(F^2 [\text{all data}]) = [w(F_o^2 - F_c^2)^2]^{1/2}$; $S(\text{all data}) = [w(F_o^2 - F_c^2)^2 / (n - p)]^{1/2}$ (n = no. of data; p = no. of parameters varied; $w = 1/[\sigma^2(F_o^2) + (aP)^2 + bP]$ where $P = (F_o^2 + 2F_c^2)/3$ and a and b are constants suggested by the refinement program.

5.3 Conclusions

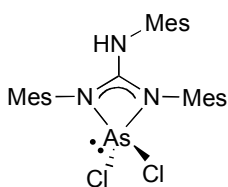
The 1:1:2 stoichiometric reactions of **2**, PnCl_3 and NEt_3 , respectively, unexpectedly gave products bearing a monoanionic guanidinate. The ability of this ligand to support neutral dihalopnictines, cationic halopnicteniums, and novel base-stabilized dicationic pnictetidiniums has been demonstrated. The synthesis of these three types of molecules was facile with moderate to high yields for $\text{Pn} = \text{As}$ and Sb . Reactions involving bismuth are prone to decomposition and low yields. This is the first example of a dicationic arsenic complex, and a rare example of an antimony dication.

5.4 Experimental section

General synthetic and crystallography experimental details can be found in Appendix 1.

5.4.1 Synthetic procedures

Compound **5.1**



To a toluene solution (5 mL) of **2** (1.00 g, 2.42 mmol), NEt_3 (0.670 mL, 4.83 mmol) and AsCl_3 (0.210 mL, 2.51 mmol) were added sequentially, resulting in a clear, yellow solution. The solution was left to stir for 1 h at rt over which time the solution precipitated white powders. The precipitate was then separated by centrifugation and the yellow supernatant transferred to a separate vial. The volatiles were removed *in vacuo* which yielded an off white solid. The solid was dissolved in CH_2Cl_2 (5 mL) and precipitated with the addition of hexane under rapid stirring. The supernatant was decanted and the solid was dried to yield a white powder.

Yield: 56% (0.757 g, 1.36 mmol);

d.p.: 190-192 °C;

^1H NMR (-30 °C): δ 7.05 (s, 2H, *m*-CH), 6.50 (s, 4H, *m*-CH), 5.65 (s, 1H, NH), 2.53 (s, 6H, *p*-CH₃), 2.33 (s, 3H, *p*-CH₃), 2.19 (s, 6H, *o*-CH₃), 2.09 (s, 12H, *o*-CH₃);

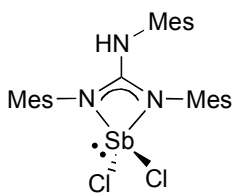
$^{13}\text{C}\{^1\text{H}\}$ NMR (-30 °C): δ 153.0, 138.6, 138.5, 137.5, 136.4, 135.6, 134.1, 133.5, 131.5, 129.9, 128.8, 129.4, 128.5, 128.4, 128.0, 127.9, 21.3(br), 20.9(br), 19.6(br), 19.1;

FT-IR (cm⁻¹(ranked intensity)): 584(14), 740(9), 857(3), 915(11), 1033(7), 1141(15), 1200(12), 1276(5), 1303(13), 1334(8), 1375(10), 1500(1), 1556(6), 2919(2), 3321(4);

FT-Raman (cm⁻¹(ranked intensity)): 97(10), 179(8), 273(5), 349(4), 370(15), 438(14), 579(3), 1278(13), 1308(12), 1333(6), 1383(7), 1482(11), 1610(1), 2921(2), 3014(9);

Elemental Analysis (%): calcd for C₂₈H₃₄N₃Cl₂As₁ C 60.22, H 6.14, N 7.52; found: C 59.92, H 5.85, N 7.55.

Compound 5.2



Compound **2** (0.501 g, 1.21 mmol) was dissolved in toluene (8 mL) and added to solid SbCl₃ (0.360 g, 1.57 mmol). Triethylamine (0.440 mL, 3.15 mmol) was added to the reaction mixture and the solution became cloudy. The reaction was left to stir at rt for 18 h.

A waxy precipitate was present on the bottom and sides of the reaction flask. The clear solution was transferred to a new vial and the volatiles removed *in vacuo* to give an off-white powder. The resulting powder was suspended in CH₃CN (6 mL) and stirred at rt for 30 min. The white powder was isolated by centrifugation and dried *in vacuo*.

Yield: 70 % (0.513 g, 0.848 mmol);

d.p.: 207-211 °C;

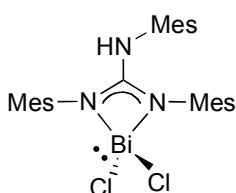
¹H NMR (-30°C): δ 7.03 (s, 2H, *aryl*), 6.49 (s, 2H, *aryl*), 6.48 (s, 2H, *aryl*), 5.60 (s, 1H, *NH*), 2.54 (s, 6H, *CH*₃), 2.32 (s, 3H, *CH*₃), 2.23 (s, 6H, *CH*₃), 2.08 (m, 12H, *CH*₃);

¹³C{¹H} NMR (-30°C): δ 157.2, 137.8 (br), 137.7, 137.4, 136.3, 135.7, 134.4, 134.1 (br), 132.2, 129.8, 128.44, 128.38, 128.1, 128.0, 21.2 (br), 20.9, 20.8, 19.8, 19.7 (br), 19.3;

FT-IR (cm⁻¹(relative intensities)): 556(11), 715(12), 852(3), 909(5), 1035(13), 1143(14), 1203(8), 1222(15), 1278(2), 1307(9), 1334(8), 1376(10), 1504(1), 2916(4), 3331(6);

FT-Raman (cm⁻¹(relative intensities)): 194(8), 275(5), 323(3), 343(14), 431(11), 503(13), 567(15), 578(4), 1278(12), 1308(2), 1336(9), 1377(10), 1525(6), 1609(1), 2917(7).

Compound 5.3



Triethylamine (0.530 mL, 3.80 mmol) was added to a CH₃CN slurry (6 mL) of **2** (0.782 g, 1.89 mmol) and BiCl₃ (0.588 g, 1.87 mmol).

The cloudy, yellow solution was left to stir for 18 h at rt. A black precipitate was present in the reaction mixture after this time. The precipitated material was removed by centrifugation, the yellow solution was transferred to a new vial, and the volatiles were removed *in vacuo* to give a yellow powder. The resulting powder was suspended in hexanes (5 mL) and stirred for 18 h at rt. The hexanes solution was decanted and the volatiles were removed from the yellow powder *in vacuo*. The product was then washed with CH₃CN (3 x 4 mL) and the volatiles were removed *in vacuo*.

Yield: 18 % (0.237 g, 0.342 mmol);

d.p.: 203-205 °C;

¹H NMR (-30°C): δ 6.97 (br, 2H, *aryl*), 6.36 (br, 4H, *aryl*), 5.18 (s, 1H, *NH*), 2.68 (br, 6H, *CH*₃), 2.35-2.17 (m, 12H, *CH*₃), 2.01 (s, 3H, *CH*₃), 1.97 (s, 6H, *CH*₃);

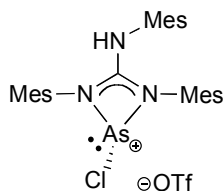
¹³C{¹H} NMR (-30°C): δ 163.2, 139.0, 136.9, 136.5, 136.2, 135.8, 132.9, 131.1, 129.5, 129.1, 128.6, 128.3, 127.5, 20.5, 20.9, 19.8, 19.3, 19.2;

FT-IR (cm⁻¹(relative intensities)): 555(13), 706(11), 852(3), 897(5), 1034(9), 1143(12), 1201(8), 1278(4), 1310(15), 1342(7), 1375(14), 1496(1), 1607(10), 2918(2), 3338(6);

FT-Raman (cm⁻¹ (relative intensities)): 85(7), 140(5), 184(14), 263(2), 425(10), 577(6), 897(12), 1009(15), 1279(9), 1309(1), 1340(13), 1381(11), 1526(8), 1608(4), 2929(3);

Elemental Analysis (%): calcd for C₂₈H₃₄Bi₁Cl₂N₃ C 48.56, H 4.95, N 6.07; found C 48.21, H 5.12, N 5.76.

Compound 5.4



Neat Me₃SiOTf (81.0 μl, 0.446 mmol) was added to a CH₂Cl₂ solution (5 mL) of **5.1** (0.254 g, 0.455 mmol), which resulted in the precipitation of a white powder after 10 min of stirring at room temperature. The suspension was allowed to stir for an additional 20 min. The volatiles were removed *in vacuo* yielding a white powder.

Yield: 96% (0.287 g, 0.427 mmol);

d.p.: 234-236 °C;

¹H NMR (CD₃CN, -40°C): δ 8.15 (s, 1H, *NH*), 7.11 (s, 2H, *aryl*), 6.72 (s, 2H, *aryl*), 6.47 (s, 1H, *aryl*), 6.42 (s, 1H, *aryl*), 2.56 (s, 3H, *CH*₃), 2.52 (s, 3H, *CH*₃), 2.44 (br s, 3H,

CH_3), 2.31 (s, 3H, CH_3), 2.27 (s, 3H, CH_3), 2.10 (br s, 3H, CH_3), 2.07 (s, 3H, CH_3), 2.05 (s, 3H, CH_3), 1.91 (br s, 3H, CH_3);

$^{13}C\{^1H\}$ NMR (CD_3CN , $-40\text{ }^\circ C$): δ 161.8, 140.6, 140.2, 139.3, 138.4, 138.0, 136.2, 132.7, 130.6, 130.3, 129.2, 129.1, 128.1, 127.8, 20.8, 20.5, 19.6, 18.4;

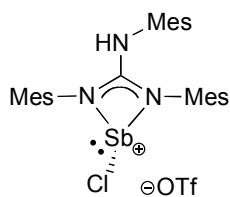
$^{19}F\{^1H\}$ NMR (CD_3CN): δ - 78.8 (s);

FT-IR (cm^{-1} (ranked intensity)): 516(10), 574(12), 637(3), 843(11), 923(9), 963(13), 1016(4), 1178(14), 1203(1), 1227(15), 1289(6), 1360(8), 1483(7), 1584(2), 2923(5);

FT-Raman (cm^{-1} (ranked intensity)): 174(9), 235(15), 324(11), 348(7), 483(6), 576(2), 763(12), 1014(5), 1323(4), 1360(8), 1484(10), 1610(3), 2061(13), 2923(1), 3024(14);

Elemental Analysis (%): calcd for $C_{29}H_{34}O_3N_3F_3S_1As_1Cl_1$ C 51.83, H 5.10, N 6.25; found C 51.99, H 5.25, N 6.36.

Compound 5.5



Neat Me_3SiOTf (154 μL , 0.849 mmol) was added to a CH_2Cl_2 solution (6 mL) of **5.2** (0.428 g, 0.707 mmol) and stirred at rt for 1 h. The volatiles were removed *in vacuo*, giving a white solid, which was washed with CH_2Cl_2 (2 x 3 mL). The decanted washings were combined and kept in the freezer overnight at $-30\text{ }^\circ C$ to give more white powder. The powders were combined, washed with pentane (2 mL) and dried *in vacuo*.

Yield: 69 % (0.350 g, 0.487 mmol);

d.p.: 183-188 $^\circ C$;

1H NMR ($-30\text{ }^\circ C$, CD_3CN): δ 7.12 (s, 1H, NH), 7.06 (s, 2H, aryl), 6.51 (br, 4H, aryl), 2.53 (s, 6H, CH_3), 2.30 (s, 3H, CH_3), 2.27(br, 6H, CH_3), 2.07(s, 6H, CH_3), 2.04 (s, 6H, CH_3);

$^{13}C\{^1H\}$ NMR ($-30\text{ }^\circ C$, CD_3CN): δ 163.0, 138.3, 138.0, 136.4, 135.3, 133.1, 130.6, 130.4, 130.1, 128.9, 128.6, 20.7, 20.5, 20.4, 19.7, 18.5;

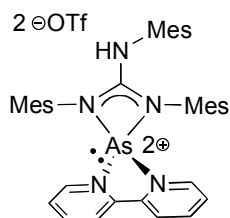
$^{19}F\{^1H\}$ NMR (CD_3CN): δ -79.5 (s);

FT-IR (cm^{-1} (relative intensities)): 461(14), 516(8), 582(11), 637(3), 716(12), 857(10), 917(7), 999(2), 1193(1), 1230(15), 1314(9), 1352(13), 1545(4), 2922(5), 3253(6);

FT-Raman (cm^{-1} (relative intensities)): 87(3), 194(7), 349(6), 440(12), 464(13), 571(5), 768(14), 1000(9), 1320(4), 1354(11), 1384(10), 1504(8), 1613(2), 2924(1), 3022(15);

Elemental Analysis (%): calcd for $C_{29}H_{34}Cl_1F_3N_3O_3S_1Sb_1$ C 48.45, H 4.77, N 5.85; found C 48.47, H 4.83, N 5.80.

Compound 5.7



A CH_3CN solution (1 mL) of 2,2'-bipyridine (0.0129 g, 0.0826 mmol) was added to a CH_3CN solution (5 mL) of **5.4** (0.0552 g, 0.0821 mmol), which resulted in a yellow reaction mixture. Neat Me_3SiOTf (14.8 μ L, 0.0818 mmol) was added with no colour change to the solution. The reaction mixture was left to stir for 2 h. The

volatiles were removed *in vacuo* yielding a yellow residue. The residue was washed with hexane (2 x 5 mL) and dried under reduced pressure to give a yellow powder.

Yield: 70% (0.0539 g, 0.0572 mmol);

m.p.: 141-145 $^{\circ}C$;

1H NMR (CD_3CN): δ 8.81 (d, 1H, *aryl*, $^3J_{H-H} = 5.6$), 8.74 (d, 1H, *aryl*, $^3J_{H-H} = 8.0$), 8.67 (m, 2H, *aryl*), 8.52 (t, 1H, *aryl*, $^3J_{H-H} = 8.0$), 8.47 (d, 1H, *aryl*, $^3J_{H-H} = 5.6$), 8.03 (t, 1H, *aryl*, $^3J_{H-H} = 6.0$), 7.78 (t, 1H, *aryl*, $^3J_{H-H} = 6.0$), 7.61 (s, 1H, *NH*), 7.17 (s, 1H, *m-CH*), 6.83 (s, 1H, *m-CH*), 6.78 (s, 1H, *m-CH*), 6.64 (s, 1H, *m-CH*), 6.49 (s, 1H, *m-CH*), 6.46 (s, 1H, *m-CH*), 2.78 (s, 3H, CH_3), 2.60 (s, 3H, CH_3), 2.28 (s, 3H, CH_3), 2.13 (s, 3H, CH_3), 2.10 (s, 3H, CH_3), 1.98 (s, 3H, CH_3), 1.91 (s, 3H, CH_3), 1.77 (s, 3H, CH_3), 1.76 (s, 3H, CH_3);

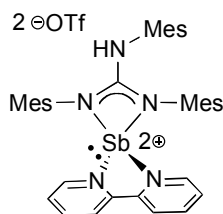
$^{13}C\{^1H\}$ NMR (CD_3CN): δ 158.0, 148.4, 147.1, 146.6, 146.5, 145.9, 140.4, 139.1, 138.5, 137.8, 137.7, 136.9, 136.2, 135.71, 135.68, 134.0, 130.9, 130.5, 129.93, 129.89, 129.6, 129.5, 129.1, 129.0, 128.7, 125.4, 125.0, 123.0, 119.8, 21.1, 20.7, 20.50, 20.45, 19.9, 19.2, 18.8, 18.6, 17.9;

$^{19}F\{^1H\}$ NMR (CD_3CN): δ -78.9 (s);

FT-IR (cm^{-1} (ranked intensity)): 518(9), 573(11), 636(3), 723(7), 780(6), 1029(2), 1158(4), 1256(1), 1287(15), 1352(12), 1449(14), 1476(13), 1501(8), 1590(5), 2928(10);

FT-Raman (cm^{-1} (ranked intensity)): 185(9), 233(15), 316(8), 570(7), 769(12), 1031(2), 1286(14), 1329(3), 1351(13), 1381(11), 1501(5), 1570(6), 1601(1), 2928(4), 3093(10);

Elemental Analysis (%): calcd for $C_{40}H_{42}O_6N_5F_6S_2As_1$ C 51.01, H 4.49, N 7.44; found C 50.14, H 4.53, N 7.24.

Compound **5.8**

A CH_2Cl_2 solution (2 mL) of 2,2'-bipyridine (0.0334 g, 0.0214 mmol) was added to a slurry of **5.5** (0.147 g, 0.0204 mmol) in CH_2Cl_2 (4 mL). The addition caused everything to dissolve and an immediate colour change from colourless to yellow. Neat Me_3SiOTf (45.0 μL , 2.45 mmol) was added to the reaction mixture and no further visible changes were observed. After stirring at rt for 1.5 h the volatiles were removed *in vacuo* to give a yellow powder. This was suspended in CH_2Cl_2 and stirred at rt for 30 min. The yellow powder was isolated after centrifugation.

Yield: 85 % (0.171, 0.173 mmol);

d.p.: 244-248°C;

^1H NMR (-30°C, CD_3CN): δ 8.62 (m, 2H, *aryl*), 8.48 (br, 2H, *aryl*), 7.84 (br, 2H, *aryl*), 7.06 (s, 1H, NH), 7.04 (br, 2H, *aryl*), 6.50 (br, 2H, *aryl*), 6.38 (br, 2H, *aryl*), 2.30 (s, 3H, CH_3), 2.27 (s, 6H, CH_3), 2.03 (s, 6H, CH_3), 2.00 (s, 6H, CH_3);

$^{13}\text{C}\{^1\text{H}\}$ NMR (-30°C, CD_3CN): δ 162.7, 138.4, 138.3, 138.0, 136.9, 136.6, 136.5, 134.0, 133.3, 130.7, 130.3, 129.28, 129.25, 129.0, 125.4, 122.9, 20.7, 20.5, 20.3, 19.1, 18.5;

$^{19}\text{F}\{^1\text{H}\}$ NMR (CD_3CN): δ -78.9 (s);

FT-IR (cm^{-1} (relative intensities)): 428(15), 518(5), 574(10), 637(2), 725(12), 784(4), 855(14), 910(11), 1027(3), 1156(7), 1250(1), 1368(9), 1498(13), 1556(6), 3167(8);

FT-Raman (cm^{-1} (relative intensities)): 85(4), 112(9), 186(14), 314(13), 350(11), 571(6), 766(12), 1030(2), 1062(15), 1316(3), 1381(10), 1498(5), 1564(8), 1599(1), 2929(7).

5.5 References

- (1) Holthausen, M. H.; Weigand, J. J. *J. Am. Chem. Soc.* **2009**, *131*, 14210.
- (2) Weigand, J. J.; Feldman, K.-O.; Henne, F. D. *J. Am. Chem. Soc.* **2010**, *132*, 16321.
- (3) Martin, C. D.; Ragogna, P. J. *Inorg. Chem.* **2010**, *49*, 8164.
- (4) Brazeau, A. L.; Caputo, C. A.; Martin, C. D.; Jones, N. D.; Ragogna, P. J. *Dalton Trans.* **2010**, *39*, 11069.
- (5) Conrad, E.; Burford, N.; McDonald, R.; Ferguson, M. J. *Chem. Commun.* **2010**, *46*, 4598.
- (6) Rupar, P. A.; Staroverov, V. N.; Baines, K. M. *Science* **2008**, *322*, 1360.
- (7) For example, see: (a) Gillespie, R. J.; Passmore, J. *Chem. Commun.* **1969**, 1333. (b) Burns, R. C.; Gillespie, R. J.; Luk, W.-C.; Slim, D. R. *Inorg. Chem.* **1979**, *18*, 3086. (c) Sato, S.; Ameta, H.; Horn, E.; Takahashi, O.; Furukawa, N. *J. Am. Chem. Soc.* **1997**, *119*, 12374. (d) Brownridge, S.; Crawford, M.-J.; Du, H.; Harcourt, R. D.; Knapp, C.; Laitinen, R. S.; Passmore, J.; Rautiainen, J. M.; Suontamo, R. J.; Valkonen, J. *Inorg. Chem.* **2007**, *46*, 681. (e) Martin, C. D.; Jennings, M. C.; Ferguson, M. J.; Ragogna, P. J. *Angew. Chem. Int. Ed.* **2009**, *48*, 2210. (f) Dutton, J. L.; Tuononen, H. M.; Jennings, M. C.; Ragogna, P. J. *J. Am. Chem. Soc.* **2006**, *128*, 12624. (g) Dutton, J. L.; Tuononen, H. M.; Ragogna, P. J. *Angew. Chem. Int. Ed.* **2009**, *48*, 4409.
- (8) Makosky, C. W.; Galloway, G. L.; Ryschkewitsch, G. E. *Inorg. Chem.* **1967**, *6*, 1972.
- (9) Vidovic, D.; Findlater, M.; Cowley, A. H. *J. Am. Chem. Soc.* **2007**, *129*, 8436.
- (10) Vargas-Baca, I.; Findlater, M.; Powell, A.; Vasudevan, K. V.; Cowley, A. H. *Dalton Trans.* **2008**, 6421.
- (11) Vidovic, D.; Findlater, M.; Reeske, G.; Cowley, A. H. *J. Organomet. Chem.* **2007**, *692*, 5683.
- (12) Rupar, P. A.; Staroverov, V. N.; Ragogna, P. J.; Baines, K. M. *J. Am. Chem. Soc.* **2007**, *129*, 15138.
- (13) Chitnis, S. S.; Peters, B.; Conrad, E.; Burford, N.; McDonald, R.; Ferguson, M. J. *Chem. Commun.* **2011**, *47*, 12331.
- (14) Schmidpeter, A.; Lochschmidt, S.; Karaghiosoff, K.; Sheldrick, W. S. *J. Chem. Soc., Chem. Commun.* **1985**, 1447.

- (15) Reed, R.; Réau, R.; Dahan, F.; Bertrand, G. *Angew. Chem. Int. Ed. Engl.* **1993**, *32*, 399.
- (16) Weigand, J. J.; Burford, N.; Decken, A.; Schulz, A. *Eur. J. Inorg. Chem.* **2007**, 4868.
- (17) For examples of metals supported by guanidates, see: (a) Green, S. P.; Jones, C.; Stasch, A. *Science* **2007**, *318*, 1754. (b) Foley, S. R.; Yap, G. P. A.; Richeson, D. S. *Chem. Commun.* **2000**, 1515. (c) Tin, M. K. T.; Thirupathi, N.; Yap, G. P. A.; Richeson, D. *J. Chem. Soc., Dalton Trans.* **1999**, 2947. (d) Jones, C.; Schulten, C.; Rose, R. P.; Stasch, A.; Aldridge, S.; Woodul, W. D.; Murray, K. S.; Moubaraki, B.; Brynda, M.; Macchia, G. L.; Gagliardi, L. *Angew. Chem. Int. Ed.* **2009**, *48*, 7406. (e) Stasch, A.; Forsyth, C. M.; Jones, C.; Junk, P. C. *New J. Chem.* **2008**, *32*, 829. (f) Jones, C.; Junk, P. C.; Platts, J. A.; Stasch, A. *J. Am. Chem. Soc.* **2006**, *128*, 2206. (g) Coyle, J. P.; Monillas, W. H.; Yap, G. P. A.; Barry, S. T. *Inorg. Chem.* **2008**, *47*, 683. (h) Milanov, A.; Bhakta, R.; Baunemann, A.; Becker, H.-W.; Thomas, R.; Ehrhart, P.; Winter, M.; Devi, A. *Inorg. Chem.* **2006**, *45*, 11008.
- (18) Green, S. P.; Jones, C.; Jin, G.; Stasch, A. *Inorg. Chem.* **2007**, *46*, 8.
- (19) Ergezinger, C.; Weller, F.; Dehnicke, K. *Z. Naturforsch., B: Chem. Sci.* **1988**, *43*, 1119.
- (20) Raston, C. L.; Skelton, B. W.; Tolhurst, V.-A.; White, A. H. *Polyhedron* **1998**, *17*, 935.
- (21) Raston, C. L.; Skelton, B. W.; Tolhurst, V.-A.; White, A. H. *J. Chem. Soc., Dalton Trans.* **2000**, 1279.
- (22) Lyhs, B.; Schulz, S.; Westphal, U.; Bläser, D.; Boese, R.; Bolte, M. *Eur. J. Inorg. Chem.* **2009**, 2247.
- (23) Day, B. M.; Coles, M. P.; Hitchcock, P. B. *Eur. J. Inorg. Chem.* **2012**, 841.
- (24) Bailey, P. J.; Gould, R. O.; Harmer, C. N.; Pace, S.; Steiner, A.; Wright, D. S. *Chem. Commun.* **1997**, 1161.
- (25) Tin, M. K. T.; Thirupathi, N.; Yap, G. P. A.; Richeson, D. *J. Chem. Soc., Dalton Trans.* **1999**, 2947.
- (26) Pauling, L. *The Nature of the Chemical Bond*; 3rd ed.; Cornell University Press: Ithaca, 1960.
- (27) Michalik, D.; Schulz, A.; Villinger, A. *Inorg. Chem.* **2008**, *47*, 11798.

Chapter 6

6 Conclusions and future directions

6.1 Conclusions

This thesis demonstrates the synthesis and studies the reactivity of *N*-heterocyclic phosphonium cations and the heavier congeners (As, Sb, Bi) with *N,N*-chelating ligands. Key to the results outlined in the previous chapters is that the ligands employed, pyridyl tethered 1,2-bis(imino)acenaphthene and guanidinate, were used almost solely for transition metals. Therefore this work represents a paradigm shift in that they have been applied to main group elements.

Similarly, the unique “clamshell” ligand, designed by Guan *et al.*, has been used as a support for Pd and Ni complexes, as catalysts for ethylene polymerization.¹ We saw an opportunity to use this ligand to support a phosphonium cation, which would place a Lewis acid in close proximity to a Lewis base (tethered pyridine). An *N*-heterocyclic phosphonium cation was synthesized *via* redox routes and halide abstraction. The Lewis amphotericism of the molecule was demonstrated separately by pyridine coordination to BH₃ and by a DMAP→P donor-acceptor complex, showing the dual reactivity of the compound. Upon our successes with phosphorus, the heavier pnictenium cations became synthetic targets in order to increase the Lewis acidity and the size of the central element to get an internal Lewis acid/Lewis base adduct. A reported redox route for the synthesis of an arsenium cation² from an α -diimine, AsCl₃ and SnCl₂ proved to be inappropriate with the “clamshell” ligand, resulting in coordination of the α -diimine to the oxidized SnCl₄. An alternate redox route using cobaltocene as the reductant was discovered to be facile and high yielding for arsenic. This route was attempted with the other trichloropnictogens and was found to be low yielding in the case of phosphorus and not viable for antimony and bismuth because both were reduced to their elemental forms by cobaltocene. Donor-acceptor complexes with the “clamshell” ligand and SbCl₃ and BiCl₃ could however be synthesized resulted in hypervalency at the central pnictogen. Halide

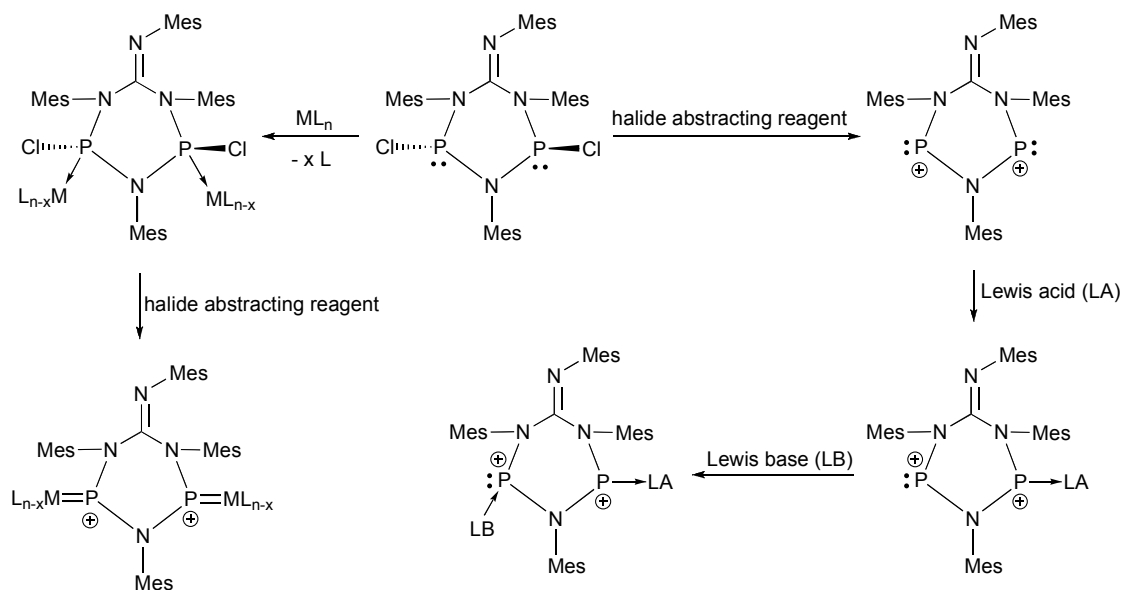
abstraction, at the PnCl_3 unit, was accomplished on these adducts resulting in base-stabilized SbCl_2^+ and BiCl_2^+ cations.

The synthesis of diaminochlorophosphines supported by various homo- and heteroleptic dianionic guanidates was accomplished for the first time and their reactivity was investigated experimentally and computationally. The lack of these compounds in the literature was surprising given the ubiquity of this ligand across the periodic table, and given that diaminohalophosphines are precursors to NHPs, of which other four-membered species are known. The seemingly easy halide abstraction from these compounds proved to be a difficult feat. Halide abstraction with common salt metathesis triflate reagents, as well as Lewis acids was unsuccessful, and in the former case led to $\text{N} \rightarrow \text{M}$ ($\text{M} = \text{Al}, \text{Ga}$) adducts. The addition of bpy, a chelating Lewis base, helps sequester the Lewis acidity at phosphorus and allows for the salt metathesis reaction to proceed, which results in a base-stabilized NHP. It was discovered that carbodiimide could be eliminated (thermally and chemically) from the ring system to form an iminochlorophosphine, which can also insert into a $\text{P} - \text{N}$ of the parent diaminochlorophosphine to give a novel six-membered ring, and upon halide abstraction can act as a cationic ligand for Pt. The analogous chemistry with heavier pnictogens (As, Sb, Bi) does not occur. Rather the 1:1:2 stoichiometric reaction of a guanidine ligand, PnCl_3 , and NEt_3 gives a diaminodichloropnictine where the supporting ligand is in the monoanionic form, instead of the anticipated diaminochloropnictine with a dianionic ligand. One chloride ion can be removed *via* halide abstraction with Me_3SiOTf , which is facile for As and Sb, however a guanidinium byproduct is concomitantly produced alongside the bismuthenium. Extra stabilization from bpy and a second halide abstraction allows for the isolation of arsenic and antimony dications, the first of its kind for the latter and a rare example for the former.

These findings contribute to the fundamental study of diaminohalophosphines, the heavier analogues, and the corresponding cyclic diaminopnictenium cations, which despite being studied for over 40 years, continue to intrigue many researchers.

6.2 Future directions

Future directions envisioned for this project involve further fundamental studies, as well as exploring the utility of some of the molecules synthesized. For example, it would be worthwhile to explore the reactivity of the dinuclear six-membered ring, **4.13**, by removing the two chloride ions to make a dicationic species with two phosphonium cations (Scheme 6.1). Given that this would be a six-membered ring containing three nitrogen atoms, and therefore six π -electrons, such a species may obtain additional stabilization from being aromatic. Interesting onward reactivity would include synthesizing homo- and hetero-dimetallic complexes, finding an appropriate substrate that could be activated by such a species and demonstrating activation at both phosphonium sites, and exploiting the amphotericity of phosphonium cations and illustrating one phosphorus acting as a Lewis acid and the other as a Lewis base (Scheme 6.1). The chemistry of the polycationic arsetidinium dication is entirely unexplored, given that our report was the first of its kind. Removing the donating bpy from this molecule would result in a highly Lewis acidic arsenic centre, which should be capable of activating small molecules, such as organic molecules with unsaturated bonds. Similar reactions should also be conducted with the antimony dication. The bismuthetidinium dication remains a synthetic target, however a clean synthesis of the diaminochlorobismuthenium must be deduced first.



Scheme 6.1: Proposed synthesis for the diphosphenium dication and its coordination to metals and formation of Lewis acid/Lewis base adducts.

Main group molecules with the “clamshell” ligand have great potential in the area of small molecule activation and catalysis. The phosphenium cation, **2.3**, presents a unique system where a Lewis acid (P^+) is proximal to a Lewis base (pyridine), which results in a pocket of reactivity akin to “frustrated” Lewis pair (FLP) chemistry (Chart 6.1a). While attempts have been made to demonstrate this with small molecules (H_2 , ethylene, CO, NH_3 , styrene, propylene oxide), no reactivity has been observed, but perhaps the right substrate has not been found. The reactivity of such a compound could be heightened with a more Lewis acidic centre, such as a group 13 cation. Metal complexes with “clamshell” molecules would also be interesting molecules to study. Electron-rich metals would be able to back-bond to the Lewis acid and the tethered pyridine may be able to act as a labile ligand on the metal, resulting in efficient catalysts (Chart 6.1b). It would also be interesting to make an NHC with the “clamshell” ligand (Chart 6.1c), given its inverse properties to the NHP and do a comparative study of their reactivities.

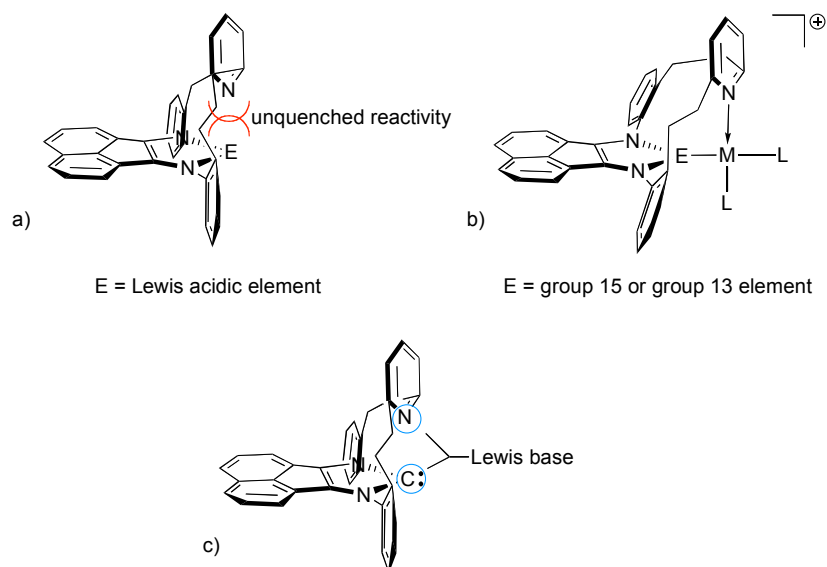


Chart 6.1: (a) “Frustrated” internal Lewis pairs; (b) metal complexes; and, (c) NHC with the “clamshell” ligand.

6.3 References

- (1) Leung, D. H.; Ziller, J. W.; Guan, Z. *J. Am. Chem. Soc.* **2008**, *130*, 7538.
- (2) Reeske, G.; Hoberg, C. R.; Hill, N. J.; Cowley, A. H. *J. Am. Chem. Soc.* **2006**, *128*, 2800.

Appendices

Appendix 1: General considerations

A1.1 General experimental considerations

All manipulations were performed in an inert atmosphere in a nitrogen filled MBraun Labmaster dp glovebox or using standard Schlenk techniques unless stated otherwise. Reagents were obtained from commercial sources. Triethylamine was distilled from CaH_2 , phosphorus(III) chloride, phosphorus(III) bromide and arsenic(III) chloride were distilled prior to use, while all other reagents were used without further purification. All solvents were dried using an MBraun controlled atmospheres solvent purification system and stored in Straus flasks under an N_2 atmosphere or over 4 Å molecular sieves in the glovebox (3 Å for acetonitrile). Chloroform-d was dried over CaH_2 , distilled prior to use, and stored in the glovebox over 4 Å molecular sieves. The synthesis of pyridyl tethered 1,2-bis(imino)acenaphthene (**1**, “clamshell”),¹ *N,N'*-bis(Dipp)carbodiimide,² *N,N'*-bis(Mes)carbodiimide,² *N,N',N''*-tris(Dipp)guanidine³ (**3**), *N,N',N''*-tris(cyclohexyl)guanidine⁴ (**6**) followed literature procedures.

Most ^1H , $^{11}\text{B}\{^1\text{H}\}$, $^{13}\text{C}\{^1\text{H}\}$, $^{19}\text{F}\{^1\text{H}\}$ and $^{31}\text{P}\{^1\text{H}\}$ data were collected on a 400 MHz Varian Inova spectrometer (399.762 MHz for ^1H , 128.27 MHz for ^{11}B , 100.52 MHz for ^{13}C , 376.15 for ^{19}F and 161.825 MHz for ^{31}P). ^1H and $^{13}\text{C}\{^1\text{H}\}$ data collected on a 600 MHz Varian Inova spectrometer is noted in the appropriate experimental sections. Spectra were recorded at room temperature, unless otherwise indicated, in CDCl_3 using the residual protons of the deuterated solvent for reference and are listed in ppm, coupling constants (J) are listed in Hz. Phosphorus, boron and fluorine NMR spectra were recorded unlocked relative to an external standard (85% H_3PO_4 , $\delta_{\text{P}} = 0.0$; $\text{BF}_3 \cdot \text{OEt}_2$, $\delta_{\text{B}} = 0.00$; $\text{CF}_3\text{C}_6\text{H}_5$, $\delta_{\text{F}} = -63.9$).

FT-IR spectra were collected on samples as KBr pellets using a Bruker Tensor 27 spectrometer, with a resolution of 4 cm^{-1} . Samples for FT-Raman spectroscopy were

packed in capillary tubes and flame-sealed. Data was collected using a Bruker RFS 100/S spectrometer, with a resolution of 4 cm^{-1} .

Melting (m.p.) and decomposition (d.p.) points were recorded in flame sealed capillary tubes using a Gallenkamp Variable Heater. High resolution mass spectrometry (HRMS) was collected using a Finnigan MAT 8200 instrument. Elemental analyses (C, H, N) were performed by Guelph Chemical Laboratories, Guelph, ON, Canada, or Laboratoire d'Analyse Élémentaire de l'Université de Montréal, Montréal, QC, Canada.

A1.2 General crystallography considerations

Single crystal X-ray diffraction data were collected on a Nonius Kappa-CCD area detector or a Bruker Apex II-CCD detector using Mo-K α radiation ($\lambda = 0.71073\text{ \AA}$) and at a temperature of 150(2) K. Suitable single crystals were selected under Paratone-N oil, mounted on MiTeGen micromounts or nylon loops then immediately placed in a cold stream of N₂ on the diffractometer. Structures were solved by direct methods and refined using full matrix least squares on F^2 using the SHELXTL suite of software.⁵ Hydrogen atoms positions were calculated.

A1.3 References

- (1) Leung, D. H.; Ziller, J. W.; Guan, Z. *J. Am. Chem. Soc.* **2008**, *130*, 7538.
- (2) Findlater, M.; Hill, N. J.; Cowley, A. H. *Dalton Trans.* **2008**, 4419.
- (3) Boéré, R. E.; Boéré, R. T.; Masuda, J.; Wolmershäuser, G. *Can. J. Chem.* **2000**, *78*, 1613.
- (4) Tin, M. K. T.; Yap, G. P. A.; Richeson, D. S. *Inorg. Chem.* **1998**, *37*, 6728.
- (5) Sheldrick, G. M. *Acta Cryst. A* **2008**, *64*, 112.

Appendix 2: Copyright permission

A2.1 American Chemical Society's policy on theses and dissertations

This is regarding request for permission to include **your** paper(s) or portions of text from **your** paper(s) in your thesis. Permission is now automatically granted; please pay special attention to the **implications** paragraph below. The Copyright Subcommittee of the Joint Board/Council Committees on Publications approved the following:

Copyright permission for published and submitted material from theses and dissertations

ACS extends blanket permission to students to include in their theses and dissertations their own articles, or portions thereof, that have been published in ACS journals or submitted to ACS journals for publication, provided that the ACS copyright credit line is noted on the appropriate page(s).

Publishing **implications** of electronic publication of theses and dissertation material

Students and their mentors should be aware that posting of theses and dissertation material on the Web prior to submission of material from that thesis or dissertation to an ACS journal may affect publication in that journal. Whether Web posting is considered prior publication may be evaluated on a case-by-case basis by the journal's editor. If an ACS journal editor considers Web posting to be "prior publication", the paper will not be accepted for publication in that journal. If you intend to submit your unpublished paper to ACS for publication, check with the appropriate editor prior to posting your manuscript electronically.

Reuse/Republication of the Entire Work in Theses or Collections: Authors may reuse all or part of the Submitted, Accepted or Published Work in a thesis or dissertation that the author writes and is required to submit to satisfy the criteria of degree-granting institutions. Such reuse is permitted subject to the ACS' "Ethical Guidelines to Publication of Chemical Research" (<http://pubs.acs.org/page/policy/ethics/index.html>); the author should secure written confirmation (via letter or email) from the respective

ACS journal editor(s) to avoid potential conflicts with journal prior publication*/embargo policies. Appropriate citation of the Published Work must be made. If the thesis or dissertation to be published is in electronic format, a direct link to the Published Work must also be included using the ACS Articles on Request author-directed link – see <http://pubs.acs.org/page/policy/articlesonrequest/index.html>

* Prior publication policies of ACS journals are posted on the ACS website at <http://pubs.acs.org/page/policy/prior/index.html>

If your paper has **not** yet been published by ACS, please print the following credit line on the first page of your article: "Reproduced (or 'Reproduced in part') with permission from [JOURNAL NAME], in press (or 'submitted for publication'). Unpublished work copyright [CURRENT YEAR] American Chemical Society." Include appropriate information.

If your paper has already been published by ACS and you want to include the text or portions of the text in your thesis/dissertation, please print the ACS copyright credit line on the first page of your article: "Reproduced (or 'Reproduced in part') with permission from [FULL REFERENCE CITATION.] Copyright [YEAR] American Chemical Society." Include appropriate information.

Submission to a Dissertation Distributor: If you plan to submit your thesis to UMI or to another dissertation distributor, you should not include the unpublished ACS paper in your thesis if the thesis will be disseminated electronically, until ACS has published your paper. After publication of the paper by ACS, you may release the entire thesis (**not the individual ACS article by itself**) for electronic dissemination through the distributor; ACS's copyright credit line should be printed on the first page of the ACS paper.

This information can be found at:
<http://pubs.acs.org/userimages/ContentEditor/1218205107465/dissertation.pdf>

A2.2 Royal Society of Chemistry rights retained by journal authors

When the author signs the exclusive Licence to Publish for a journal article, he/she retains certain rights that may be exercised without reference to the RSC. He/she may:

- Reproduce/republish portions of the article (including the abstract).
- Photocopy the article and distribute such photocopies and distribute copies of the PDF of the article that the RSC makes available to the corresponding author of the article upon publication of the article for personal or professional use only, provided that any such copies are not offered for sale.
- Adapt the article and reproduce adaptations of the article for any purpose other than the commercial exploitation of a work similar to the original.
- Reproduce, perform, transmit and otherwise communicate the article to the public in spoken presentations (including those which are accompanied by visual material such as slides, overheads and computer projections).

The author(s) must submit a written request to the RSC for any other use than those specified above. All cases of republication/reproduction must be accompanied by an acknowledgement of first publication of the Work by the RSC. The acknowledgement depends on the journal in which the article was published.

For all other journals the acknowledgement is: [Original citation] - Reproduced by permission of The Royal Society of Chemistry (RSC).

The acknowledgement should also include a hyperlink to the article on the RSC website.

The author also has some rights concerning the deposition of the whole article, details of which are given on the Author Deposition pages.

This information can be found at:

<http://www.rsc.org/AboutUs/Copyright/RightsRetainedbyJournalsauthors.asp>

Appendix 3: Supplementary data

A3.1 Corroborating ^1H NMR spectra for elemental analyses of compounds **3.3-3.5**.

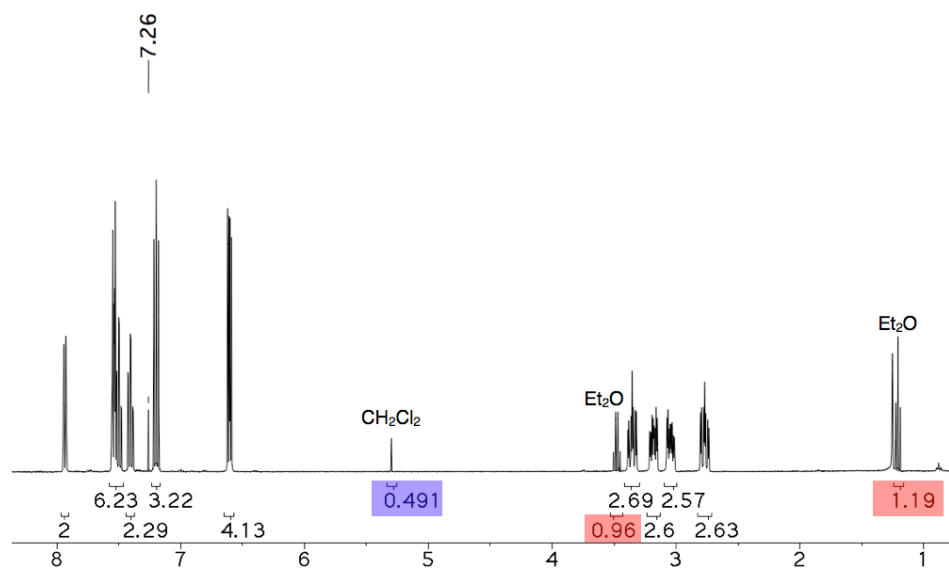


Figure A3.1: Corroborating ^1H NMR spectrum for the elemental analysis of **3.3** showing $\frac{1}{4}$ equivalents of CH_2Cl_2 (blue) and $\frac{1}{4}$ equivalents of Et_2O (red).

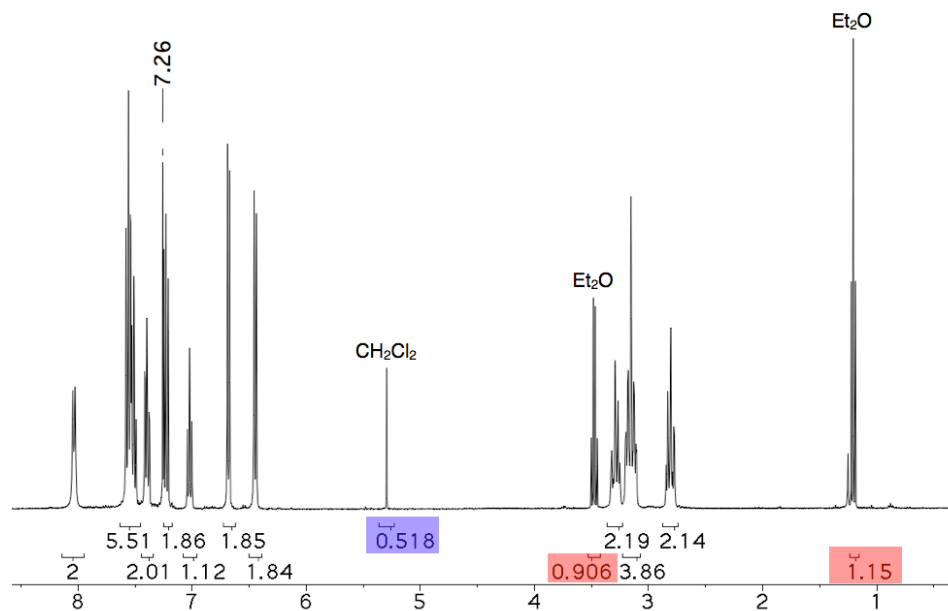


Figure A3.2: Corroborating ¹H NMR spectrum for the elemental analysis of **3.4** showing $\frac{1}{4}$ equivalents of CH₂Cl₂ (blue) and $\frac{1}{4}$ equivalents of Et₂O (red).

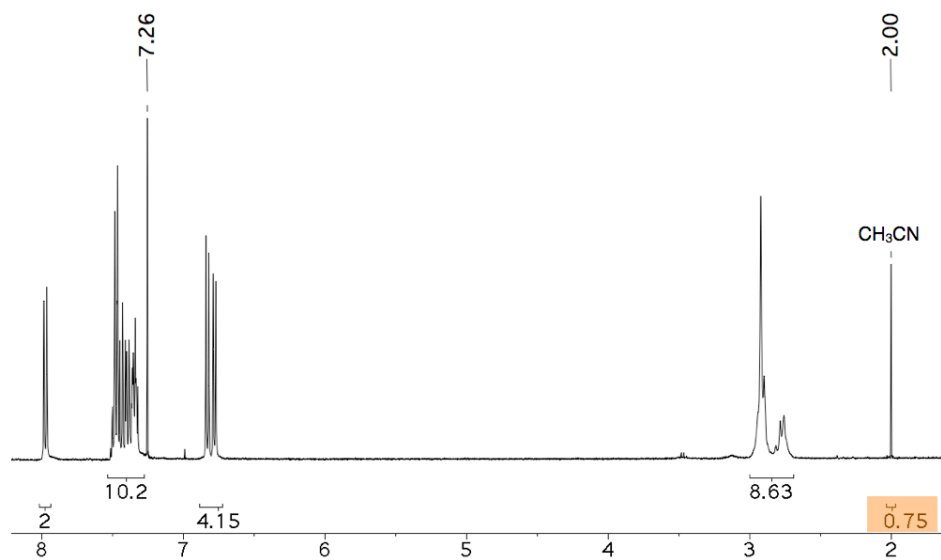


Figure A3.3: Corroborating ¹H NMR spectrum for the elemental analysis of **3.5** showing $\frac{1}{4}$ equivalents of CH₃CN.

Curriculum Vitae

Name: Allison Brazeau

Post-secondary Education and Degrees: Carleton University
Ottawa, Ontario, Canada
2001-2005 B.Sc. with Honours in Chemistry

Carleton University
Ottawa, Ontario, Canada
2005-2007 M.Sc.

The University of Western Ontario
London, Ontario, Canada
2008-2012 Ph.D.

Honours and Awards: Inorganic Discussion Weekend Poster Prize Winner
2011, 2006

EWPC-8 Travel Grant
2011

Western Graduate Thesis Research Fund
2011

Western Graduate Research Scholarship
2008-2011

Natural Sciences and Engineering Research Council Alexander
Graham Bell Canada Graduate Scholarship
2008-2011(CGS-D), 2006-2007(CGS-M)

Ontario Graduate Scholarship
2009(declined), 2008-2009, 2006(declined)

Fluorosense Inc. Scholarship in Chemistry
2005-2006

Senate Medal for Outstanding Academic Achievement –
Undergraduate
2005

Related Work Experience**Teaching Assistant**
Carleton University
2004-2007The University of Western Ontario
2008, 2011**Publications:**

“Chemistry of the heavy group 15 elements with the pyridyl tethered 1,2-bis(imino)acenaphthene "clamshell" ligand” Allison L. Brazeau, Nathan D. Jones and Paul J. Ragona.* *Dalton Trans.* **2012**, *41*, 7890 (invited submission for “*New Talent: Americas*” special issue).**Artwork featured on back cover.

“Synthesis, Reactivity, and Computational Analysis of Halophosphines Supported by Dianionic Guanidinate Ligands” Allison L. Brazeau, Mikko M. Hänninen, Heikki M. Tuononen, Nathan D. Jones and Paul J. Ragona.* *J. Am. Chem. Soc.* **2012**, *134*, 5398.

“Electrogenerated chemiluminescence of triazole-modified deoxycytidine analogues in *N,N*-dimethylformamide” Kalen N. Swanick, David W. Dodd, Jacquelyn T. Price, Allison L. Brazeau, Nathan D. Jones, Robert H. E. Hudson and Zhifeng Ding.* *Phys. Chem. Chem. Phys.* **2011**, *13*, 17405.

“A base-stabilised arsenic(III) dication” Allison L. Brazeau, Anton S. Nikouline and Paul J. Ragona.* *Chem. Commun.* **2011**, *47*, 4817.

“A new approach to internal Lewis pairs featuring a phosphonium acid and a pyridine base” Allison L. Brazeau, Christine A. Caputo, Caleb D. Martin, Nathan D. Jones and Paul J. Ragona.* *Dalton Trans.* **2010**, *39*, 11069.

“Blue fluorescent deoxycytidine analogues: convergent synthesis, solid-state and electronic structure, and solvatochromism” David W. Dodd, Kalen N. Swanick, Jacquelyn T. Price, Allison L. Brazeau, M. J. Ferguson, Nathan D. Jones and Robert H. E. Hudson.* *Org. Biomol. Chem.* **2010**, *8*, 663.

“A Cation-Captured Palladium(0) Anion: Synthesis, Structure, and Bonding of [PdBr(PPh₃)₂]⁻ Ligated by an N-Heterocyclic Phosphonium Cation” Christine A. Caputo, Allison L. Brazeau, Zachery Hynes, Jacquelyn T. Price, Heikki M. Tuononen and Nathan D. Jones.* *Organometallics* **2009**, *28*, 5261.

“Growth Mechanisms in Nanocrystalline Lead Sulfide by Stopped-Flow Kinetic Analysis” Allison L. Brazeau and Nathan D. Jones.* *J. Phys. Chem. C* **2009**, *113*, 20246.

“Atomic Layer Deposition of Aluminum Oxide Thin Films from a Heteroleptic, Amidinate-Containing Precursor” Allison L. Brazeau and Seán T. Barry.* *Chem. Mater.* **2008**, *20*, 7287.

“Chiral, Hemilabile Palladium(II) Complexes of Tridentate Oxazolidines, Including C₂-Symmetric “Pincers”” Elizabeth T. J. Strong, Steven A. Cardile, Allison L. Brazeau, Michael C. Jennings, Robert McDonald and Nathan D. Jones.* *Inorg. Chem.* **2008**, *47*, 10575.

“Theoretical and Experimental Investigations of Ligand Exchange in Guanidinate Ligand Systems for Group 13 Metals” Allison L. Brazeau, Gino A. DiLabio, Kevin A. Kreisel, Wesley Monillas, Glenn P. A. Yap and Seán T. Barry.* *Dalton Trans.* **2007**, *30*, 3297.

“Synthesis and Thermolysis of Aluminum Amidinates: A Ligand-Exchange Route for New Mixed-Ligand Systems” Allison L. Brazeau, Zhaohui Wang, Chris N. Rowley and Seán T. Barry.* *Inorg. Chem.* **2006**, *45*, 2276.

Conference Presentations:

“Metal Complexes with a “Clamshell” Phosphenium Ligand” Allison L. Brazeau, Nathan D. Jones and Paul J. Ragogna.* 44th Inorganic Discussion Weekend, *The University of Western Ontario*, Niagara Falls, ON, August 2011. (poster)

“Pnictenium Cations: Redox Reactions and the Freedom to Choose the Counteranion” Allison L. Brazeau, Nathan D. Jones and Paul J. Ragogna.* 94th Canadian Chemistry Conference and Exhibition, Montreal, QC, June 2011. (oral)

“N-heterocyclic phosphenium cations with new ligand frameworks” Allison L. Brazeau and Paul J. Ragogna.* 8th European Workshop on Phosphorus Chemistry, Universität Münster, Münster, Germany, March 2011. (oral)

“Cationic Arsenic Complexes Featuring a Bulky Guanidinate Ligand” Allison L. Brazeau, Anton S. Nikouline and Paul J. Ragogna.* 43rd Inorganic Discussion Weekend, University of Windsor, Windsor, ON, November 2010. (oral)

“Synthesis and Reactivity of a Phosphenium Cation Supported by an Axially Donating BIAN Derivative” Allison L. Brazeau, Christine A. Caputo, Nathan D. Jones and Paul J. Ragogna.* 93rd Canadian Chemistry Conference and Exhibition, Toronto, ON, May 2010. (oral)

“Towards Four-Membered N-Heterocyclic Phosphenium Cations Supported by Dianionic Guanidinate Ligands” Allison L. Brazeau, Nathan D. Jones and Paul J. Ragogna.* 93rd Canadian Chemistry Conference and Exhibition, Toronto, ON, May 2010. (poster)

“New Ligand Frameworks for Supporting N-Heterocyclic Phosphenium Cations” Allison L. Brazeau, Jacquelyn T. Price and Nathan D. Jones.* 42nd Inorganic Discussion Weekend, University of Guelph, Guelph, ON, November 2009. (oral)

“Investigation of Lead Sulfide Nanocrystal Growth Kinetics by Stopped-Flow Spectrophotometry” Allison L. Brazeau and Nathan D. Jones.* 41st Inorganic Discussion Weekend, Brock University, St. Catharines, ON, November 2008. (poster)

“Lead Sulfide Nanocrystal Growth Investigation *via* Stopped-Flow Spectrophotometry”
Allison L. Brazeau and Nathan D. Jones.* 91st Canadian Chemistry Conference and
Exhibition, Edmonton, AB, May 2008. (poster)